NASA Reference Publication 1381

November 1995

1995 Scientific Assessment of the Atmospheric Effects of Stratospheric Aircraft

Richard S. Stolarski, Assessment Chair

Steven L. Baughcum
William H. Brune
Anne R. Douglass
David W. Fahey
Randall R. Friedl
Shaw C. Liu
R. Alan Plumb
Lamont R. Poole
Howard L. Wesoky
Douglas R. Worsnop

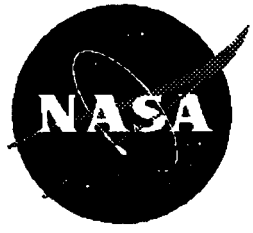

National Aeronautics and Space Administration

1995 SCIENTIFIC ASSESSMENT OF THE ATMOSPHERIC EFFECTS OF STRATOSPHERIC AIRCRAFT

Table of Contents

FOREWORD

The following report is an assessment of scientific predictions for the atmospheric effects of a proposed fleet of high-speed civil transport (HSCT) aircraft. It was commissioned by the Atmospheric Effects of Stratospheric Aircraft (AESA) element of the National Aeronautics and Space Administration (NASA) High-Speed Research Program (HSRP), which has technology goals that, if achieved, would promise environmental compatibility and economic practicability for the HSCT fleet. When the program was conceived in 1989, this latest revival of interest in supersonic transport (SST) was greeted with healthy skepticism by those who well recalled the related atmospheric studies of the 1970s. For the technology of that era, it was predicted that nitrogen oxides (NO_x) from a fleet of SSTs would do significant damage to stratospheric ozone [Johnston, 1971].

Our understanding of the atmosphere had grown significantly by the beginning of the AESA program [Johnston *et al.*, 1991; Douglass *et al.*, 1991], and today we are on the verge of having predictive tools that can be applied with a high degree of confidence. However, today's best informed opinion regarding HSCT technology is the same as before; that the SSTs studied in the 1970s would have been an environmental problem. But in reading the present report and projecting to where the science may be in a few years, it is important to realize that aircraft technology has also progressed and will continue to advance.

Earlier atmospheric predictions assumed that jet engine combustors produced NO_x at a rate of about 30 grams of equivalent nitrogen dioxide (NO_2) per kilogram of fuel burned. The original HSRP target emission, 5 grams per kilogram of fuel burned [Shaw *et al.*, 1993, Sweetman, 1995, Williams, 1993], has now been achieved in tests of practical combustor configurations. At that low level of emissions, current atmospheric models suggest that HSCT technology indeed can be environmentally compatible [Stolarski and Wesoky, 1993a]. Therefore, it is the parallel development of science and technology that offers the promise of success for the HSRP.

Recognition of the progress made in understanding the atmospheric processes to which an HSCT fleet would contribute, and the technological means for controlling resulting emissions, is demonstrated by a September 1994 recommendation from the International Coordinating Council of Aerospace Industry Associations to the Emissions Working Group (WG3) of the International Civil Aviation Organization's (ICAO) Committee on Aviation Environmental Protection (CAEP):

> WG3 should recommend to CAEP that it charter a sub-group, with appropriate Terms of Reference, to develop Annex 16 emissions certification requirements for future supersonic aeroplanes, consistent with technical practicability and economic reasonability, for consideration at CAEP/4.

The next meeting of CAEP (i.e., CAEP/3) will be in December 1995, with CAEP/4 likely to occur three to five years later.

Although this progress in the regulatory forum is also very promising for HSCT technology, it must be recognized that ICAO has indicated [CAEP, 1992] that any future emission standard will likely occur only "when the environmental need has been accepted by an international consensus (e.g., by UNEP/WMO)." And, although significant "developments [have] changed decidedly the scientific

community's judgment with respect to the expected impact of the NO_x component of the HSCT effluent" [Anderson, 1995], such a consensus does not yet exist. The most current ozone assessment of the United Nations Environment Programme (UNEP) and World Meteorological Organization (WMO) [WMO, 1995] clearly recognizes the progress of the NASA program and other research, but also states that there are "important uncertainties in supersonic assessments."

These uncertainties have been highlighted in an evaluation by the National Research Council (NRC) of the National Academy of Sciences that NASA requested in 1992. A panel of ten experts, including four from Europe, received extensive briefings from NASA managers and investigators before an interim assessment report [NASA, 1993] was transmitted to them in June 1993. In Congressional testimony [Graedel, 1994] regarding the NRC [1994] report, the panel chairman noted that the then

> current assessment of environmental effects resulting from HSCT fleet emissions reveals no paramount concerns, but this assessment is clearly preliminary ... Although many AESA studies during the next year or two will increase our understanding of aspects of the atmosphere-aircraft interaction, the assessment's overall reliability will not change significantly by 1995.

The present report seeks to incorporate AESA results from the last two years into an updated assessment. It will also serve to initiate the second phase of AESA, in direct response to the NRC evaluation [Graedel, 1994] which recommended that

> The extension of AESA through 1998, coupled with strong program emphasis on resolving key uncertainties through a combination of airborne missions and computer model incorporation of mission results, would markedly increase the confidence one could bring to the assessment results.

Convergence of a confident scientific assessment, the related HSCT technology, and the regulatory policy at the end of this decade would be a truly exciting achievement.

Howard L. Wesoky
Manager, Atmospheric Effects of Aviation
Office of Aeronautics
National Aeronautics and Space Administration

EXECUTIVE SUMMARY

1. What are the concerns about high-speed civil transport operations in the stratosphere that motivate this assessment?

The operation of high-speed civil transport (HSCT) aircraft will introduce exhaust gases and particulates directly into the stratosphere. These exhaust components could alter stratospheric ozone and the Earth's climate.

- Important emissions from HSCTs include water vapor, carbon dioxide (CO_2), nitrogen oxides (NO_x), sulfur oxides (SO_x), carbon monoxide (CO), nonmethane hydrocarbons (NMHCs), and soot. The atmospheric impact of these emissions depends on how they change the steady-state abundance over background atmospheric amounts and their role in atmospheric photochemical, dynamical, and radiative processes. Atmospheric ozone change is possible because these HSCT emissions directly affect photochemical processes which control the ozone abundance. Climate change is also possible because these HSCT emissions are directly involved in the radiative balance of the atmosphere.

2. What processes are important in today's atmosphere and in a future atmosphere perturbed by HSCT emissions?

The amount of stratospheric ozone is determined by photochemical production and loss processes, and by the transport of air throughout the atmosphere. Photochemical loss of ozone is dominated by catalytic reactions involving NO_x, hydrogen oxides (HO_x), and halogen radicals (chlorine oxides (ClO_x) and bromine oxides (BrO_x)). Heterogeneous reactions which occur on or in stratospheric aerosol particles play an important role by reducing the ozone loss due to NO_x and increasing that due to HO_x and halogens. Atmospheric circulation determines the time spent by air in regions of photochemical loss and the distribution of exhaust gases emitted by a fleet of HSCTs.

- NO_x catalytically destroys stratospheric ozone but also inhibits ozone destruction by the HO_x and halogen radical catalytic cycles through the formation of more stable gases. The effect of adding NO_x to the atmosphere by HSCTs is sensitive to the balance of these two effects. In the stratosphere above ~26 km, NO_x catalysis is the most important ozone loss process; increased NO_x leads to increased local ozone loss. In the lower stratosphere, NO_x interference with the dominant HO_x and halogen catalysis of ozone destruction is more important. For increased NO_x (e.g., from HSCT exhaust), the sign and magnitude of the local chemical ozone change in the lower stratosphere depend on the background amounts of trace gases and aerosol surface area.

- Reactions on sulfate aerosols composed of sulfuric acid (H_2SO_4) and water (H_2O) play an important role in determining the abundance of NO_x. Because of these reactions, the concentration of NO_x depends on the variable input of volcanic SO_2 to the stratosphere. Observations show that the concentration of NO_x falls in response to increases in aerosol surface area. Because increases in sulfur, water vapor, and soot from HSCT emissions will change the surface area, composition, and number of particles in the lower stratosphere, the emissions indirectly influence ozone loss rates. In low-temperature regions near the poles, both liquid and frozen aerosols form that contain nitric acid (HNO_3) in addition to H_2O and H_2SO_4. Reactions on these aerosols enhance halogen-catalyzed loss of ozone and may sediment from the stratosphere, effectively reducing NO_x. The increased

water vapor and H_2SO_4 from HSCT exhaust could increase the importance of such processes, especially if the stratosphere is cooled by climate change.

- Transport of air between mid-latitudes and the tropics is restricted, especially between 20 and 28 km. Transport of air from the primary flight corridors in mid-latitudes into the tropics results in a more rapid spread of HSCT exhaust from the lower to upper stratosphere, where the catalytic destruction of ozone by NO_x is more efficient.

- For a projected fleet of HSCT aircraft, climate can be affected by changes in the abundance of water vapor, soot, or sulfate in the stratosphere. Climate also can be affected by changes in cirrus cloud properties or by the radiative consequences of changes in ozone and its vertical distribution.

3. What has been learned about the character of engine emissions and the chemical and fluid-dynamic processing that occur in the aircraft wake?

In situ aircraft exhaust sampling experiments and modeling of engine processes and the dilution of exhaust gases into the atmosphere are used to define the important chemical and dynamical features of exhaust plumes in the stratosphere.

- Measurements of reactive nitrogen (NO_y) species, condensation nuclei (CN), and CO_2 were recently made in the exhaust of the Concorde supersonic aircraft and the NASA ER-2 subsonic aircraft while in flight. The emission indices (EIs) were calculated independently of plume dynamics because measurements of CO_2 provide a measure of fuel burned. The measured EI of NO_x, expressed as grams of equivalent nitrogen dioxide (NO_2) per kilogram of fuel burned, is in excellent agreement with earlier results deduced from altitude chamber measurements of exhaust from the Concorde engine as part of the Climatic Impact Assessment Program (CIAP). These results suggest that the methodology developed to calculate the EI of NO_x at cruise from altitude chamber data will be appropriate to evaluate new HSCT engines.

- Observations show that NO_x is the most abundant NO_y species in both supersonic and subsonic aircraft plumes. The presence of only a small percentage of HNO_3 and nitrous acid (HONO) is in agreement with observations of HO_x in the plume and theoretical model calculations.

- The large number of detectable particles in the Concorde plume conflicts with the results of plume models that predict the formation of a large number of much smaller sulfate particles and a smaller fractional conversion of SO_x to condensed sulfate. These results indicate that current understanding of plume chemistry and particle formation processes is not complete. If new HSCT aircraft produce particles at a rate comparable to the Concorde, significant increases in particle number and surface area could occur in the lower stratosphere of the Northern Hemisphere. Including these increases in predictive models could change calculated ozone and climate impacts from an HSCT fleet.

4. What are the predicted atmospheric changes associated with HSCTs?

Five two-dimensional (2-D) photochemical models were used to calculate the impact of an HSCT fleet for a variety of cases including sensitivity tests for the EI of NO_x, cruise altitude, background atmospheric chlorine amount, and fleet size. Individual models were used to test sensitivity to a variety of effects not included in these basic predictive calculations.

- The range of model results is shown in Table ES-1. Conditions include a baseline fleet of 500 Mach 2.4 aircraft burning 8.2 x 10^{10} kg of fuel per year in an atmosphere with a background stratospheric aerosol amount equivalent to a relatively clean period between major volcanic eruptions. The models do not include the formation or reactivity of polar stratospheric cloud (PSC) particles. The calculated changes in ozone in Table ES-1 result from a decrease in the middle and upper stratosphere and an increase in the lower stratosphere and troposphere. The time required for photochemistry and transport to effect these ozone changes precludes large ozone changes near the assumed HSCT flight corridors. The EI_{NO_x} values in Table ES-1 reflect those expected for future HSCT combustors (5 g NO_2/kg fuel) and those closer to current engines (15 g NO_2/kg fuel).

- Laboratory observations continue to refine photolysis and reaction rate coefficients of importance to the lower stratosphere and to identify important reactions on surfaces of stratospheric aerosol particles. The formulation of the chemistry in the 2-D models is derived from the latest recommendation of a NASA panel that conducts a biennial review [DeMore *et al.*, 1994].

- Four of the five models used in the calculations were tested against two benchmarks, one for photolysis rates and one for chemistry. These indicate mostly minor differences, implying that the range in model results follows, at least in part, from differences in the 2-D representation of dynamics. The chemistry benchmark tested the model chemistry integrators against a photochemical steady-state model that has been used in detailed comparisons with atmospheric measurements of key radicals involved in the chemistry of stratospheric ozone.

- When the background aerosol surface area used in the models is increased by a factor of 4 (roughly equivalent to the median amount in the stratosphere over the last 2 decades), the calculated perturbation to total ozone is less negative by a few tenths of a percent. Variations in future

Table ES-1. Calculated steady-state total column ozone change (%) in the Northern Hemisphere averaged over a year for several HSCT fleet scenarios.

Scenario				2-D model results
Mach number	Cl_y (ppbv)	EI_{NO_x} (g NO_2/kg fuel)	Number of aircraft	Ozone change (%)[a]
2.4	3	0	500	-0.3 to -0.1
2.4	3	5	500	-0.3 to +0.1
2.4	3	5	1000	-0.7 to +0.03
2.4	3	10	500	-0.5 to 0.0
2.4	3	15	500	-1.0 to -0.02
2.4	3	15	1000	-2.7 to -0.6
2.4 Cruise +1 km	3	5	500	-0.5 to +0.02
2.4 Cruise -2 km	3	5	500	-0.06 to +0.1
2.4	2[b]	5	500	-0.4 to +0.02

[a] Range of average values obtained from the five 2-D models used in this assessment.

[b]Expected in a 2050 atmosphere.

stratospheric aerosol levels, primarily due to the frequency of large volcanic eruptions, are a source of uncertainty in HSCT ozone impact predictions.

- Sulfur emitted by a fleet of HSCTs can increase the sulfate aerosol surface area throughout the lower stratosphere. Although the increase in surface area decreases the impact of NO_x emissions, it also in-creases ozone loss due to the existing chlorine and hydrogen radicals in the stratosphere. If the sulfur emitted by HSCTs immediately forms small particles in the plume, then the global increase in sulfate surface area is maximized.

- A model that included aerosol processes was used to calculate ozone changes when 100% of the sulfur (EI_{SO_2} = 0.4 g sulfur/kg fuel) from an HSCT fleet was emitted as small particles into a volcanically unperturbed stratosphere. The change in total column ozone from the injection of small particles depended in a complex way on EI_{NO_x} and background chlorine amount. For EI_{NO_x} = 5 g/kg fuel, the calculated ozone depletion increased when small particles were formed; the overall perturbation became as large or larger than that for the EI_{NO_x} = 15 g/kg fuel case. Inclusion of the reaction of $BrONO_2$ with water on aerosols increased the effect of the small particles.

- The model results for ozone change in the basic scenarios vary more widely when heterogeneous reactions on PSCs are included. This results from uncertainty in PSC microphysical processes and from ambiguity in how to best represent such processes in a 2-D model.

- A general circulation model (GCM) was used to calculate the global surface air temperature and stratospheric temperature responses to predicted changes in ozone and water vapor from a fleet of HSCTs with EI_{NO_x}= 15 g NO_2/kg fuel. Since the resulting changes in temperature are smaller than the climatic fluctuations in the model, they likely would not be detectable in the atmosphere.

- Climate effects due to sulfur and soot emissions, while likely to be small, have yet to be evaluated. Formation of persistent contrails from HSCTs is expected to be infrequent.

5. How consistent are atmospheric and laboratory measurements with the current representation of processes in the 2-D models used to predict the HSCT effects on ozone?

Atmospheric observations can provide tests of our understanding of the photochemical and transport processes responsible for controlling the distribution of ozone and the potential impact of HSCTs. Laboratory measurements define the formulation of chemistry in models. Subsets of this formulation are tested by comparing the model predictions against a sufficiently complete set of atmospheric observations. Although constraints on transport formulations in 2-D models are less direct, observations of the distribution of and the correlations between long-lived gases provide a test of these formulations. An extensive series of 2-D model tests, conducted in 1992 [Prather and Remsberg, 1993], led to improvements in the models and an understanding of the differences among them. Comparisons to observations made since that time are ongoing, as are further model improvements.

- Models reproduce the basic features of the ozone column and vertical profile. Consistent with observations, the models suggest that ozone concentrations should have decreased in the past decade. However, the predicted changes are smaller than those measured by a factor of 1.5 to 2, particularly in the lower stratosphere. Inclusion of a realistic representation of the temporal changes in stratospheric sulfate aerosol in a model improves the agreement with the observed trends, but the predicted changes are still smaller than observed. These differences suggest that important uncertainties remain in the ozone changes calculated for an HSCT fleet.

- Model simulations reproduce some, but not all, of the basic features of the distribution of long-lived trace gases in the stratosphere. Since trace gases are the sources of the free radicals that catalyze ozone removal, model-measurement differences reflect inaccuracies in the model transport formulation and affect comparisons of reactive species calculations with measurements.

- Important regions for simulation of atmospheric transport are those with high spatial gradients in long-lived species such as N_2O, NO_y, or ozone. Examples are the regions in the stratosphere between the tropics and subtropics and at the edge of the polar vortices in winter. Aircraft and satellite observations have increased the level of understanding of the gradients and the barriers to transport that create them. In general, the 2-D models used to predict HSCT effects exhibit weak gradients, suggesting that they have too much mixing across these barriers.

- Observations of HO_x, NO_x, ClO_x, and BrO_x in the stratosphere allow direct evaluation of the photochemical destruction cycles of ozone. Above 25 km altitude, observations of HO_x and NO_x free radicals agree with photochemical models to within ~40% when the models are constrained by observed abundances of long-lived chemical species, temperature, aerosol surface area, and overhead ozone column. Observations of chlorine monoxide (ClO) at these altitudes are up to a factor of 2 lower than model predictions. Below 20 km, midday observations of HO_x, NO_x, ClO_x, and BrO_x also generally agree with similarly constrained models to within ~40%. However, HO_x observations exceed model calculations by more than a factor of 3 near sunrise and sunset, times when HO_x concentrations are small. Incorporation of the reaction of bromine nitrate ($BrONO_2$) with H_2O on sulfate aerosols reduces this discrepancy but increases the discrepancy in other species. Between about 20 and 25 km, observations of HO_x and ClO_x radicals are not available to provide a rigorous test of models.

- The observations and modeling of NO_x, HO_x, and ClO_x free radicals in the lower stratosphere agree in showing that the concentrations of HO_x and ClO_x depend on NO_x radicals. When the NO_x concentration is low, such as observed in the lower stratosphere of the Northern Hemisphere during the fall of 1992 and spring of 1993, the HO_x and ClO_x/BrO_x reactions dominate the local ozone loss rates. Thus, according to model calculations, when NO_x from HSCTs is added to these regions, reductions in HO_x and ClO_x/BrO_x abundances generally result in reductions in local ozone loss rates.

- Observations show that PSCs occur during the Antarctic winter and spring and Arctic winter. Heterogeneous reactions on these PSC surfaces activate large fractions of the available chlorine that can then destroy ozone in the presence of sunlight. Widespread ozone destruction does occur in the Antarctic because sedimenting PSC particles also denitrify the stratosphere and alter the buffering of ClO_x by NO_x. The proper inclusion of PSC processes in the 2-D predictive models would reduce an important uncertainty in the HSCT impact results.

6. What are the uncertainties in the atmospheric impacts of HSCT operations?

Several classes of uncertainty are associated with predictions of HSCT impacts made with 2-D models as shown in Table ES-1. Uncertainties in some model parameters can be readily quantified and evaluated directly with the models. Other sources of uncertainty have been identified but not yet quantified. Finally, uncertainty from the possibility of missing processes or major errors in understanding cannot be quantified, but only discussed in terms of the overall confidence in the assessment.

- The only quantified uncertainty in this assessment is that due to uncertainties in gas-phase reaction rate coefficients. These have been propagated through a model to give an estimated uncertainty of ~1% (1-σ) in the calculated ozone column perturbation in the Northern Hemisphere. Uncertainties in heterogeneous chemical reactions and photolysis rates will increase the overall chemical uncertainty. Constraining these results with atmospheric observations will reduce the uncertainty.

- A number of parametric sensitivity tests were performed for processes not included in the basic assessment scenarios. If the combined range of these tests is taken as an estimate of uncertainty, the overall uncertainty due to the processes not included in the basic scenarios is equal to or greater than the reaction-rate uncertainty.

- Uncertainties in microphysics include both the formation of numerous small particles in the HSCT exhaust plume and the possibility of increased denitrification in polar regions due to increases in condensible gases from the HSCT exhaust. Although the numerous small particles in the HSCT plume can indirectly affect ozone loss rates, the particle formation process is poorly understood and the uncertainties are large. Although the likelihood of a significant increase in Arctic denitrification and in polar ozone loss through chlorine and bromine chemistry is small, the implications of such processes for this assessment are large.

- Uncertainties in model transport remain important and difficult to quantify. Observations of seasonally varying and short- and long-lived tracers provide diagnoses of the degree of mixing and rates of transport between tropical and mid-latitude regions of the stratosphere, as well as providing information on residence times for stratospheric trace species.

- The impact of ozone and water vapor from HSCTs on climate was calculated to be within the climatic fluctuations of the model used. Thus, the expected perturbation and its uncertainty are difficult to quantify.

- The possibility of missing processes in the models creates an unquantifiable uncertainty in the HSCT assessment. However, the probability that important processes have been overlooked decreases as we continue to explore HSCT perturbations with models and continue to challenge these models with atmospheric measurements.

7. How can uncertainties in the predicted atmospheric effects of HSCTs be reduced?

Future efforts to reduce the overall assessment uncertainty are expected to focus on the major unquantified uncertainties and attempts to quantify them. The primary methodology for improving our predictive capability continues to involve testing model representations of the atmosphere through comparison with observational data. Substantial progress in that direction will be realized in the near term by systematic comparisons with recent data from the Upper Atmospheric Research Satellite (UARS), the Atmospheric Laboratory for Applications and Science (ATLAS) on the Space Shuttle, and ER-2 aircraft, as well as a host of balloon platforms. Specific additional strategies for addressing the major uncertainties identified in this assessment are listed below in no specific order of priority:

- Extension of the observational database for long-lived tracers and radicals to include a number of seasonal cycles and undersampled regions of the atmosphere, notably the summer high latitudes and tropics.

- Systematic development of 3-D chemical-transport models for testing transport formulations and zonal-symmetry assumptions in 2-D predictive models.

- Inclusion of standardized descriptions of particle formation and evolution in 2-D predictive models and comparison with global aerosol distributions derived from existing satellite and aircraft data.

- Further characterization, through laboratory and atmospheric observations, of the composition and temporal evolution of aircraft exhaust aerosols in the wake/plume regime, and of the composition and microphysics of PSCs.

1995 SCIENTIFIC ASSESSMENT OF THE ATMOSPHERIC EFFECTS OF STRATOSPHERIC AIRCRAFT

INTRODUCTION

The High-Speed Civil Transport (HSCT) is a proposed aircraft that would dramatically shorten intercontinental commercial flights. For example, transit times from Los Angeles to Tokyo would be shortened from over 10 hours to less than 4 1/2 and flights from Los Angeles to Sydney from 14 hours to 7 1/2 hours, including a refueling stop. Such an aircraft might fly at Mach 2.4 (1600 mph) at an altitude of 20 km (65,000 ft), well into the stratosphere where most atmospheric ozone resides.

The ozone abundance in the stratosphere above us is important for three reasons. One is that the amount of ultraviolet radiation from the sun reaching the surface of the Earth depends upon the amount of stratospheric ozone, particularly for the wavelengths that cause sunburn and skin cancer. The concern has been that reductions in the amount of stratospheric ozone might occur as a result of emissions from supersonic airliners and industrial production of long-lived halogenated compounds, thus leading to involuntary exposure of the human population to increased risk of skin cancer. The second reason is that the enhanced ultraviolet radiation at the surface could damage the biosphere, particularly the oceanic plankton which are so vital to the marine food chains. The third reason is that ozone is one of the three atmospheric trace gases (water (H_2O) and carbon dioxide (CO_2) are the others) that largely determine the transmission of ultraviolet, visible, and infrared radiation through the atmosphere, and hence affect climate. Chlorofluorocarbons (CFCs), nitrous oxide (N_2O), and methane (CH_4) are other gases which can affect climate and whose abundances are being affected by human activity.

Figure 1 is a simple schematic of the atmosphere between the ground and 30 km. The sunlight absorbed at the surface produces a rapidly overturning, convective thermal structure in the lower atmosphere, called the troposphere, in which temperature decreases with height. However, above approximately 12-16 km the temperature increases with altitude due to the absorption of ultraviolet sunlight by ozone. This region of permanent temperature inversion is called the stratosphere. Because of this inversion, the stratosphere is characterized by slower removal of injected pollutants. The boundary between the troposphere and the stratosphere is marked by a temperature minimum called the tropopause. Air crosses it in an upward direction in the tropics at an altitude of ~16 km (10 miles), and is dried by the very low temperatures there. Although clouds and rain can remove soluble molecules from the troposphere, they cannot do so in the dry stratosphere except for the special case of the very low-temperature regions occurring during winter over the poles. Air returns to the troposphere at mid- to high latitudes, where the height of the tropopause is 12 km or less.

By the mid-1960s, it was realized that the distribution of ozone in the stratosphere could not be quantitatively understood using only simple photochemistry. Balancing the production of ozone (O_3) from the photolysis of molecular oxygen (O_2) by sunlight with loss via the recombination of atomic oxygen and ozone led to significant overes-

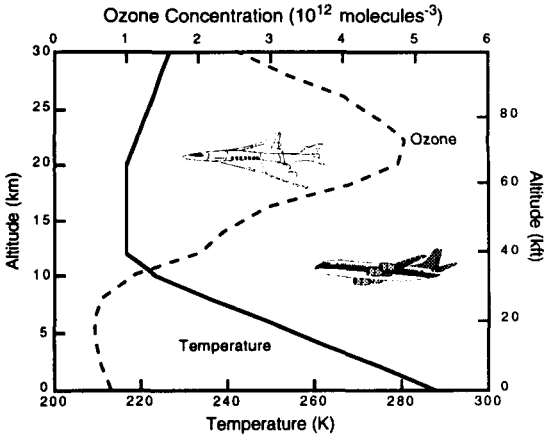

Figure 1. A simple schematic of the atmosphere between the ground and 30 km. Temperature is shown by the solid curve using the bottom scale and concentration of ozone molecules is shown as a dashed curve using the top scale. Both are for mid-latitude conditions from the U.S. Standard Atmosphere [1976]. Typical cruise altitudes for HSCTs and subsonic aircraft are indicated.

timates of the total amount of ozone. In addition, this model could not explain quantitatively why overhead column abundances of ozone observed at high latitudes are larger than in the tropics.

These calculations showed two things. One was the importance of winds in moving ozone from where it is produced in the tropics to the polar regions where it more easily accumulates. The other was that some additional chemical processes must be destroying ozone. It is these processes that make it possible for industrial chemicals to affect ozone, and that together make it a complicated task to produce an assessment of the effects of a specific activity, such as the operation of a fleet of HSCT aircraft.

Missing from the earlier models was the knowledge that certain molecules existing naturally in the atmosphere - such as H_2O and N_2O (produced biologically) - could react with energetic oxygen atoms in the stratosphere to form reactive molecular fragments called free radicals. These radicals, although present in very small amounts, can destroy many ozone molecules by series of reactions in which ozone is consumed but the free radicals are not, a process called catalytic destruction. These series of reactions can repeat many times as long as the free radicals remain in the stratosphere. The free radicals of concern were the hydroxyl radical (OH) and the hydroperoxy radical (HO_2) from H_2O, and nitric oxide (NO) and nitrogen dioxide (NO_2) from N_2O. In 1970 and 1971, it was suggested that the emission of water and NO from a proposed supersonic transport fleet could significantly reduce stratospheric ozone via these reactions.

We will now turn to the question of why the proposed supersonic aircraft might have a much larger effect than subsonic ones, and why the redistribution of chemicals in the stratosphere by the winds is both important and difficult to estimate accurately. The most efficient altitude at which an aircraft can fly is determined by its speed. For a Mach 2.4 aircraft, the optimum cruise altitude is ~20 km (13 miles), well into the stratosphere. Transport of the exhaust products to the troposphere is slow and occurs episodically, so material injected at 20 km stays in the atmosphere for months to years. These long residence times give the emitted exhaust material time to affect the ozone as it is redistributed over the globe by winds.

An important attribute of the chemical and dynamical processes linking aircraft exhaust to ozone concentrations is nonlinearity. In a nonlinear system, relatively small changes may result in complex and sometimes amplified responses. When a system consists, as the stratosphere does, of nonlinear chemistry coupled with nonlinear meteorology, it is possible that the response of the system to perturbations such as aircraft exhausts will be complicated. A good example of a nonlinear response of a system to a small change is that of water just above its freezing point. If the temperature of the system is lowered only slightly, the water will freeze. However, if the system is at room temperature, the same change in temperature does not cause any appreciable effect.

During the 1970s and early 1980s, the focus moved away from nitrogen oxides (NO_x) emitted by aircraft to the effects of chlorine from CFC molecules released from aerosol spray cans and refrigeration systems and also to bromine contained in agricultural fumigants and fire extinguishers. The primary radicals of concern in these cases are chlorine monoxide (ClO) and bromine monoxide (BrO). During this period, it was appreciated that different free radicals are coupled by reactions between members of these families to produce species which were mixed, such as chlorine nitrate ($ClONO_2$), bromine nitrate ($BrONO_2$), and nitric acid (HNO_3). This meant that the response of the stratosphere to aircraft would be complex and would depend on the amount of chlorine in the stratosphere.

In 1985, a vivid demonstration of the nonlinearity of the system became apparent - the ozone hole over Antarctica. It was seen in the historical ozone record only when the stratospheric chlorine content reached a certain value, after which the magnitude of the ozone loss grew rapidly. The explanation was provided by a series of ground-based and airborne observations, later confirmed and put into a global context by satellite observations. The ozone hole chemistry demonstrated that reactions occurring on the surfaces of aerosol and cloud particles consisting of mixtures of sulfuric acid (H_2SO_4), HNO_3, and H_2O are important in the stratosphere. The abundances of these species are

all affected directly by aircraft emissions. A second important feature was that the rate of the primary gas-phase reaction sequence destroying the ozone increased nonlinearly with increasing chlorine abundance.

These events led investigators to examine whether chemistry occurring on aerosol particles could have important effects, not just at the low temperatures over Antarctica and the Arctic during winter, but also in mid-latitudes. In the last five years it has been shown, both in the laboratory and in the atmosphere, that reactions occurring on H_2SO_4 aerosols play an important role throughout the lower stratosphere. The effect of this chemistry is to reduce the calculated amount of NO_x, which destroys ozone catalytically, and to increase HNO_3, which does not. Including this chemistry in models made the calculated impact of aircraft exhaust upon the ozone layer considerably smaller than in earlier calculations.

The effect of the heterogeneous chemistry is not limited to changes in NO_x alone; the coupling between NO_x and the chlorine and bromine chemistry on one hand and between the NO_x and hydrogen oxides (HO_x) chemistry on the other is such that changes in NO_x also induce changes in the free radical abundances in these other chemical families. The close coupling between the chemical families and the large influence of heterogeneous chemistry in the lower stratosphere suggests that emissions from supersonic aircraft engines can affect stratospheric ozone two ways. First, emissions of NO_x can alter all the free radical abundances, thus directly affecting ozone loss. Second, emissions of water vapor and particles can alter the characteristics of the existing aerosols and cloud particles, thus affecting the heterogeneous chemistry and indirectly influencing ozone loss. These effects further underscore the complexity of the stratospheric response to the emissions from supersonic aircraft.

Model calculations suggest that ozone should have decreased from the early 1980s at least in part as a result of the increase in chlorine emissions from 1945 to the present. Such a decrease is evident in the observed mean record of total ozone in northern mid-latitudes in the overhead column over the last 30 years, which is shown in Figure 2 [Bojkov and Fioletov, 1995]. The ozone record in Figure 2

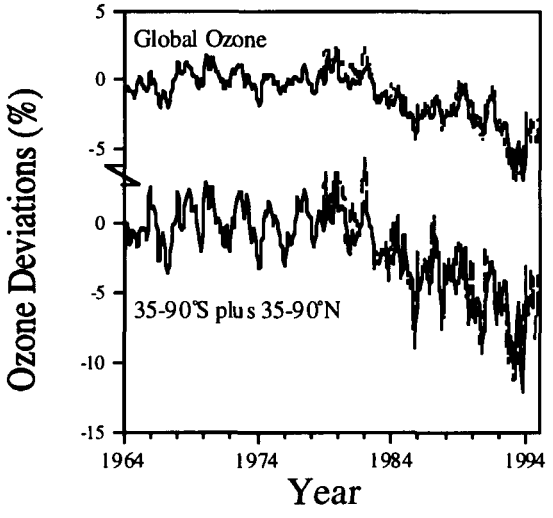

Figure 2. Deviations from the average of the 1964-1980 column ozone level for the global average and for middle and polar latitudes (35°-90°S plus 35°-90°N). Both data sets show a dramatic decline (about 5% for the global average) over the last 15 years. Solid line represents ground-based data (smoothed by a 1-2-1 weight function); dotted line represents TOMS data. Note that the data is plotted against two separate scales on the left axis. [Adapted from Bojkov and Fioletov, 1995]

shows a marked reduction in the last 15 years, the interpretation of which is both a complicated exercise and an important goal. This figure shows many variations that occur naturally and which are the result of the nonlinear chemical and meteorological systems interacting with each other. The disentangling of the causes and effects in this time history is not easy, nor can it alone tell us everything that is needed to understand the system.

This report focuses on calculating the pattern of ozone concentration changes arising from a projected fleet of HSCTs. It pays less attention to climatic effects and none to effects on the biosphere. Such factors have been dealt with at length in the United Nations Environmental Programme/World Meteorological Organization (UNEP/WMO) and Intergovernmental Panel on Climate Change (IPCC) assessments [WMO 1986, 1989, 1990, 1992, 1995; IPCC, 1992, 1995], which also make it clear that the assessment of the effects of HSCTs must be set in a context of parallel effects on the ozone layer arising from CFCs, subsonic aircraft, and increasing amounts of greenhouse gases.

The basic path in the assessment methodology leads from a determination of HSCT fleet operation and emissions, to calculation of the atmospheric distribution of HSCT emissions, and finally to the calculation of steady-state changes in column ozone throughout the atmosphere. The computational tool primarily employed is the two-dimensional (2-D) model, in which the time-consuming complexity of the real three-dimensional (3-D) atmosphere is reduced to more manageable proportions by averaging around latitude circles.

An important source of information used to place the 2-D model results in a realistic context is the set of observations gathered from aircraft, balloons, and satellites; it is an important objective to link the observational perspective with the uncertainties on the numerical estimates. It is important to appreciate that because of this simplification, 2-D models do not adequately simulate all of the features of the atmosphere, either with or without HSCT operations. They are an advance on the one-dimensional (1-D) models used in the assessments made 20 years ago [CIAP, 1975] in that they include seasonal and pole-to-pole variations rather than a representation of a single atmospheric column. The imperfections of the simulations are accompanied within the Atmospheric Effects of Stratospheric Aircraft (AESA) component of the National Aeronautics and Space Administration (NASA) High-Speed Research Program (HSRP) by efforts to provide a description of uncertainties, with the objective of providing a balanced assessment of the current state of predictive ability. A significant portion of text in the main body of this report is devoted to a consideration of the uncertainties in 2-D calculations.

This scientific assessment seeks to describe research performed in the last few years and to help direct efforts that would further improve the ability to quantify and reduce uncertainties. Advances in the knowledge of stratospheric transport, chemistry, and aerosol microphysics are discussed in Chapter 1 along with a brief discussion of observed changes in ozone over the last 20 years. The implication of these advances in understanding are discussed within the context of predicting the effect of stratospheric aircraft, and areas of uncertainty are underlined. Chapter 2 presents and discusses the basic assessment scenarios and the calculations, mostly by two-dimensional models, of HSCT impact. Chapter 3 presents an evaluation of the assessment based on an understanding of how the stratosphere works and how this knowledge is represented in models. Studies of sensitivity to effects not included in the basic assessment are shown. Finally, Chapter 4 summarizes the current knowledge of the potential impacts of HSCTs and discusses the implications of this knowledge, including uncertainties for AESA Phase II.

1 ADVANCES IN ATMOSPHERIC CONCEPTS AND SCIENTIFIC ASSESSMENT APPROACH

1.1 Observations of Stratospheric Ozone

Observations of stratospheric ozone establish a context for conducting the assessment of the effects of HSCTs. Particularly important are the mid-latitude observations taken over the last three decades, as shown in Figure 2 of the Introduction. The total ozone column shows clear variations that are related to physical and chemical processes in the stratosphere. Most important is the overall decline over the last 15 years. Observations of the altitude distribution of ozone shows that this change is greatest below 25 km in the lower stratosphere (Figure 3). This region contains a large fraction of the ozone column. It is a region where gas-phase chemistry, transport, and heterogeneous chemistry on small particles are all important. This decreasing trend, the altitudes of greatest change, and our current understanding of stratospheric chemistry all suggest that at least some of this ozone change is caused by increases in stratospheric chlorine and bromine chemicals.

Shortly after the large injection of sulfur into the stratosphere by Mt. Pinatubo in June 1991, global stratospheric ozone concentrations decreased significantly. For several years following the eruption, values were found to be outside the range of observations made during the 1979-1990 period (Figure 4). Studies suggest that these ozone changes resulted from changes in transport, radiation, and chemistry caused by the enhancement of sulfate aerosol in the stratosphere. Because aerosols are gradually removed from the stratosphere, the large decrease in ozone was temporary, and within two to three years the ozone trends returned to values present before the eruption (Figure 2).

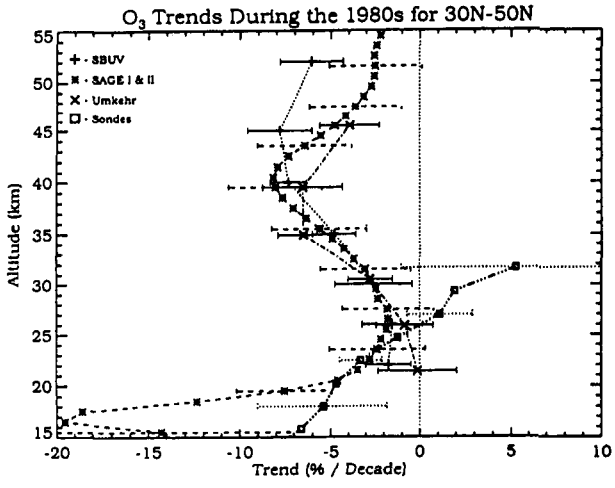

Figure 3. Comparison of trends in the vertical distribution of ozone during the 1980s. Ozonesonde and Umkehr trends are those from Miller *et al.* [1995]. Trends are given in percent per decade relative to 1980. 95% confidence limits are shown. [WMO, 1995]

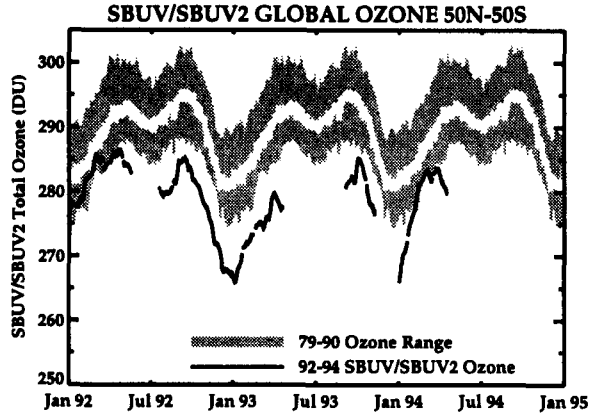

Figure 4. Total ozone measured by SBUV and SBUV(2) since January 1992 compared with the 1980s range and average: 50°N-50°S; global ozone. [WMO, 1995]

The most pronounced ozone changes, i.e., the ozone hole over Antarctica, have been observed at the high latitudes (Figure 5). Ozone losses similar in structure but smaller in magnitude also have been observed over the Arctic in March. These rapid changes result directly from chlorine and bromine catalytic destruction of ozone, but the reduction of the NO_x in these regions, initiated by the presence of particles, is essential for such rapid ozone loss.

Because HSCTs would fly in the lower stratosphere, their exhaust would interact with the processes that caused the observed ozone change. The exhaust of proposed HSCTs will contain CO_2, H_2O, NO_x, carbon monoxide (CO), sulfur dioxide (SO_2), and soot, just as the exhaust from other aircraft do. Understanding the effects of this exhaust on the stratosphere, particularly on stratospheric ozone, requires a detailed knowledge of the aircraft exhaust and the processes that control ozone. Advances in this understanding have come from atmospheric ob-

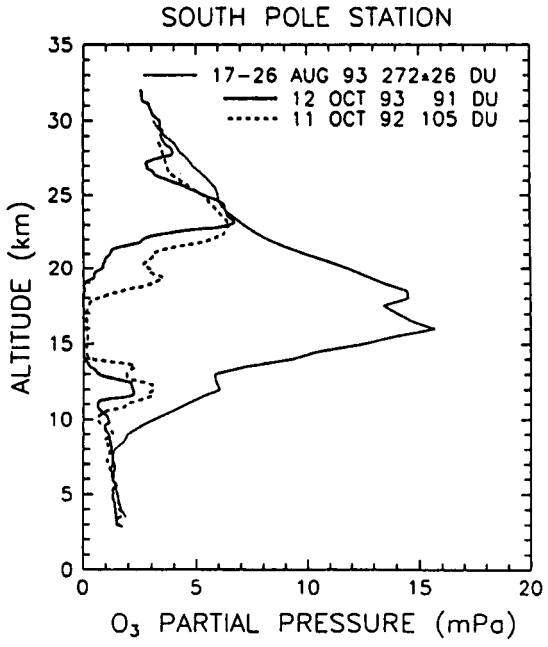

Figure 5a. Comparison of the South Pole pre-depletion ozone profile in 1993 (average of four soundings) with the profile observed when total ozone reached a minimum in 1992 and 1993. [Adapted from Hofmann *et al.*, 1994]

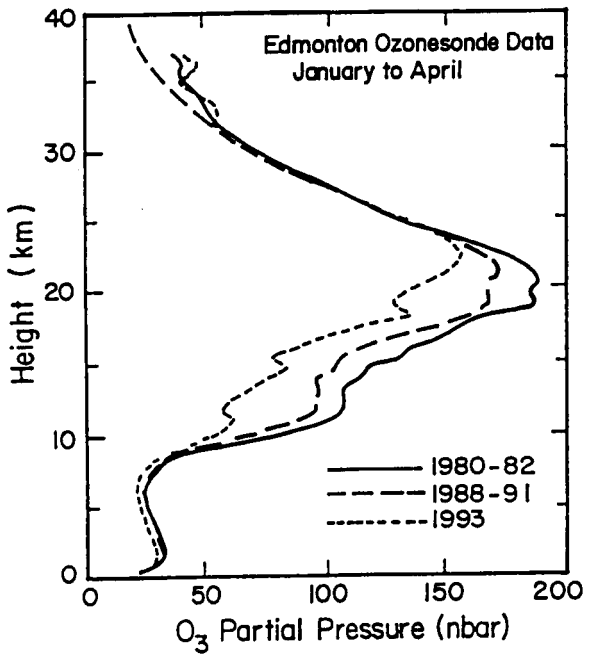

Figure 5b. Average ozone profiles found from ozonesonde measurements of Edmonton in spring (January to April) for 1980-1982 (46 sondes), 1988-1991 (42 sondes), and 1993 (13 sondes). [Adapted from Kerr *et al.*, 1993].

servations, laboratory studies, and model calculations supported by the HSRP. Other research programs participate in this effort, including NASA's Upper Atmosphere Research Program (UARP) and Atmospheric Chemistry Modeling and Analysis Program (ACMAP), and programs at the National Oceanic and Atmospheric Administration (NOAA) and the National Science Foundation (NSF).

1.2 Current Concepts of Stratospheric Processes

A simple view of stratospheric circulation is that air, while circling the globe, enters the stratosphere from the tropical troposphere, slowly ascends, moves from the tropics to mid-latitudes, and reenters the troposphere at middle and high latitudes a few years later (Figure 6). During this transit, sunlight produces ozone from O_2 and also produces, from source gases, those reactive species that destroy ozone. The amount of ozone results from its photochemical production and loss, and transport from regions with different ozone concentrations. In the middle stratosphere above 30 km, production and loss are much faster than transport, so that ozone reaches a steady-state amount for which its production equals its loss. In the lower stratosphere, both chemistry and transport affect the ozone amount as transport processes occur on time scales comparable to those of photochemical ozone production or loss. Photochemical loss of ozone is much smaller than production in the tropics, while at high latitudes photochemical production is much smaller than loss. Thus, ozone

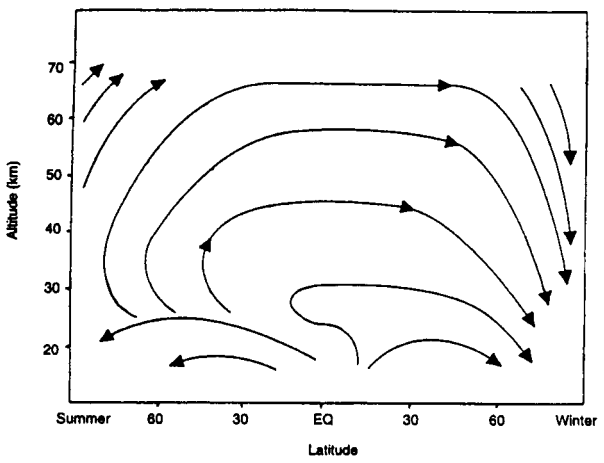

Figure 6. Streamlines associated with Lagrangian-mean velocities for equinoctial conditions. [Dunkerton, 1978]

changes due to HSCTs at any location can result both from local photochemical changes and from changes in the ozone transported to that region.

1.2.1 ADVANCES IN UNDERSTANDING STRATOSPHERIC CHEMISTRY

Ultraviolet sunlight and the ensuing chemistry decompose some gases that enter the stratosphere into chemically active gases. These chemically active gases can be grouped into chemical families. Oxygen atoms and ozone together are called odd oxygen (O_x). The OH and HO_2 reactive species together are called HO_x. The sum of NO, NO_2, and nitrogen trioxide (NO_3) is called NO_x. The sum of NO_x and the more stable gases such as HNO_3, dinitrogen pentoxide (N_2O_5), and $ClONO_2$ is called odd nitrogen (NO_y). The sum of stable hydrogen chloride (HCl), $ClONO_2$, reactive ClO, and other chlorine species is called inorganic chlorine (Cl_y). The sum of reservoir $BrONO_2$, reactive BrO and other bromine species is called inorganic bromine (Br_y). The partitioning, which refers to the fraction of the family found in each of the chemical species, is sensitive to chemical processes. The total amounts of NO_y, Cl_y, and Br_y are sensitive mainly to transport.

Stratospheric ozone is produced primarily through the decomposition of O_2 by solar ultraviolet light. Chemical removal results from chemical destruction by NO_x, HO_x, halogen (ClO and BrO), and atomic oxygen (O) free radicals. Prior to 1990, photochemical models predicted that throughout the middle and lower stratosphere, the NO_x catalytic cycle:

$$NO + O_3 \rightarrow NO_2 + O_2$$
$$O + NO_2 \rightarrow O_2 + NO$$
$$\text{Net: } O + O_3 \rightarrow 2O_2$$

and other NO_x catalytic cycles would dominate the photochemical destruction of ozone from below 20 km to ~40 km altitude. If this was the case, then an increase in NO_x would always result in a decrease in ozone.

Recent free radical measurements in all chemical families demonstrate a different picture. Above 26 km, where somewhat less than half the ozone column resides, the catalytic destruction of ozone can result mainly from the NO_x catalytic cycle [Jucks *et al.*, 1995]. However, in the lower stratosphere below 20 km, the chemistry becomes more complex, the overall ozone removal rate decreases, and the fraction of the catalytic removal by NO_x becomes smaller. In the air masses observed from NASA's ER-2 high-altitude research aircraft in May 1993 during the Stratospheric Photochemistry, Aerosols, and Dynamics Expedition (SPADE), ozone destruction was dominated by reactions involving HO_x, ClO, and BrO (Figure 7) [Wennberg *et al.*, 1994].

Absolute ozone removal rates depend on chemical reactions that couple NO_x with HO_x, ClO_x, and BrO_x. Observations show that the concentrations of HO_2 and ClO are inversely correlated with the concentration of NO_x [Cohen *et al.*, 1994; Stimpfle *et al.*, 1994; Froidevaux *et al.*, 1994]. The inverse correlation is consistent with the understanding of the chemical mechanisms based on laboratory studies. Reaction with NO converts HO_2 to OH; reaction with NO_2 converts ClO and BrO to $ClONO_2$ and $BrONO_2$. In each case, the NO_x reactions suppress

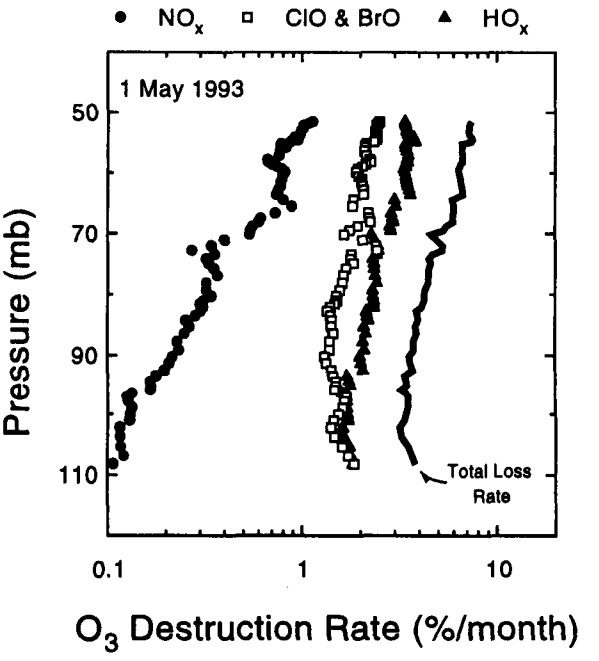

Figure 7. Photochemical removal rates for ozone. Measurements of the concentrations of OH, HO_2, ClO, NO, and ozone obtained on 1 May 1993 are used to infer the ozone removal rates. The HO_x radicals were responsible for more than 40% of the photochemical loss in the lower stratosphere. The catalytic action of the halogen radicals accounted for nearly one-third of the total. [Adapted from Wennberg *et al.*, 1994]

the rate of ozone catalysis; thus, NO_x is critical in determining free radical concentrations and the removal rate of ozone.

Increases in NO_x, such as from aircraft exhaust, can cause either increases or decreases in the local ozone chemical loss rate (Figure 8) [Wennberg *et al.*, 1994]. In regions where HO_x and halogen free radicals dominate ozone loss, increasing concentrations of NO_x decreases the concentrations of HO_x and halogen radicals, and thus the ozone loss rates by HO_x and halogen radicals. For regions of sufficiently large NO_x concentrations, NO_x catalysis more than compensates for the decreases in the HO_x and halogen radical catalysis. In these regions, the local chemical ozone loss increases with increasing NO_x. In the limit where NO_x is driven toward zero, such as can happen in the winter polar stratosphere, ozone loss rates increase by one to two orders of magnitude because nearly all the available chlorine exists as ClO. Thus the preexisting concentrations of ClO, BrO, HO_x, and, in particular, NO_x determine the sign and magnitude of changes in local ozone loss rates that will occur when exhaust NO_x is added.

Photochemical reactions couple NO_x to other members of the nitrogen chemical family, NO_y, such as

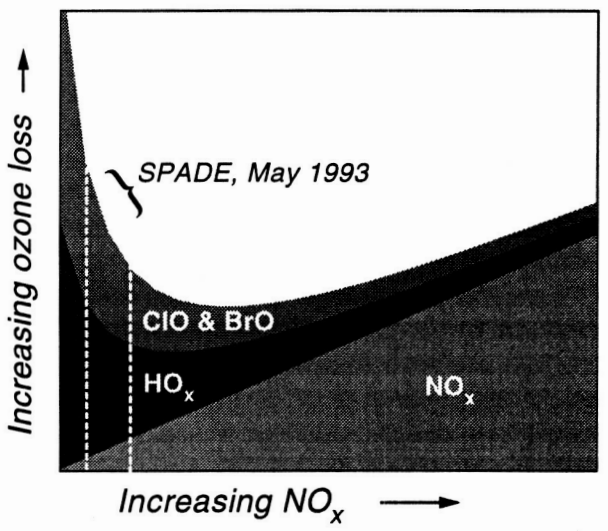

Figure 8. Schematic of the ozone removal rate vs. NO_x. Because of the coupling that exists between the radical families, the response of the total ozone removal rate to changes in NO_x is highly nonlinear. At sufficiently low NO_x such as that observed during the SPADE campaign, the removal rates are inversely correlated with NO_x. [Adapted from Wennberg *et al.*, 1994]

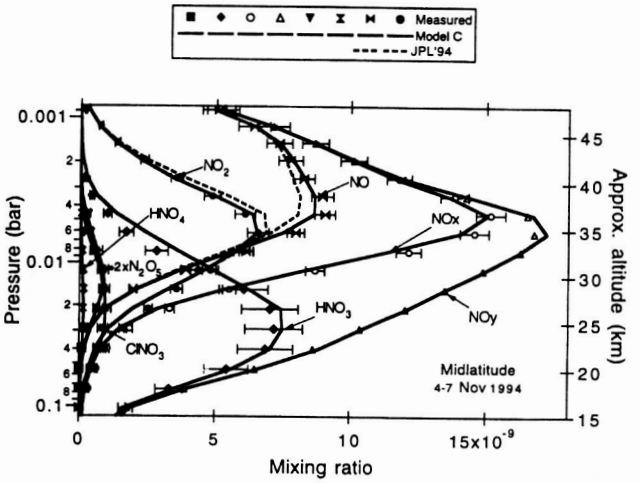

Figure 9. Partitioning of nitrogen oxide species between 18 and 45 km. Symbols represent measurements made by the Atmospheric Trace Molecule Spectroscopy (ATMOS) instrument during the ATLAS-3 Space Shuttle mission. The measurements were made at northern mid-latitudes (40°-48°N) during sunset in the first days of the mission (4-7 November 1994). The lines represent the results of a zero-dimensional photochemical model constrained by simultaneous measurements of HCl + $ClNO_3$, HNO_3 + NO + NO_2 + HNO_4 + $2N_2O_5$ + $ClNO_3$, CH_4, O_3, H_2O, C_2H_6, CO, and temperature from ATMOS and aerosol surface area measurements from SAGE II, assuming a balance between production and loss for each calculated species over a 24-hour period. Model C (solid lines) uses rates for the reactions of Cl + CH_4 and OH + HCl from a reanalysis of laboratory data and allows for a 7% yield of HCl from the reaction of ClO + OH. [Adapted from Michelsen *et al.*, 1995]

HNO_3, N_2O_5, and $ClONO_2$ within hours to weeks. The fraction of NO_y that exists in reactive form (NO_x/NO_y) depends on the amount of solar ultraviolet light (and thus altitude, season, and latitude) and on the surface area of the aerosol particles that provide the sites for heterogeneous chemical reactions. In the sunlit mid-latitudes, the partitioning of NO_y has two distinct regimes (Figure 9). Above ~30 km, NO_x dominates the budget of NO_y; while below, NO_x becomes a much smaller fraction [Michelsen *et al.*, 1995]. Figure 9 also shows comparisons to a photochemical model which are discussed in Section 3.2.3.1.

Over the last few years, laboratory studies and atmospheric observations have led to identification of new mechanisms that partition NO_y. Prior to 1990, the

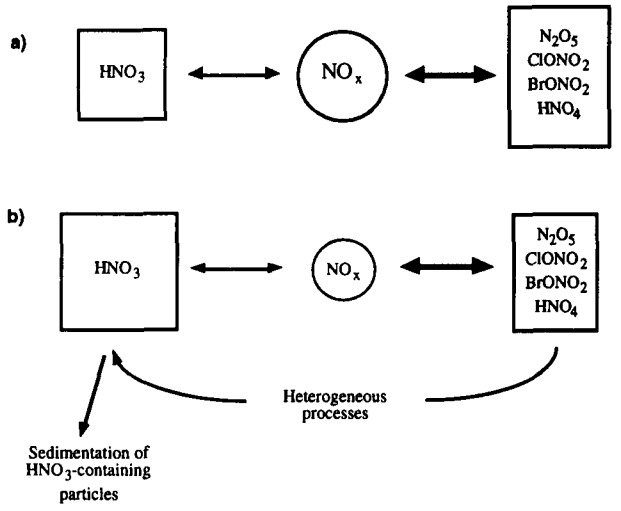

Figure 10. Processes connecting the various NO_y species and NO_x. a) The picture circa 1990, the easily-photolyzed reservoirs of NO_x, such as N_2O_5, $ClONO_2$, $BrONO_2$, and HNO_4, are connected to the much more stable HNO_3 only via gas-phase reactions involving NO_x; b) Recent laboratory and atmospheric measurements demonstrate that heterogeneous reactions directly convert N_2O_5, $ClONO_2$, and $BrONO_2$ to HNO_3 [Mozurkewich and Calvert, 1988; Van Doren *et al.*, 1991, Tolbert *et al.*, 1988; Hanson and Ravishankara, 1993, 1994, 1995; Molina *et al.*, 1987; Williams *et al.*, 1994].

view was that NO_x radicals interconverted with the easily photolyzed NO_y reservoirs such as N_2O_5, $ClONO_2$, $BrONO_2$, peroxynitric acid (HNO_4), and with the much more stable HNO_3, but that no reactions converted one reservoir species to another (Figure 10a). It is now recognized that heterogeneous reactions on particle surfaces existing in the lower stratosphere convert N_2O_5, $ClONO_2$, and $BrONO_2$ directly to HNO_3 (Figure 10b). These reactions indirectly reduce NO_x concentrations by reducing the abundance of easily photolyzed reservoirs and accumulating NO_y as HNO_3. Stratospheric observations in the mid-latitudes provide evidence supporting the conclusions of laboratory studies for N_2O_5 to HNO_3 conversion [McElroy *et al.*, 1992; Fahey *et al.*, 1993; Koike *et al.*, 1994]. An important sink of NO_x is sedimentation of particles containing HNO_3. This process apparently occurs only in polar regions during winter [Fahey *et al.*, 1990; Santee *et al.*, 1995]. The resulting decrease of NO_x affects the chemistry of the polar vortex, and may have some global consequences when the affected polar air mixes with mid-latitude stratospheric air.

Chemical ozone destruction at higher altitudes allows ultraviolet sunlight to penetrate further into the stratosphere. This increased amount of ultraviolet sunlight produces more ozone at these lower altitudes. This effect, called "self-healing," partially compensates for the chemical destruction of ozone, but the net impact still may be ozone loss. This coupling between ozone at different levels means that changes in the local ozone production and loss rates depend on ozone changes at higher altitudes.

These results illustrate several features of the potential effects of HSCT exhaust on stratospheric chemistry:

- NO_x catalytically destroys stratospheric ozone but also inhibits catalytic ozone destruction by the HO_x and halogen radical catalytic cycles through the formation of more stable gases. In the stratosphere above 26 km, NO_x catalysis is the most important ozone loss process; increased NO_x leads to increased local ozone loss. In the lower stratosphere, NO_x interference with the dominant HO_x and halogen catalysis of ozone destruction is more important. For increased NO_x (e.g., from HSCT exhaust), the sign and magnitude of the local chemical ozone change in the lower stratosphere depend on the meteorological conditions and the background amounts of trace gases and aerosol surface area.

- HSCT exhaust would increase the water vapor and sulfur in the lower stratosphere and indirectly influence ozone loss by increasing the amount of sulfate aerosol. An increase in the amount of sulfate aerosol will lower NO_x and thus reduce the direct impact of aircraft-generated NO_x on ozone. The aerosol increase also will lead to increased catalysis of ozone destruction by HO_x and halogens. The net effect of the HSCT exhaust will depend on magnitude of the aerosol surface area changes and the impact of these changes on each of the chemical destruction cycles for ozone.

Local chemical production and loss is not the only means by which ozone is changed. The ozone concentration in a region of the atmosphere is also sensitive to transport of air from adjoining regions. Changes in chemical loss rates by catalysis do not necessarily result in proportional changes in ozone. The ozone concentration in a region is sensitive, not

only to the chemical losses that can occur in that region, but also to the magnitude of the perturbations which have occurred elsewhere in the stratosphere and then propagated to that region by transport.

1.2.2 ADVANCES IN UNDERSTANDING STRATOSPHERIC TRANSPORT

A calculation of zonal-mean mass transport in the stratosphere is shown in Figure 6. The exchange of mass between the tropics and mid-latitudes appears to be restricted at certain altitudes, and may include some transport from the mid-latitudes back into the tropics. In the fall, the rapid cooling and formation of a strong polar wind jet cause polar air to subside many kilometers and leads to the development of a transport barrier between the polar regions and mid-latitudes. Transport of stratospheric air across the tropopause, which determines in part the mean residence time of air in the stratosphere, occurs sporadically when stratospheric air gets folded into the troposphere. The paths of the air parcels and their rate of mixing with other air parcels are important for understanding the response of the stratosphere to HSCT exhaust.

Transport and the dispersal of HSCT exhaust are key issues for understanding the potential effects on stratospheric ozone. An important aspect is that fraction of HSCT exhaust which would be transported from the heavily traveled flight corridors in mid-latitudes to the tropics where it can be lofted to higher altitudes. Subsequent transport back to mid-latitudes would be at altitudes where the NO_x from the exhaust causes increased ozone loss. The degree of isolation between the winter polar vortices and mid-latitudes determines the extent to which chemistry occurring in the vortices, and any change in that chemistry resulting from HSCT emissions, will affect global ozone levels. Thus, the deposition of HSCT exhaust in the lower stratosphere becomes a global issue because of transport.

Recent observations have led to new insights into stratospheric dynamics, and a clearer conceptual picture of transport is emerging. The most powerful of the observations involve simultaneous measurements of suites of long-lived gases, called tracers, with contrasting sources, sinks, and lifetimes in the stratosphere (e.g., N_2O, NO_y, CFCs, CO_2, H_2O, CH_4, CO, ozone, and aerosols). These measurements have been obtained from aircraft, balloon, and satellites. Mixing ratios of stratospheric constituents fluctuate at a fixed location due to reversible horizontal and vertical displacements, but examining changes in one tracer relative to another effectively removes this variability [Ehhalt *et al.*, 1983]. Observations of compact, simple relationships between tracers in the lower stratosphere [Fahey *et al.*, 1989; Woodbridge *et al.*, 1995] (Figure 11) suggest that the surfaces of constant mixing ratio, or "isopleths," are similar for these species if quasi-horizontal mixing is faster than their local chemical lifetimes [Holton, 1986; Mahlman *et al.*, 1986; Plumb and Ko, 1992].

If the observed relationships hold from pole to pole, then the global stratospheric tracer transport would be well represented by the "global diffuser" model (Figure 12a). In this model, transport occurs by the

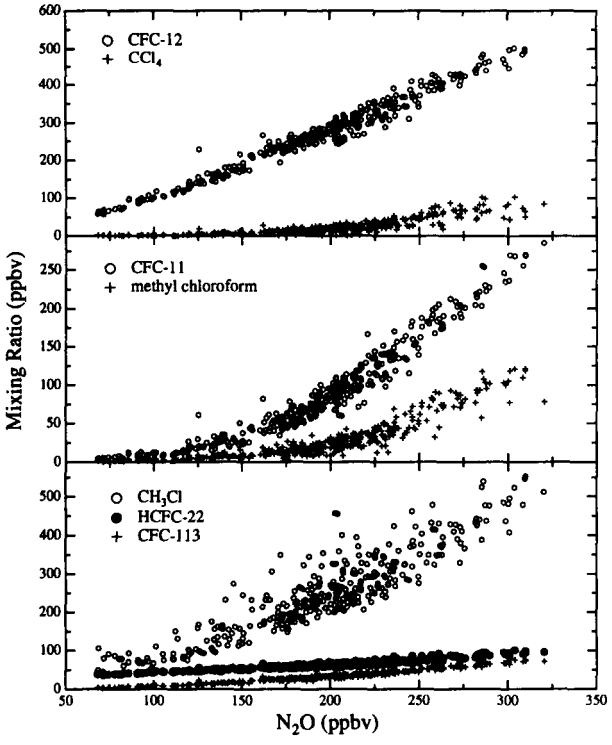

Figure 11. Concentrations of halocarbons in the lower stratosphere from Whole Air Sampler vs. N_2O from the Airborne Tunable Laser Absorption System. These relationships have been discussed for NO_y and N_2O by Fahey *et al.* [1990]. Their theoretical basis is discussed by Holton [1986], Mahlman *et al.* [1986], and Plumb and Ko [1992]. [Adapted from Woodbridge *et al.*, 1995]

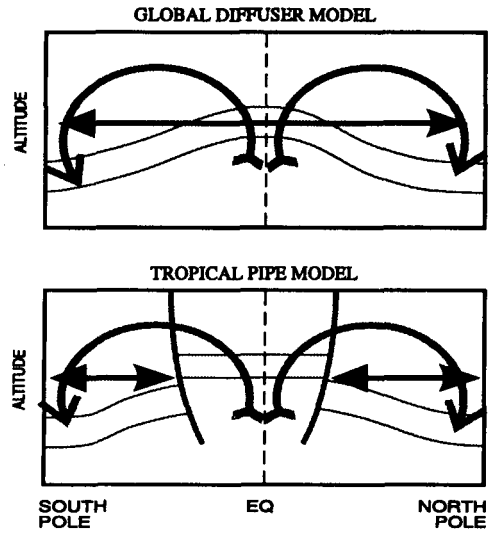

Figure 12. Idealized models for global-scale transport of tracers. a) Global diffuser model, with rapid exchange between mid-latitudes and tropics due to quasi-isentropic mixing in the winter mid-latitude surf zone. b) Tropical pipe model, with vertical advective transport in the tropics, entrainment of tropical air into mid-latitudes, and quasi-isentropic mixing restricted to subtropical latitudes and higher. [Adapted from Plumb, 1995]

simple, mean motions depicted in Figure 6 and rapid mixing from pole to pole along quasi-horizontal surfaces. The result is globally uniform mixing surfaces and therefore globally uniform tracer-tracer correlations.

However, observations showed confinement of Mt. Pinatubo and background aerosols in the tropics [Trepte and Hitchman, 1992; Trepte *et al.*, 1993] (Figure 13); tracer gradients across the subtropics [Randel *et al.*, 1993]; and gradients in ozone, NO_y, and the ozone/NO_y ratio between the tropics and mid-latitudes in the lower stratosphere [Murphy *et al.*, 1993]. These observations led to the idea of a subtropical "barrier" to transport of air from mid-latitudes into the tropics and to the development of another conceptual picture - the "tropical pipe" model (Figure 12b). This model is similar to the global diffuser model except that air can travel across the "subtropical barrier" only from the tropics to mid-latitudes, resulting in tracer-tracer correlations that are significantly different in the tropics than in mid-latitudes.

The atmospheric effects of HSCTs are different in the two concepts. If only the global diffuser model is applicable, HSCT exhaust would freely enter the tropics and be lofted to high altitudes where it would lead to enhanced ozone loss. If only the tropical pipe model is applicable and all upwelling is confined to the tropics, then the middle stratosphere would be largely protected from exhaust products released outside the tropics; changes to atmospheric composition would be largely confined to low altitudes and mid- to high latitudes.

Consistent with aspects of both models, aircraft and satellite observations indicate that air enters the stratosphere in the tropics and indeed is transported rapidly poleward into mid-latitudes up to ~20 km [McCormick *et al.*, 1993; Trepte *et al.*, 1993; Boering *et al.*, 1994, 1995]. The observed propagation of seasonal variations in CO_2 and H_2O implies a vertical ascent rate in the tropics of ~20 meters per day, comparable to that expected from calculated heating rates, and transport to mid-latitudes on time scales as short as one month.

Likewise, the isolation of the tropics from mid-latitude air is not complete and may have seasonal and interannual variations. Analyses of tropical tracer correlations demonstrate that 25 to 40% of air in the tropics at 20 km was transported from mid-latitudes [Avallone and Prather, 1995; Minschwaner *et al.*, 1995]. Thus, the tropical pipe is "leaky," though indications are that the pipe becomes less leaky and the tropics become more isolated at altitudes above 20 km [Michelsen *et al.*, 1995; Mote *et al.*, 1995].

Another critical issue is the residence time of the aircraft emissions, which is determined by the rate at which the emissions are flushed out of the lower stratosphere into the troposphere. The final stage of transport across the tropopause is effected through "tropopause folding" events associated with active upper tropospheric synoptic weather systems. Until a few years ago, it was thought that these processes controlled the overall rate of stratosphere-troposphere exchange, but it is now recognized that the rate of mass exchange is controlled by the large-scale stratospheric circulation [Haynes *et al.*, 1991; Holton *et al.*, 1995]. However, synoptic-scale folding events may be a controlling influence on the residence time of exhaust gases injected into the very low mid-latitude stratosphere (below ~16 km).

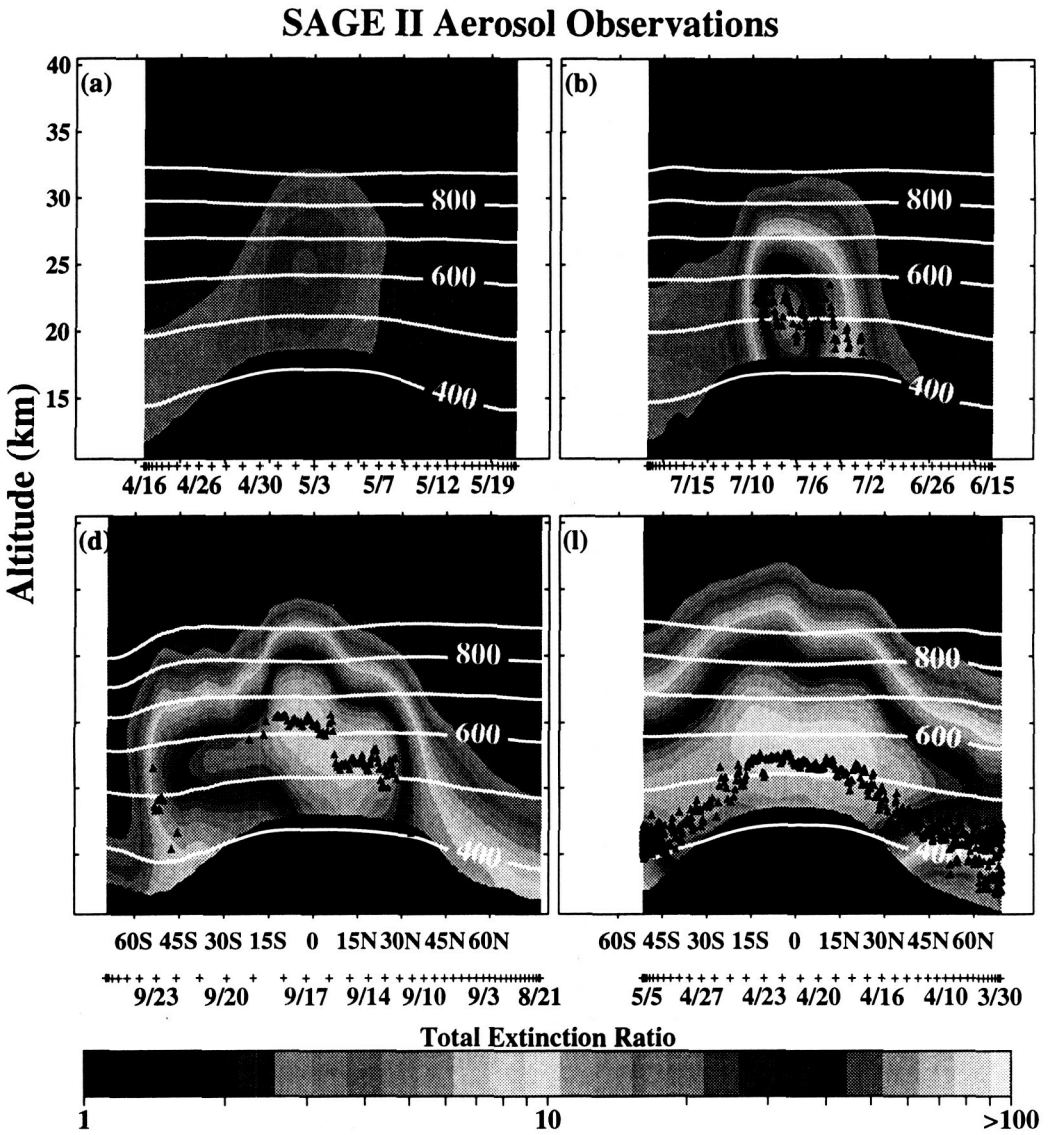

Figure 13. Latitude-altitude cross sections of the SAGE II 1- μm extinction ratio measurements that show the effect of the Mt. Pinatubo eruption in June 1991 on aerosol abundance in the lower atmosphere. The specific observation dates are indicated with crosses below each panel for the periods: a) 15 April to 25 May 1991 (pre-eruption); b) 14 June to 26 July 1991 (early austral winter); d) 20 August to 30 September 1991 (late austral winter); and, i) 29 March to 9 May 1992 (full dispersal). No data were used 2 km below the tropopause (blacked out). Small triangles indicate truncation altitude for the SAGE II data. Lidar data were used below this altitude. Isentropes (constant potential temperature in K) appear as white contour lines. Similar concepts come from observations of UARS data [Randel *et al.*, 1993] and NO_y and ozone by ER-2 instruments in the lower stratosphere [Murphy *et al.*, 1993]. [Adapted from Trepte *et al.*, 1993]

Understanding the transport of air into and out of the polar vortex is also important, since chemical and microphysical processes which occur solely in the vortices may be affected by HSCT exhaust. Recent observations from balloons, aircraft, and satellites suggest that above ~16 km the polar vortices are largely isolated from exchange with the mid-latitudes [Vömel *et al.*, 1995; Mote, 1995; Waugh *et al.*, 1995]. Concentrations of trace species at mid-latitudes are not dramatically affected during winter by transport out of the vortex. However, transport of material out of the vortex in spring and exchange of material near the vortex edge may be important.

Transport controls the dispersal of the HSCT exhaust and thus the concentration of its constituents and its

distribution throughout the stratosphere. Because the abundance of the exhaust constituents and the meteorological conditions of their location dictate the chemical reactions that will occur, transport and chemistry both determine the potential effects of HSCT exhaust.

1.2.3 ADVANCES IN UNDERSTANDING AEROSOL MICROPHYSICS

HSCT exhaust emits condensible gases and particles (aerosols) into the atmosphere. Sulfate aerosols result from the conversion of fuel sulfur to sulfur oxides (SO_x) in the engine combustor, followed by conversion to H_2SO_4 in the expanding exhaust plume or in the free atmosphere and, in turn, growth of preexisting particles or nucleation of new particles. Soot aerosols are a product of incomplete fuel combustion.

Increases in atmospheric sulfate and soot aerosols could affect both climate and chemistry. Sulfate aerosols are primarily scatterers of incoming solar radiation, while soot aerosols are primarily absorbers. Therefore, increases in sulfate and soot may affect the radiative forcing of the atmosphere-Earth system. These aerosols may also impact the formation, and thus the radiative effects, of cirrus clouds. From a chemistry perspective, increased surface area from HSCT exhaust aerosols and condensible gases could change the rates of heterogeneous reactions that alter the stratospheric NO_y partitioning, and consequently the HO_x, Cl_y, and Br_y partitioning.

Advances have occurred in the quantification of aircraft-induced aerosol effects. Measurements show that both soot and sulfate from HSCT exhaust could increase the abundance of small particles in the lower stratosphere. Soot emissions could double or triple the amount of natural stratospheric soot. Because the natural soot loading is only 1% that of sulfate, the potential impact of this increase is unclear. Other observations have shown that significant numbers of persistent small sulfate particles form in the exhaust plume of supersonic aircraft, with appreciable total surface area available for catalyzing heterogeneous reactions [Fahey *et al.*, 1995a]. Sulfur-soot interactions in the near-field region behind the aircraft are possible, such as the activation of soot particles as nuclei for condensation of H_2O and H_2SO_4.

There is a greater understanding of the complex microphysics that occur in the low-temperature atmospheric regions such as the Arctic and Antarctic. Observations of polar stratospheric clouds (PSCs) show considerable variability that is consistent with the complex ternary phase diagram of HNO_3, H_2O, and H_2SO_4 rather than the simpler model of equilibrium nitric acid trihydrate (NAT) thermodynamics. For temperatures above 195 K, the behavior of stratospheric aerosols is consistent with liquid sulfate composition in the range of 50 to 80% H_2SO_4 by weight. At temperatures of ~192 K, both HNO_3 and H_2O can condense to form ternary solution droplets whose composition depends on the ambient HNO_3/H_2SO_4 ratio. The existence of supercooled liquid particles at these temperatures is consistent with earlier *in situ* and remote sensing observations and with laboratory and theoretical studies that predict significant thermodynamic barriers to freezing of both binary H_2SO_4-H_2O and ternary H_2SO_4-H_2O-HNO_3 solutions. Other laboratory studies show multiple metastable solid phases are possible when the solution droplets freeze. Understanding the detailed temperature-dependent behavior of these particles is a key in determining their efficiency in catalyzing heterogeneous reactions and in triggering denitrification, the irreversible removal of NO_y in polar regions. The mechanisms underlying the steep temperature dependence of both microphysical and reaction kinetic processes must be accurately coupled in order to model high-latitude, cold-temperature photochemical cycles.

1.3 Advances in HSCT Emissions Characterization: Measurements in the Plume of the Concorde

During the Airborne Southern Hemisphere Ozone Experiment/Measurements for Assessing the Effects of Stratospheric Aircraft (ASHOE/MAESA) ER-2 campaign in 1994, measurements of NO, NO_y, CO_2, H_2O, condensation nuclei (CN), N_2O, OH, and HO_2 were made in the exhaust plume of a Concorde supersonic aircraft while in flight (Figure 14) [Fahey *et al.*, 1995a]. The emission indices (EIs) were calculated independently of plume dynamics because measurements of CO_2 provide a measure of fuel burned. The observations show:

- The measured EI of NO_x, 23 ±5 grams as equivalent NO_2 per kilogram of fuel burned, is in agreement with the earlier results deduced from

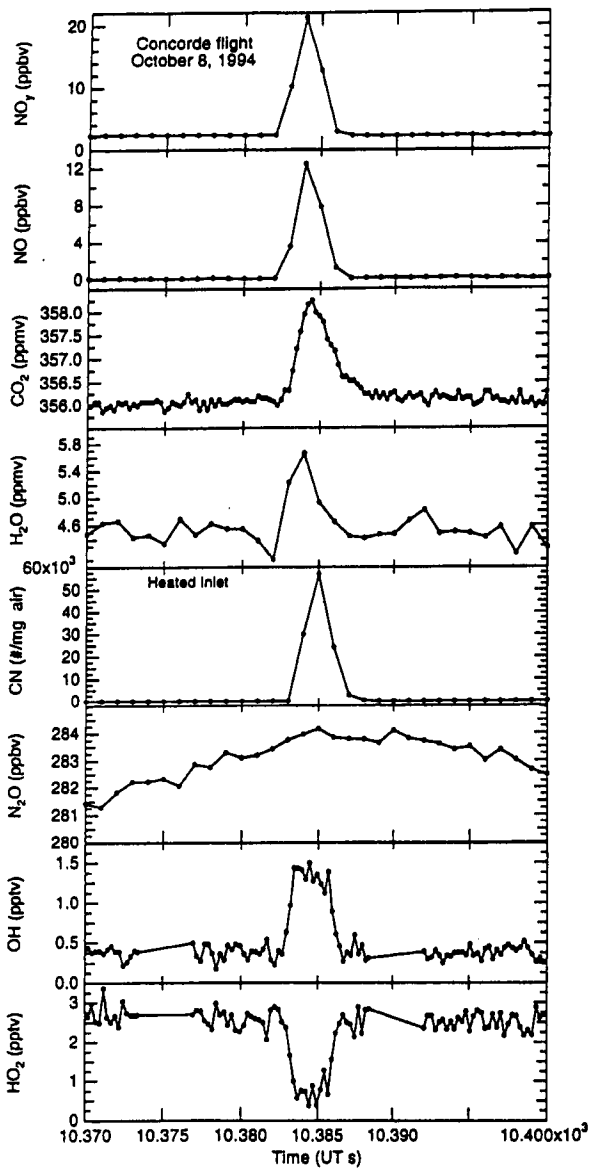

Figure 14. Emissions from an Air France Concorde measured *in situ* from the ER-2 on 8 October 1994. The bottom axis indicates Universal Time (UT). [Adapted from Fahey *et al.*, 1995a]

altitude chamber measurements as part of the Climatic Impact Assessment Program (CIAP). These results suggest that the methodology developed to extrapolate the EI of NO_x at cruise from altitude chamber data will be appropriate to evaluate new HSCT engines.

- No enhancements in CO above stratospheric background levels were observed in the plume. This limits the EI of CO to be less than 3.5 g CO/kg fuel. Provided the combustion efficiency of the future HSCT fleet is no lower than that of the Concorde, CO emissions will be negligible.

- The measurements of OH in the plume suggest that hydroxyl emissions are approximately 3 to 5% of the NO_x emissions and that the OH reacts quickly with NO to form nitrous acid (HONO) [Arnold *et al.*, 1992; Hanisco *et al.*, 1995]. During daylight, the regeneration of OH through HONO photolysis increases OH above background values. The measured OH values suggest that only a small fraction of NO_x (5%) and SO_2 (1%) are oxidized by OH in the plume. Heterogeneous chemistry involving HONO may be important, particularly at night [Zhang *et al.*, 1995].

- The emission index for total particles as measured with a CN counter exceeded 10^{17} (kg fuel)$^{-1}$. Approximately 70 to 90% of these particles were volatile when heated to 192°C. Laboratory studies indicate that the volatile particles are likely sulfuric acid and water mixtures and not soot. The lower size-limit of the CN counter (0.009 μm diameter) implies that between 12 and 45% of the fuel sulfur is oxidized to form H_2SO_4 [Fahey *et al.*, 1995a]. The OH radical is generally assumed to be responsible for sulfur oxidation; however, the level of OH measured in the Concorde plume is consistent with no more than 1% oxidation. These results suggest that sulfur oxidation by OH is not the dominant process in the plume. A suitable mechanism rationalizing the observed degree of oxidation has yet to be identified.

The Concorde plume measurements highlight the issue of particulate (i.e., soot and sulfur) emissions from HSCTs. The potential for the aircraft emissions of H_2O, sulfur, and particulates to change the NO_x/NO_y ratio in both the polar and mid-latitudes may be more significant than the emissions of NO_x. These results heighten the requirement that characterization and understanding of the potential changes in aerosol chemistry be appreciated.

1.4 HSCT Perturbations: The Assessment Approach

The AESA component of NASA's HSRP is designed to assess the potential atmospheric effects of a fleet of HSCT aircraft operating in the stratosphere. As in

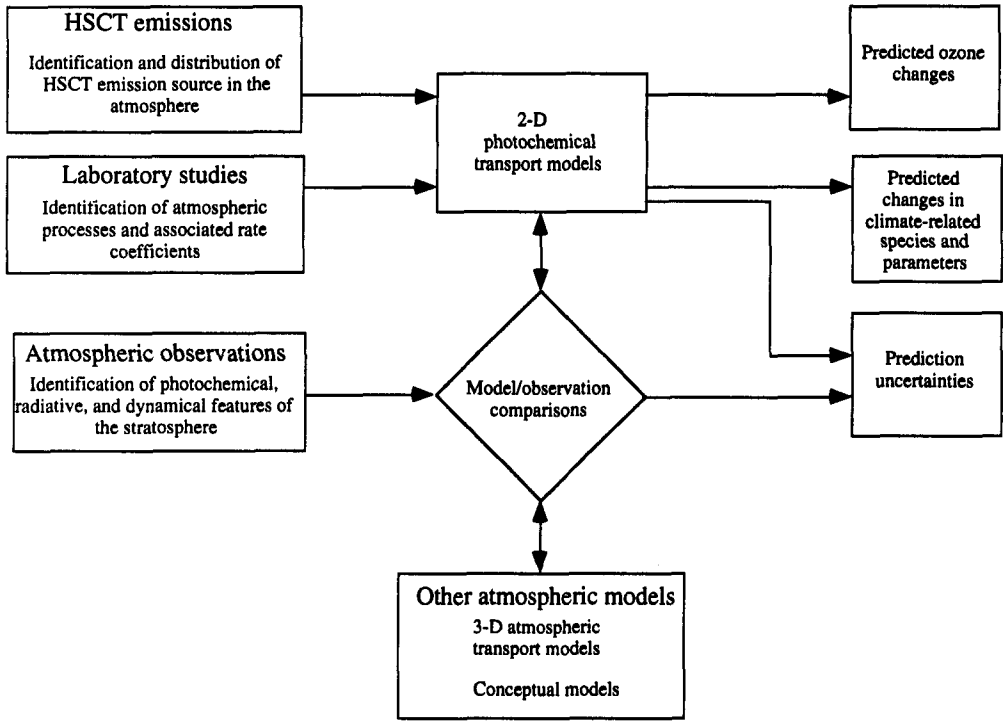

Figure 15. Schematic of the HSCT Scientific Assessment Process.

previous assessments, the current effort emphasizes changes in ozone that could result from HSCT operations, although preliminary studies of changes in climate are also included. As outlined in previous AESA reports [Prather and Wesoky, 1992; Stolarski and Wesoky, 1993a, b, 1995; Prather and Remsberg, 1993; NASA, 1993], significant resources have been devoted to carefully handling the details of the assessment process.

This document describes predictions of the steady-state ozone changes that might result from HSCT operation (Figure 15). The predictions cannot be obtained directly from observations or the concepts outlined in this chapter; they must come from photochemical transport model calculations. 2-D photochemical transport models have been chosen for this task.

The end result of the assessment process is not just the predicted column ozone change or changes in the climate-related chemical species, temperature, and atmospheric dynamics. As important is the statement of the uncertainty in the prediction. The discussion of uncertainties provides the greatest information about confidence in the prediction of ozone change and about advancement in the understanding of stratospheric processes and ozone.

The assessment is based on a large array of tools, of which the 2-D models are one component. Other tools used in the assessment include atmospheric observations, laboratory studies, HSCT emissions inventories, emissions characterization, and a variety of photochemical transport and process models. Atmospheric observations supported under AESA allow many key processes and constituents to be observed directly in the lower stratosphere using specialized instruments on airborne platforms. Laboratory studies have expanded the number of reactions, particularly heterogeneous reactions, that must be considered in the models and have provided measured rate coefficients. Ground-based data sets indicate significant trends in long-lived source gases that are produced in the troposphere and transported to the stratosphere.

An essential part of this process is the comparison of models and observations. These provide the basic understanding of stratospheric processes, the development of conceptual models, and means to test the quality of model performance. Observations have been most usefully compared with process models

that can mimic the meteorological and chemical conditions of the individual observations. However, 2-D and 3-D model results have been compared only in limited cases. Of the advances in understanding outlined above, only some have been included in the 2-D predictive models. Sensitivity tests have been performed for the aerosol effects and transport, but the advances in transport and aerosol effects have not yet been fully implemented.

Particles formed in HSCT exhaust plumes may have an important role in changing global stratospheric aerosol abundances and in increasing the rates of heterogeneous reactive processes. Climatic effects by an HSCT fleet have been recognized as a potential concern, but appear to be small compared to other anthropogenic climate perturbations. Climatic assessments are preliminary and depend on future improvements of the climate models and their application to this issue. The direction and emphasis of the AESA Phase II program will be influenced by the understanding of the relative importance of the ultraviolet and climate effects caused by ozone changes.

The atmosphere is changing. Climate is changing as radiatively active gases are being added to the atmosphere. Stratospheric chemistry is changing as CFCs and thus stratospheric chlorine are reduced. The subsonic aircraft fleet is expected to approximately double in size by the year 2015. The framework that is being developed for this assessment must be robust enough to make confident predictions in the face of atmospheric change.

2 MODEL PREDICTIONS OF HSCT EFFECTS FOR BASIC SCENARIOS

An initial inventory of emissions from an HSCT fleet was given in [Miake-Lye *et al.*, 1992] in the first AESA Program Report [Prather and Wesoky, 1992], which concluded that the nonexhaust emissions are unlikely to affect the chemical content and radiative balance of the atmosphere. The primary emissions (in term of mass emitted) from aircraft are H_2O and CO_2, which are the end products of jet fuel combustion. NO_x (= NO + NO_2), CO, hydrocarbons (HCs), and soot also are produced in aircraft engine combustors and vary in quantity according to the combustor temperature, pressure, and design. Sulfur is present as an impurity in the fuel. For a given engine, the EIs of NO_x, CO, and HCs will vary with the power setting and, thus, will be different for different phases of the flight [ICAO, 1995]. For example, NO_x levels are highest at high thrust (takeoff and climb) and lowest during descent. Table 1 gives typical EIs of the HSCT engines based on the NASA Interim AESA Assessment Report [NASA, 1993] and on a recent Boeing report [Baughcum *et al.*, 1994]. The emission characteristics of Concorde, as measured in an altitude chamber simulating supersonic cruise conditions [CIAP, 1975], are included for comparison. As described in the previous section, recent measurements in the wake of the Concorde flying at supersonic cruise yielded an EI of 23 ±5 g NO_x/kg fuel, which is in agreement with the CIAP results [Fahey *et al.*, 1995a].

The EIs given in Table 1 can be combined with the expected fuel use of an HSCT fleet to give the total emission into the stratosphere. The increase in stratospheric burden of a species can be obtained by using the emitted amount and an estimated residence time of the species in the stratosphere. Table 2 summarizes the estimated range of perturbations from an HSCT fleet with supersonic cruise fuel use of ~50 x 10^9 kg yr^{-1}. The effect from the emitted sulfur may depend on the assumed gas-to-particle conversion rates in the plume (see Sections 3.2.4.3 and 3.2.4.5).

2.1 Description of Fleet Scenarios

In order to assess the potential impact of a fleet of HSCTs, an inventory of the HSCT emissions as a function of latitude and altitude is needed as model input. Two combustor concepts are being evaluated:

Table 1. Typical EIs (in units of grams emission per kilogram fuel) for the Concorde and the projected HSCT engines at stratospheric cruise altitudes.

Species	Concorde	Projected HSCT Engines
Carbon Dioxide (CO_2)	3155	3155
Water (H_2O)	1237	1237
CO	3.5	2.9
NO_x (as NO_2)	18	5-15
Hydrocarbons (HCs)	0.2	0.3
Soot (as carbon)	0.03	0-0.02
Sulfur Dioxide (SO_2)	0.8	0.4

lean, premixed, prevaporized and two-stage rich-burn, quick-quench [see Shaw *et al.*, 1993]. Although full-scale combustors utilizing these concepts have not been built, preliminary measurements suggest that low-NO_x levels can be achieved. However, because of uncertainty in what NO_x EIs can be achieved in future engine designs, the HSCT assessment has been conducted treating EI_{NO_x} as a parameter over the range of 5-15 g NO_x/kg fuel. The EIs for HSCT engines at stratospheric cruise conditions used in the calculations are given in Table 1.

To calculate a 3-D inventory of HSCT emissions, it is necessary to determine the ground rules under which an HSCT would operate (e.g., no supersonic flight over land), identify which cities would be connected via HSCT flights, and calculate the number of flights between each city. These assumptions were based on a forecast of passenger demand in the year 2015. Then, based on the preliminary design of the aircraft and the engine, the fuel burn and emissions were calculated for each flight, placed onto a 3-D grid, and summed to produce the emission inventory for the fleet. For the HSCT assessments, emission inventories were developed on a 1° longitude by 1° latitude by 1 km altitude grid.

For the 1993 AESA Interim Assessment [NASA, 1993], emission inventories were developed for various HSCT fleets (Mach 1.6, 2.0, and 2.4), assuming a passenger demand corresponding to that of a fleet

Table 2. Catalog of potential stratospheric perturbations by HSCT fleet of 500 aircraft.

Emittant	Projected Perturbation	Potential Atmospheric Interactions
Ozone Effects		
NO_x	Peak 50-100% increase [a]	Ozone depletion by NO_x catalysis, interference with ClO_x, HO_x, and BrO_x catalysis
		Conversion to HNO_3, NAT condensation, increased ClO_x catalysis in polar vortex
H_2O	Peak 10-20% increase	HO_x formation and ozone depletion, interference with NO_x catalysis, enhanced ClO_x catalysis
		NAT/ice condensation, denitrification in polar vortex, increased ClO_x catalysis
Sulfur	10-200% increase [b] in surface area	Increased aerosol surface area, enhanced ozone depletion by ClO_x, decreased ozone depletion by NO_x
Soot	Highly uncertain: 0-300% increase	Additional nucleation sites for aerosols, increased surface area-changes in chemical reactivity of aerosols
Hydrocarbons	~0.1% increase compared to CH_4	Source of CO, HO_x, H_2O
CO	5-20% increase	Modification of catalysis by HO_x and NO_x
Radiative Forcing Effects		
CO_2	Current subsonic ~3% of CO_2 from fossil fuel - HSCT ~1%	Direct change in IR radiative forcing
H_2O	Peak 10-20% increase	NAT/Ice condensation, cirrus cloud formation, change in radiative forcing
		Direct change in IR radiative forcing
Sulfur	10-200% increase [b] in surface area	Increased aerosol mass loading, change in radiative forcing
Soot	Highly uncertain: 0-300% increase	Additional nucleation sites for aerosols, increased surface-area change in radiative forcing
NO_x	Peak 50-100% increase	Ozone depletion, change in radiative forcing

[a] Estimated for $EI_{NO_x} = 5$

[b] Depends on assumptions concerning gas to particle conversion in the plume

of 500 Mach 2.4 aircraft. Simple ground rules were used which assumed that the HSCT would capture a constant fraction of the passenger flow between the candidate cities [Wuebbles *et al.*, 1993; Baughcum *et al.*, 1994; Landau *et al.*, 1994]. Subsonic air traffic emissions were also evaluated and displacement of subsonic aircraft by HSCTs was considered explicitly.

Since some routes are more profitable for airlines than others and since the biggest benefit of the HSCT for passengers is the shorter travel time, an HSCT

marketing analysis was completed to take these factors into account. Updated emission scenarios for Mach 2.0 and 2.4 HSCTs were calculated using a Boeing projection of year 2015 passenger demand [Baughcum and Henderson, 1995]. HSCTs were scheduled assuming a universal (i.e., single, world-wide) airline. The fleet sizes calculated were for a very active, high-utilization HSCT fleet and should represent an upper limit of the amount of emissions generated by that number of aircraft. Revised subsonic aircraft scenarios were also developed to be consistent with this HSCT fleet. The new scenarios predict more emissions in the Southern Hemisphere and in the tropics than did the 1993 Interim Assessment scenarios. The total estimated fuel usage for a 500-aircraft, Mach 2.4 fleet in these scenarios is 82 x 10^9 kg per year. Figure 16 shows the percentage of fuel burned at altitudes above 13 km as a function of latitude for a fleet of 500 Mach 2.4 HSCTs. Figure 17 shows the fuel burned as a function of altitude for an all-subsonic fleet and for a modified subsonic fleet plus 500 Mach 2.4 HSCTs in 2015. The NO_x emissions at supersonic cruise altitudes are assumed to be proportional to fuel burned for a constant supersonic cruise EI_{NO_x}.

For the following assessment model runs, the Mach 2.4 HSCT with $EI_{NO_x} = 5$ at stratospheric cruise has been chosen as the standard scenario. Such an aircraft would cruise in the 18- to 21-km altitude range. For an assumption of constant HSCT passenger demand, the studies have shown the

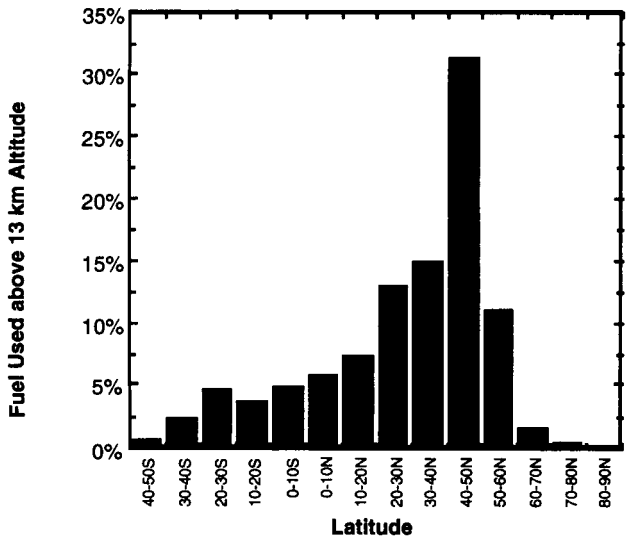

Figure 16. Latitudinal distribution of fuel used above 13 km altitude by a Mach 2.4 HSCT fleet.

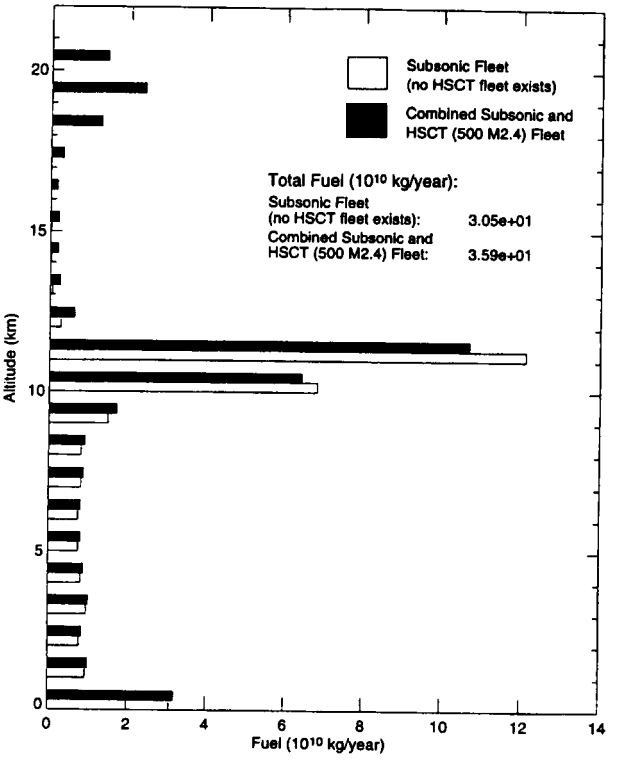

Figure 17. Total estimated fuel burn as a function of altitude for an all-subsonic 2015 fleet and for a 2015 fleet which includes a modified subsonic fleet plus 500 Mach 2.4 HSCTs.

emission levels for a Mach 2.0 fleet to be comparable to the Mach 2.4 fleet shifted to lower altitude by 2 km [Baughcum *et al.*, 1994; Baughcum and Henderson, 1995]. Because of this, the altitude sensitivity has been evaluated in the model scenarios by shifting the Mach 2.4 HSCT emissions by +1 km and -2 km.

In order to evaluate how growth in the HSCT fleet size would affect the geographical distribution of engine exhaust, emission scenarios were calculated by both Boeing [Baughcum and Henderson, 1995] and McDonnell Douglas [Metwally, 1995] for fleets of ~1000 HSCTs. (As a reference point, ~1000 Boeing 747s have been produced over the last 25 years.) The Boeing study was based on a universal airline fleet of 991 active HSCTs. The McDonnell Douglas study used four regional airlines (European, Far East, Americas-east, and Americas-west) to schedule departures of 1059 HSCTs. Both studies used the same baseline aircraft and emission characteristics, but different assumptions about

market penetration and utilization. Thus, while they generated similar amounts of global fuel burned and emissions, some differences in the geographical distribution were predicted. The market penetration model determines the fraction of the HSCT passenger demand between two cities; hence, differences in geographical distribution for a given total passenger demand are due largely to the different market penetration assumptions. For the same model, changes in airline scheduling (e.g., a universal airline vs. four regional airlines) would be expected to modify somewhat the number of HSCTs required to meet the passenger demand but not the total emissions deposited within the stratosphere.

To evaluate the effects of doubling the HSCT fleet size, two model runs (EI_{NO_x} = 5 and 15) were made using the Boeing study. The emissions from the McDonnell Douglas study are sufficiently similar that it was deemed unnecessary to perform a different set of scenarios. The total fuel burned for the HSCT component of this scenario was 157 x 10^9 kg per year, with ~63% between 17 and 21 km.

The 2-D models used the 3-D emission data by summing the emissions within a latitude belt and introducing them into the model grid box representing that latitude belt. This procedure assumes that the emitted materials are instantly mixed zonally. Previous model studies showed that the effects on the calculated ozone changes from adjusting the source function for subsidence of the plume [Rodriguez *et al.*, 1994] and for the nonzonal excursion of the plume before it is zonally mixed [Plumb *et al.*, 1995] are small. The annual amount was put into the model at a uniform rate through the year without accounting for possible seasonal variations in HSCT traffic.

2.2 Description of 2-D Models Used in the Assessment

For the practical purpose of accomplishing long-term simulations for an assessment such as this, approximations are made to reduce computing time. One approach that has proven to be practical is the use of 2-D models that solve systems of equations for zonal-mean quantities. These 2-D models take advantage of the fact that atmospheric transport occurs rapidly around a latitude circle on a time scale of one to two weeks. Thus, they consider only longitudinally averaged or zonal-mean quantities. They include a relatively complete suite of chemicals and reactions as a function of latitude and altitude.

The behavior (as a function of latitude, altitude, and time) of the zonal-mean concentrations of the key chemical constituents are obtained by solving a set of continuity equations. The time rate of change of the concentration of a species at a particular location is given in terms of the changes due to photochemical interactions and transport to and from neighboring locations. A number of inputs are required to specify these quantities. These include boundary conditions at the ground and the top of the atmosphere to specify the exchange rates, chemical reaction rate coefficients and absorption cross sections to calculate the photochemical rates, and the transport fields to specify the transport rates.

The dynamical foundation for describing the transport of the zonal-mean quantities in 2-D models was developed in the 1960s [Murgatroyd and Singleton, 1961; Reed and German, 1965]. These ideas were refined and incorporated into numerical models with chemistry during the 1970s and early 1980s [see review in Tung, 1984]. While all the models that participated in this assessment use some form of residual mean circulation calculated from diabatic heating rates as an approximation to the advective transport circulation for constituents, they differ in the choice of the circulation and eddy diffusion coefficients [see Prather and Remsberg, 1993]. The diabatic heating rates are calculated off-line or taken from published results such as those of Dopplick [1972, 1979], Shine [1987], Rosenfield *et al.* [1987], and Briegleb [1992a, b]. The calculated diabatic heating rates differ from one another because of differences in the assumptions in the radiative code and differences in the background temperatures assumed in the calculation. The 2-D models also differ in their assumptions concerning mixing processes by large-scale eddies (planetary waves) and small-scale processes. Formulations are being developed following Garcia *et al.* [1992] that self-consistently represent eddy processes, but these have not yet been applied to the aircraft assessment.

The set of equations for the different species are coupled because the local photochemical rate for a species depends on the concentration of other species at that location. Even in the 2-D approximation, these integrations take significant computer time. Thus, some of the models employ grouping schemes

Table 3. Models participating in the assessment.

Model	Investigators/Institution
AER	M. Ko and D. Weisenstein, Atmospheric and Environmental Research, Inc. (USA)
CAMED	R. Harwood, J. Kinnersley, Y. Roberts, J. Pyle, University of Edinburgh/ University of Cambridge (UK)
CSIRO	K Ryan, I. Plumb, P. Vohralik, and L. Randeniya, Commonwealth Science Commonwealth Scientific and Industrial Research Organization (Australia)
GSFC	C. Jackman, D. Considine, and E. Fleming, NASA Goddard Space Flight Center (USA)
LLNL/UI	D. Kinnison and P. Connell, Lawrence Livermore National Laboratory/ D. Wuebbles and K. Patten, University of Illinois (USA)

for constituents to reduce the number of equations. Several constituents such as those in the NO_x family are grouped together and the continuity equation with transport terms is solved for the family. The chemical partitioning occurring within the family is calculated under the assumption that a steady state is reached.

The 2-D models that provided results for this assessment are identified in Table 3. With the exception of the Commonwealth Scientific and Industrial Research Organization (CSIRO), the models provided results for the 1993 Interim Assessment Report. Descriptions of these four models were given in that report [NASA, 1993]. However, these models have been modified since then, not only in the chemistry used but also in their treatment of atmospheric processes. These models will continue to evolve as our knowledge of atmospheric processes improves. It is inappropriate to ascribe the differences in ozone predictions in this and previous reports solely to changes in the models, since significant changes have been made in the boundary conditions chosen for the assessment and in the emission scenarios. Brief descriptions of the model changes, together with a full description of the CSIRO model, are given in Appendix A.

Heterogeneous processes on background sulfate aerosols have been shown to play an important role in controlling the chemistry of NO_x, HO_x, ClO_x, and BrO_x which, in turn, control the concentration of ozone in the stratosphere [WMO, 1995]. The effect of such reactions is to reduce the role of NO_x relative to the other ozone catalysts, implying a smaller potential effect of NO_x from HSCT exhaust on stratospheric ozone [e.g., Weisenstein *et al.*, 1991]. All the 2-D predictive models include heterogeneous chemistry on sulfate aerosols in the stratosphere using specified sulfate aerosol distributions. For the assessment calculations, PSCs were not included in the 2-D model runs. With the reduction in the importance of NO_x as a catalyst of ozone depletion, HO_x from exhaust water vapor emissions takes on a larger role. Thus, the 1993 AESA Interim Assessment Report [NASA, 1993] and this assessment emphasize model evaluations of the combined effects of NO_x and H_2O from HSCT exhaust. The current report, however, also discusses other factors that previously were given less emphasis, such as PSC formation (see Section 3.2.4.6) and the effect of sulfur and soot emissions on aerosol loading in the stratosphere (see Sections 3.2.4.5 and 3.2.4.7).

2.3 Model Intercomparisons

Variations among the predictive model results arise from combinations of differences in the model components of transport, radiation, and photochemistry. Two exercises were carried out recently to examine the differences in radiation and photochemistry.

2.3.1 PHOTOLYSIS BENCHMARK

Radiation subroutines within 2-D models usually make approximations to speed up the calculation. During the Models and Measurements exercise [Prather and Remsberg, 1993] and in previous model intercomparisons, differences were discovered among model photolysis calculations even when the cross sections and overhead ozone were specified. For this assessment, a benchmark photolysis calculation has been developed for which several detailed radiation models [Anderson and Lloyd, 1990; Dahlback and Stamnes, 1991; M. Prather, personal communication] have achieved the same answers to within 2%. The benchmark gives us the ability to check directly the precision of the radiation modules used in the 2-D predictive codes. The

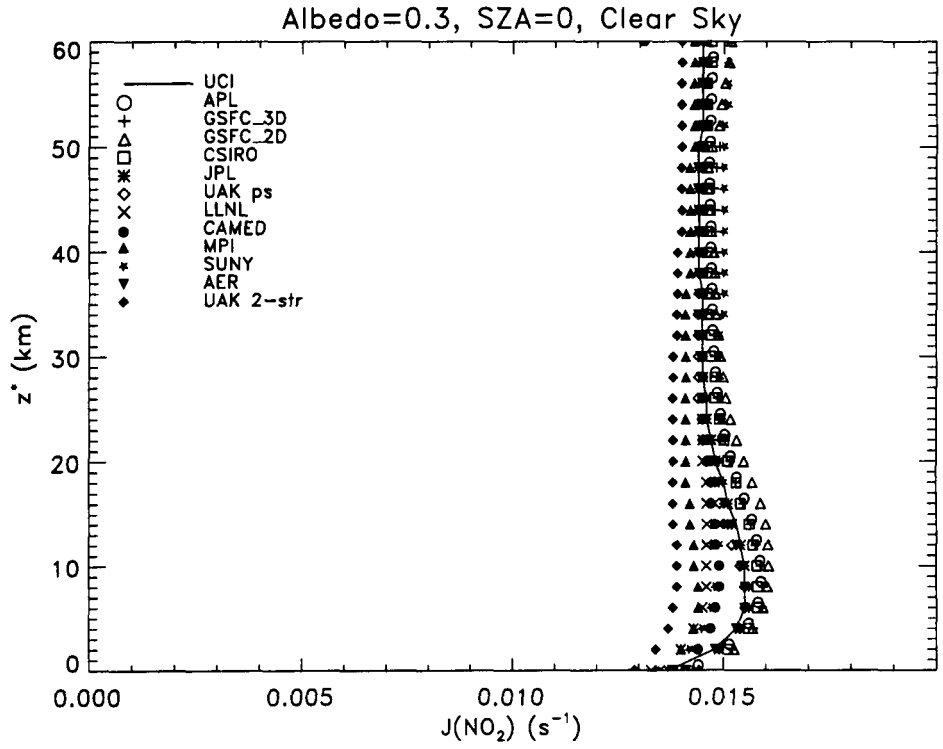

Figure 18. Photolysis benchmark intercomparison for $J(NO_2)$ as a function of altitude for 13 models for a clear-sky calculation at 0° solar zenith angle and ground albedo of 0.3. The solid line is the UCI benchmark. The models with similar values (>0.015 sec^{-1}) in the upper troposphere are multi-stream calculations, while the lower group are two-stream calculations. The AER model used in the runs now includes the UCI code.

initial intercomparisons yielded differences between some of the 2-D model radiation routines and the benchmark. These variations were deemed unacceptable by the 2-D modeling groups, who then upgraded their radiation calculations or converted to a parameterized look-up table derived from a more accurate radiation code. One example of the results of this intercomparison, the photolysis rate for NO_2 as a function of altitude, is shown in Figure 18. The spread of the calculations for this benchmark case is ~±5% in the upper stratosphere. In the lower stratosphere and troposphere, the results fall into two groups: multi-stream calculations with photolysis coefficients peaking at a little over 0.015 sec^{-1}, and two-stream calculations with peak photolysis coefficients under 0.015 sec^{-1}. This is significantly better agreement than in previous intercomparisons.

2.3.2 CHEMISTRY SOLVER BENCHMARK

After considering chemical kinetic theory and practice, numerical accuracy, and computational speed, a variety of photochemistry solution techniques have been chosen by the 2-D predictive model groups. In the same manner as the photolysis benchmark discussed above, a chemistry benchmark calculation was used to identify differences in the steady-state solutions calculated by the different chemistry solvers.

This initial benchmark was defined using a Gear-type integration code with a consensus set of chemical species and reactions common to the majority of the 2-D predictive models using rate coefficients from JPL-94-26 [DeMore *et al.*, 1994]. The chemical code in each 2-D model was used to calculate the constrained-equilibrium concentrations of the radical species with fixed values for ozone; CH_4; H_2O; CO; molecular hydrogen (H_2); and fixed family totals of inorganic NO_y, Cl_y, and Br_y. In the calculation, all models used the same photolysis rates.

Three cases or regions were chosen to represent situations in which different families dominate ozone loss: A) 40 km/2.7 hPa, 65°N, April 11, with fixed

species and families measured or inferred from the Atmospheric Trace Molecule Spectroscopy (ATMOS) measurements outside the polar vortex between April 8 and 14, 1993; B) 20 km/67 hPa, 38°N, May 11 with concentrations from the SPADE aircraft campaign diurnal flights in 1993; and C) 20 km/64 hPa, 59°N, November 4 with concentrations from the ASHOE/MAESA aircraft mission northern survey flight in 1994.

The benchmark diurnally averaged volume mixing ratios for several important radical species were compared to 2-D model results. Models (e.g., CSIRO and the Lawrence Livermore National Laboratory/ University of Illinois (LLNL/UI)), which calculate diurnal coefficients directly using short time steps, agree with a variety of key radicals to within better than 1%. The Atmospheric and Environmental Research, Inc. (AER) model, which also calculates diurnal coefficients directly but with a longer time step to speed up the calculations, agrees with the benchmark to within a few percent for key radicals. The Goddard Space Flight Center (GSFC) model gets somewhat larger differences, from a few percent up to 10 to 15%. This arises from their more approximate approach to calculating diurnal effects so as to obtain sufficient model speed to make many runs.

The benchmark mechanism results have also been compared for region C to the solver module in the photostationary state (PSS) model used by Salawitch and coworkers [e.g., Salawitch *et al.*, 1994a, b] in their studies of aircraft observations. (The photolysis rates used in the benchmark were provided by Salawitch.) Diurnal-average radical concentrations are almost uniformly consistent to within 1% between the benchmark result and PSS solver results with a closely similar mechanism. This begins to provide a connection between the predictive 2-D models and the data now available to evaluate their accuracy.

2.4 Model Predictions of Ozone Response to HSCT Emissions

2.4.1 The Scenarios

A scenario is defined by specifying the boundary conditions for the trace gases in the atmosphere and the emissions from a HSCT fleet. To obtain the ozone change for each scenario, the 2-D model background case is run using the prescribed boundary conditions without any HSCT emissions (but with projected subsonic emissions for the year 2015) until a repeating seasonal cycle is achieved. The perturbed case includes emissions due to the HSCT fleet and subsonic emissions modified to account for subsonic flights displaced by the HSCT fleet. The model calculated change in ozone for the scenario is given by the difference in the calculated ozone distributions between the background and the perturbed cases.

Aircraft emissions of NO_x, H_2O, HCs (as CH_4), and CO were included in the calculations. Some of the assessment scenarios were developed to evaluate the sensitivity of the effect of HSCTs to changes in the background atmosphere (e.g., background chlorine amount), and changes in the HSCT fleet (e.g., changes in altitude of injection, EI_{NO_x}, and fleet size). In most scenarios, the trace gas concentrations in the background atmosphere are those predicted to be appropriate for 2015. In particular, the ground-level concentrations of CFCs were specified to give a stratospheric mixing ratio for Cl_y = 3 parts per billion by volume (ppbv), consistent with the projected concentration given in WMO [1995]. The bromine concentration is assumed to be at 19 parts per trillion by volume (pptv) [WMO, 1995]. Additional calculations were performed for Cl_y = 2.0 ppbv corresponding to the chlorine level for 2050, and 0.6 ppbv corresponding to the natural background. Variations in the HSCT fleet include different values of EI_{NO_x} (0, 5, 10 and 15), different cruise altitudes, and different fleet size.

Background aerosol surface areas, assuming relatively little volcanic activity, were as given in the lower limit case specified in WMO [1992] and were assumed not to be perturbed by the aircraft operation. The sensitivity of the HSCT ozone perturbations to ambient sulfate aerosol loading is discussed in Section 3.2.4.4. Effects from emitted sulfur compounds (due to fuel impurities) are discussed in Section 3.2.4.5.

For the calculations, all models used the chemical reaction rate coefficients and photolysis cross sections recommended in the most recent Jet Propulsion Laboratory (JPL) review [DeMore *et al.*, 1994]. The runs did not include the heterogeneous reaction of $BrONO_2 + H_2O$ or any consideration of PSCs. Calculations on the effects of $BrONO_2$ hydrolysis

Table 4a. Calculated steady-state total column ozone change (%) in the Northern Hemisphere averaged over a year for the basic assessment scenarios.

Scenario					Model				
	Mach Number	Cl_y (ppbv)	EI_{NO_x} (g NO_2/kg fuel)	Number of Aircraft	AER	GSFC	CSIRO	LLNL/ UI	CAMED
I.	2.4	3	0	500	-0.3	-0.3	-0.2	-0.1	—
II.	2.4	3	5	500	-0.3	-0.07	-0.2	-0.3	+0.08
III.	2.4	3	10	500	-0.4	+0.0	-0.3	-0.5	-0.4
IV.	2.4	3	15	500	-0.7	-0.02	-0.5	-0.9	-1.0
V.	2.4 Cruise +1 km	3	5	500	-0.4	-0.2	-0.3	-0.5	+0.02
VI.	2.4 Cruise +1 km	3	15	500	-1.2	-0.3	-0.9	-1.4	-1.4
VII.	2.4 Cruise -2 km	3	5	500	-0.04	+0.03	+0.0	-0.06	+0.1
VIII.	2.4 Cruise -2 km	3	15	500	-0.03	+0.2	+0.08	-0.1	-0.3
IX.	2.4	2	5	500	-0.4	-0.2	-0.3	-0.4	+0.02
X.	2.4	2	15	500	-1.0	-0.3	-0.7	-1.2	-1.2
XI.	2.4	0.6	15	500	-1.5	-0.7	—	—	—
XII.	2.4	3	5	1000	-0.6	-0.2	-0.4	-0.7	+0.03
XIII.	2.4	3	15	1000	-1.9	-0.6	-1.4	-2.1	-2.7

and PSCs are discussed in Sections 3.2.3.2 and 3.2.4.6, respectively.

2.4.2 CALCULATED CHANGES IN COLUMN AMOUNT OF OZONE

Analysis of the results from these updated models confirm the previous finding that the effect on ozone from the emitted CO and HCs (as CH_4) is small. Sensitivity calculations from the National Center for Atmospheric Research (NCAR) model [Tie *et al.*, 1994] show that the effect in the model of the emitted HC, when treated as nonmethane hydrocarbons (NMHCs), is also small.

Table 4a gives model-calculated steady-state ozone changes for a number of basic assessment scenarios relative to the all-subsonic aircraft cases, averaged over a year for the Northern Hemisphere, while Table 4b gives calculated changes for a latitude band between 40°N and 50°N. The basic HSCT fleet was the Mach 2.4, 500-aircraft fleet with EIs of 0, 5, 10, and 15 g NO_x/kg fuel burned (scenarios I through IV). The EI_{NO_x} = 0 case represents the effects from HSCT H_2O emissions in the absence of interference from emitted NO_x. For the EI_{NO_x} = 0, 5, and 10 cases, all of the models calculated ozone depletions in the Northern Hemisphere of ≤0.5%. The calculated ozone depletions generally increase with larger EI_{NO_x}. All the models, except GSFC, calculated a Northern Hemisphere total ozone decrease of between ~0.5 and ~1% for EI_{NO_x} = 15. Figure 19 shows the calculated ozone column change in the 40 to 50° latitude band as a function of EI_{NO_x}. Note that while most models show a similar response to changes in EI_{NO_x}, the gradient calculated by the University of Cambridge/University of Edinburgh (CAMED) model is much steeper.

The effect of changing flight altitudes is shown in Figure 20. Scenarios V and VI are cases where the Mach 2.4 fleet was assumed to be cruising 1 km higher in altitude than in the basic scenarios. The results for EI_{NO_x} = 5 were more negative than the basic scenario. For EI_{NO_x} = 15, most models calculated depletions of greater than 1%. The results shown for scenarios VII and VIII are for calculations in which the Mach 2.4 fleet was assumed to cruise 2

Table 4b. Calculated steady-state total column ozone change (%) between 40°N and 50°N averaged over a year for the basic assessment scenarios.

Scenario					Model				
	Mach Number	Cl_y (ppbv)	EI_{NO_x} (g NO_2/kg fuel)	Number of Aircraft	AER	GSFC	CSIRO	LLNL/ UI	CAMED
I.	2.4	3	0	500	-0.4	-0.3	-0.3	-0.1	—
II.	2.4	3	5	500	-0.3	-0.05	-0.2	-0.3	+0.2
III.	2.4	3	10	500	-0.5	+0.07	-0.3	-0.6	-0.4
IV.	2.4	3	15	500	-0.8	+0.06	-0.5	-1.0	-1.2
V.	2.4 Cruise +1 km	3	5	500	-0.5	-0.2	-0.4	-0.6	+0.09
VI.	2.4 Cruise +1 km	3	15	500	-1.3	-0.2	-1.1	-1.6	-1.5
VII.	2.4 Cruise -2 km	3	5	500	-0.03	+0.07	+0.04	-0.06	+0.2
VIII.	2.4 Cruise -2 km	3	15	500	-0.01	+0.3	+0.2	-0.2	-0.2
IX.	2.4	2	5	500	-0.4	-0.2	-0.3	-0.4	+0.07
X.	2.4	2	15	500	-1.1	-0.3	-0.8	-1.4	-1.4
XI.	2.4	0.6	15	500	-1.7	-0.7	—	—	—
XII.	2.4	3	5	1000	-0.7	-0.2	-0.5	-0.7	+0.1
XIII.	2.4	3	15	1000	-2.2	-0.6	-1.6	-2.3	—

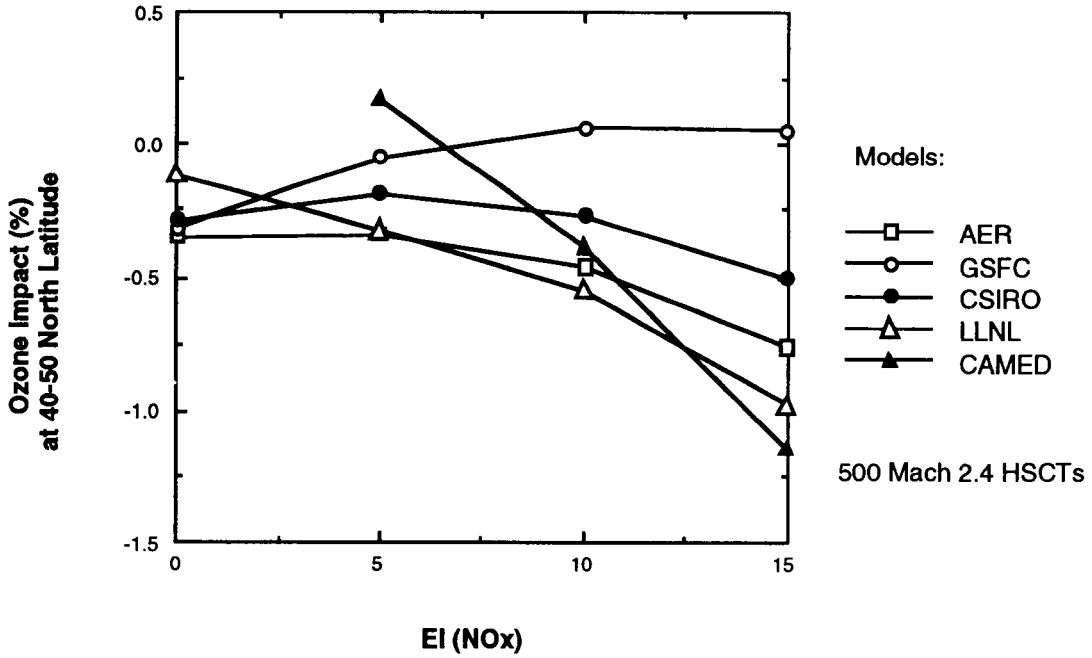

Figure 19. Predicted column ozone change (%) in the 40° to 50°N latitude band as a function of EI_{NO_x} for a fleet of 500 Mach 2.4 HSCTs.

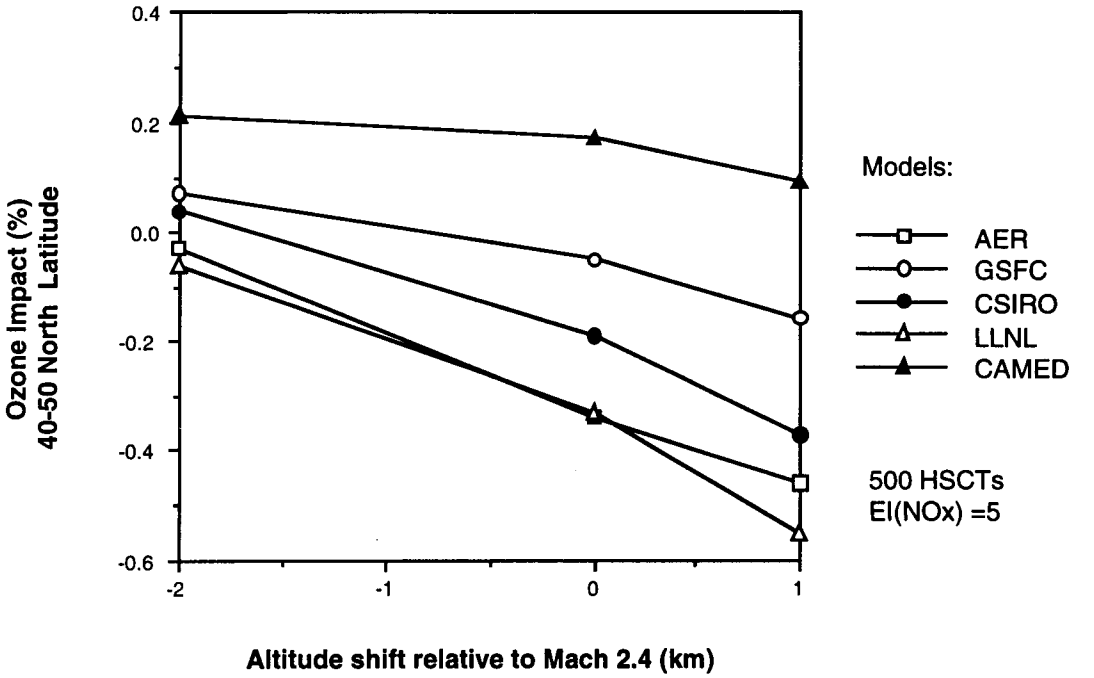

Figure 20. Predicted column ozone change (%) in the 40° to 50°N latitude band as a function of altitude displacement from the Mach 2.4 base case, assuming 500 HSCTs with $EI_{NO_x} = 5$.

km lower in altitude than the basic scenario, simulating a Mach 2.0 fleet. In these cases, all models calculated very small (≤0.3%) depletions for both $EI_{NO_x} = 5$ and 15. This demonstrates the strong sensitivity of the effects of NO_x to altitude. All the models show a similar dependence on flight altitude.

The effect of decreasing chlorine was tested by running the Mach 2.4 fleet with $EI_{NO_x} = 5$ and 15 and a background chlorine amount of 2 ppbv (expected to be reached in ~2050), and the $EI_{NO_x} = 15$ case with $Cl_y = 0.6$ ppbv (scenarios IX through XI). As expected, the models calculate a more negative perturbation as the chlorine background decreases because of reduced interference between the ClO_x and NO_x cycles. The calculated globally and annually averaged ozone de-pletion varies linearly with the Cl_y concentration and is more negative for smaller Cl_y.

Scenarios XII and XIII are for the double Boeing fleet described in Section 2.1. The increased perturbation over the basic Mach 2.4 fleet calculations for $EI_{NO_x} = 5$ is nearly linear, except for the GSFC and CAMED models which started with a result near zero. The perturbation increase is greater than linear for $EI_{NO_x} = 15$. Note that the calculated depletion for the double fleet at $EI_{NO_x} = 5$ is greater than for the $EI_{NO_x} = 10$ case with the smaller fleet. This is primarily because the mature fleet is not just a doubling of the flights in the same corridors, but includes a higher percentage of flights crossing the tropics where the exhaust is more readily lofted to high altitudes. Another difference is that the double fleet at $EI_{NO_x} = 5$ emits twice the water vapor as a fleet of 500 HSCTs with $EI_{NO_x} = 10$.

Figure 21 shows the calculated depletion in column ozone as a function of latitude for each model for the month of March. All of the models show a greater calculated ozone change near the poles than at low latitudes. There is significant variation in the latitude dependence because the various models have a different crossover point in altitude from ozone increase in the lower stratosphere to ozone decrease in the middle and upper stratosphere (see Section 2.4.3). At 60°N, the model-calculated ozone changes for the $EI_{NO_x} = 15$ case range from near zero for the GSFC model to -1.3% for the LLNL/UI model. For $EI_{NO_x} = 5$, the range is from -0.1% to nearly -0 .5%. The model-to-model variation is less in the Southern Hemisphere.

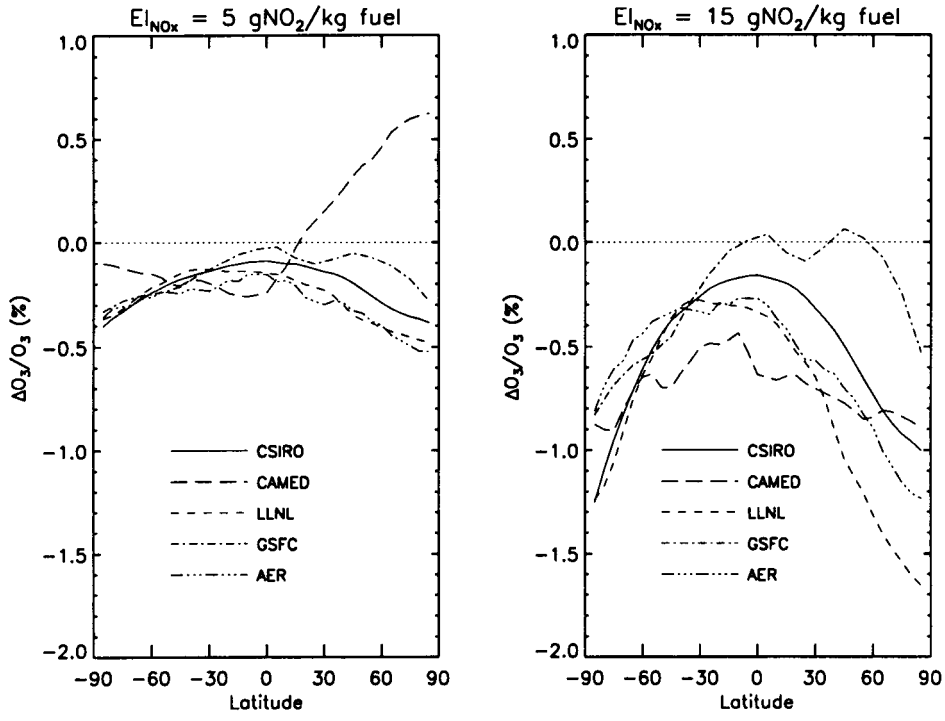

Figure 21. Calculated column ozone change (%) during March as a function of latitude for a Mach 2.4 HSCT fleet from the several models; a) EI_{NO_X} = 5 g NO_2/kg fuel, and b) EI_{NO_X} = 15 g NO_2/kg fuel. The changes reflect the difference between a calculation of the projected 2015 supersonic and subsonic fleets and the projected 2015 subsonic fleet in the absence of a supersonic fleet.

2.4.3 CALCULATED LOCAL CHANGES IN OZONE CONCENTRATION

The above discussions represent a brief overview of the column integrals of ozone change. The change in ozone column is made up of a calculated decrease in the middle to upper stratosphere and a calculated increase in the lower stratosphere and troposphere. The balance between these increases and decreases is dependent on the dispersion of the aircraft effluent by atmospheric transport processes as well as the transport of long-lived species, including ozone, in the background atmosphere. An example of the dispersion of aircraft-generated NO_x (converted to NO_y), calculated by the AER model, is shown in Figure 22. All of the models used in this study obtained similar total amounts of perturbed NO_y, but showed differences in its distribution with altitude and latitude. The calculated added amount of NO_y in the HSCT-perturbed atmosphere corresponded to a residence time of 13 to 16 months. Figure 23 shows the corresponding calculation of ozone change as a function of latitude and season from the AER model for EI_{NO_X} = 5 and 15 g NO_2/kg fuel. The residence time for exhaust gases and the photochemical response time of ozone in the lower stratosphere imply that the perturbation would decrease to less than half its value in a few years if HSCT operations in the stratosphere were to cease.

Figure 24 compares the calculated change in ozone concentration as a function of altitude from 5 models at 45°N for the Mach 2.4 EI = 5 case. All of the models predict ozone depletion at altitudes above 24 km, while most of the models predict ozone increase between 14 and 20 km. With the exception of the CAMED model, the models predict relatively small contributions to the integrated ozone column due to their treatment of tropospheric processes. To isolate the changes that are the result of changes in the subsonic fleet, an extra model scenario was run in which the emissions above 13 km altitude were assumed to be zero. The models obtained ozone changes of 0 to -0.03% relative to the subsonic-only case. This demonstrates that the tropospheric emissions from supersonic aircraft and the change in subsonic emis-

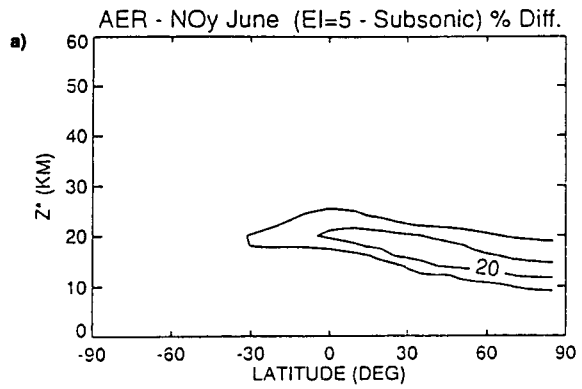

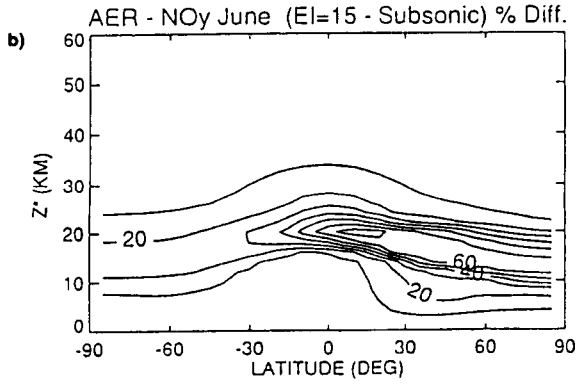

Figure 22. Calculated change in the total odd nitrogen (NO_y) concentration during June (in percent) as a function of latitude and altitude for a Mach 2.4 HSCT fleet from the AER model; a) EI_{NO_x} = 5 g NO_2/kg fuel, and b) EI_{NO_x} = 15 g NO_2/kg fuel. The changes reflect the difference between a calculation of the projected 2015 supersonic and subsonic fleets and the projected 2015 subsonic fleet in the absence of a supersonic fleet.

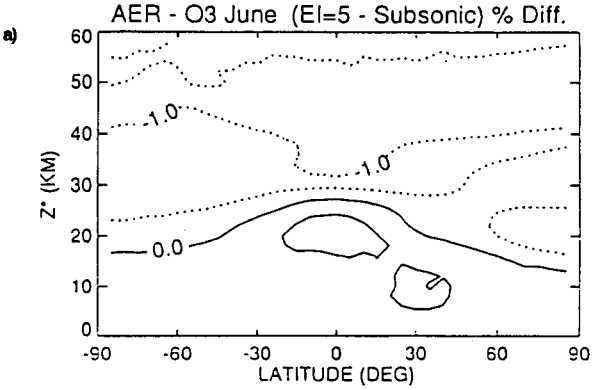

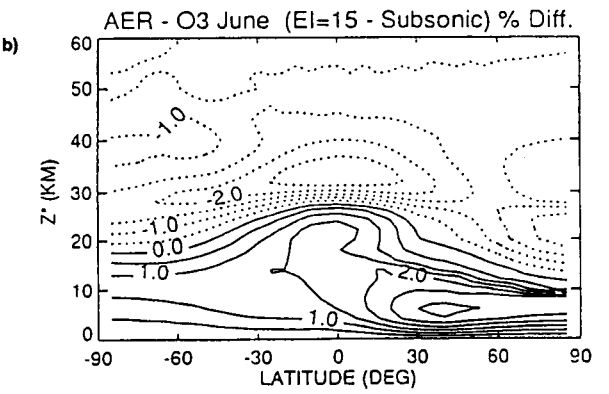

Figure 23. Calculated change in the ozone concentration during June (in percent) as a function of latitude and altitude for a Mach 2.4 HSCT fleet from the AER model; a) EI_{NO_x} = 5 g NO_2/kg fuel, and b) EI_{NO_x} = 15 g NO_2/kg fuel. The changes reflect the difference between a calculation of the projected 2015 supersonic and subsonic fleets and the projected 2015 subsonic fleet in the absence of a supersonic fleet.

sions in the HSCT scenario are small effects on column ozone.

Ozone profiles as a function of altitudes calculated by the models are very similar at altitudes above ~26 km (see Figure 25). Between approximately 16 and 26 km, the calculated ozone profiles show a wider spread of results. This is a critical region for understanding the HSCT perturbation and is the altitude band where the variations between models of HSCT impact at 45°N latitude were greatest. These differences in ozone concentrations in the lower stratosphere are, at least in part, due to transport effects. Partitioning of the chemical families is a function of the ozone concentration (see Section 3.2.3.2). The differing background ozone amounts in the models will thus lead to different chemical sensitivities to added NO_x.

Figure 26 shows the percentage of ozone loss in the background atmosphere due to each catalytic cycle as a function of altitude and latitude calculated in a representative 2-D model (LLNL/UI) for March. Catalytic destruction due to NO_x is one of the significant background atmospheric ozone loss mechanisms in the middle and upper stratosphere. In

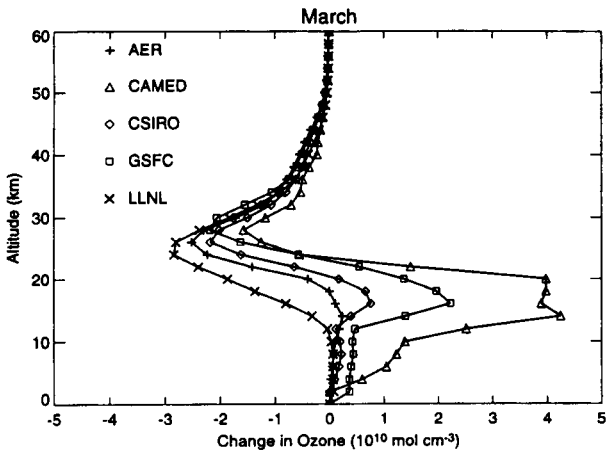

Figure 24. Calculated change in ozone concentration as a function of altitude for a fleet of 500 Mach 2.4 HSCTs (EI_{NO_X} = 5). The results are shown at 45°N latitude for the month of March.

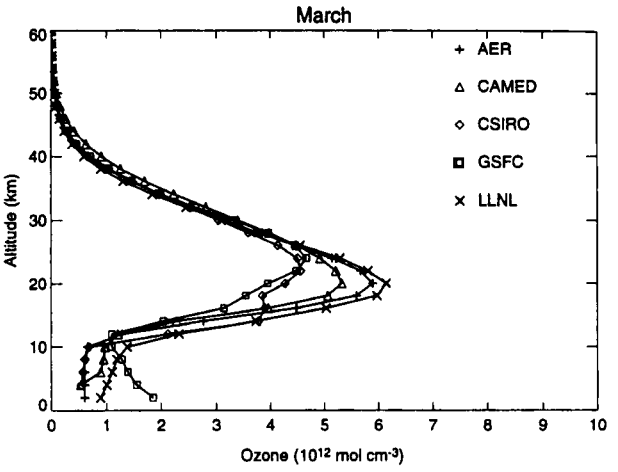

Figure 25. Calculated ozone concentrations as a function of altitude for the 2015 all-subsonic scenario (Cl_y = 3 ppbv). The results are shown at 45°N latitude for the month of March.

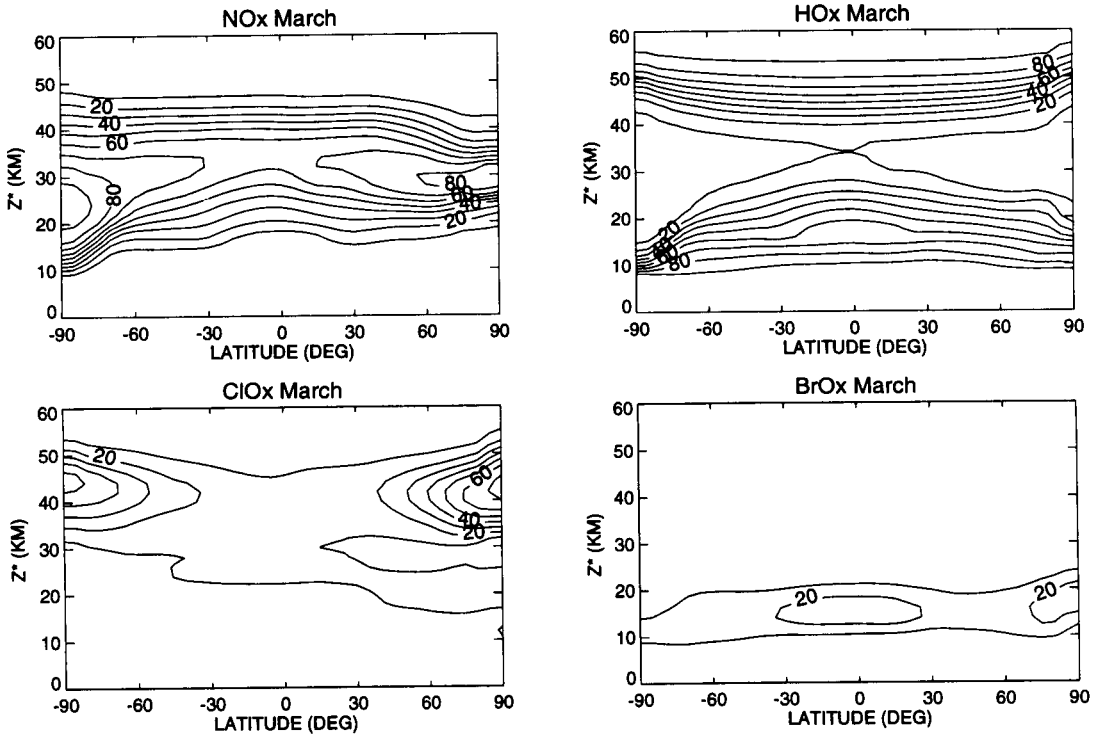

Figure 26. Percentage of ozone loss rate due to each catalytic cycle as a function of latitude and altitude for March in the 2015 atmosphere without HSCTs from the LLNL model: NO_X, HO_X, ClO_X, and BrO_X. BrO_X chemistry does not include hydrolysis of $BrONO_2$ on aerosols. Reactions involving bromine and chlorine molecules are classified as BrO_X. Reactions involving chlorine and nitrogen are classified as ClO_X. Reactions involving nitrogen and hydrogen are classified as NO_X.

the lower stratosphere, NO_x catalysis is a minor mechanism and loss is dominated by HO_x catalysis with significant contributions from ClO_x and BrO_x. Similar calculations for the other models yield qualitatively similar results. They do, however, differ in detail. Some of this can be attributed to variations in the dynamics that yield differing background concentrations, while part can be attributed to variations in the counting schemes used to assign O_x loss to each chemical family. When rate-determining steps for catalytic cycles are used, several differing assignments for O_x loss can be made which yield equivalent results.

One analysis that can be made is the change in catalytic cycles as NO_y and H_2O are added from the aircraft exhaust. Figure 27 shows the CSIRO model-calculated change in the loss term from each catalytic cycle when the aircraft perturbation is added for EI_{NO_x} = 15 during March. The quantity plotted is $-100 \cdot (L_{NO_x}(\text{pert}) - L_{NO_x}(\text{base}))/L_{\text{total}}(\text{base})$ for the NO_x term in the upper left panel and the equivalent terms for the HO_x, ClO_x, and BrO_x cycles in the other panels. In the region below 20 km, the added NO_x and H_2O each interfere with both the HO_x and the NO_x cycles, causing a partial cancellation of the negative effects of the NO_x cycle. Nearer to the pole, the BrO_x cycle interferes with the negative NO_x perturbation.

The model results show that there is no simple spatial correspondence between changes in NO_y and changes in production and loss. The portion of the added NO_y that is transported to the tropics above ~25 to 30 km altitude leads to a large change in ozone removal rate. This is because the sulfate aerosol surface area decreases at higher altitudes, and photolysis of HNO_3 is faster in the tropics and at high altitudes, leading to an increase in the NO_x/NO_y ratio and, therefore, an increase in the sensitivity to

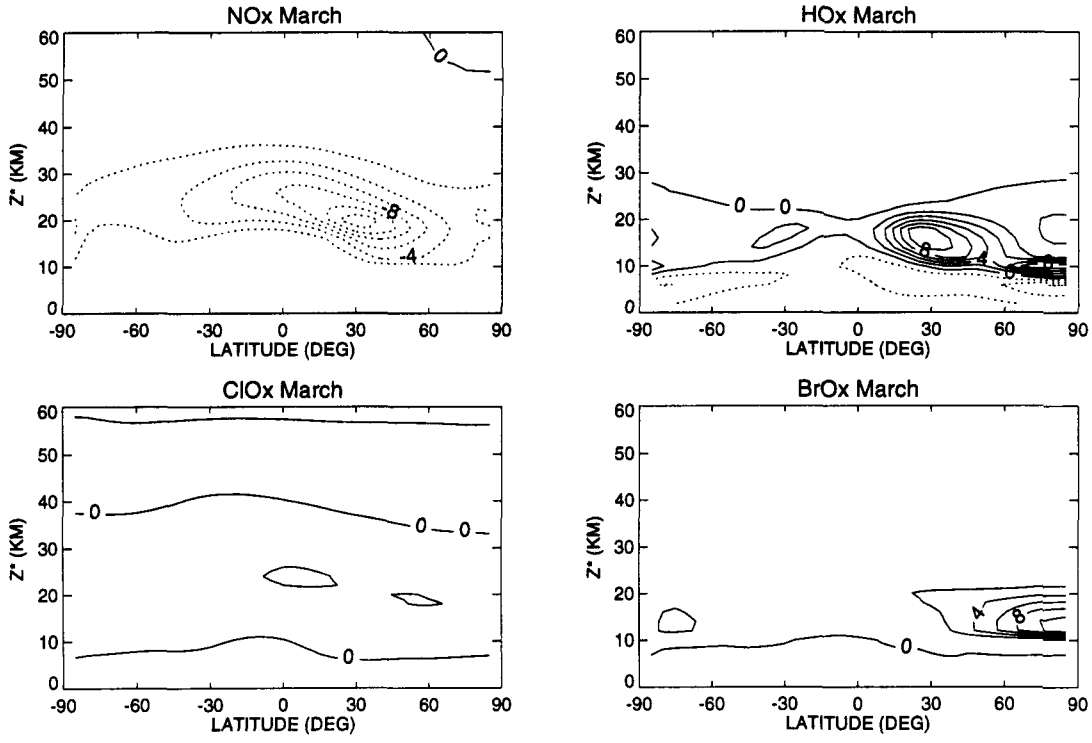

Figure 27. Change in loss term for each catalytic cycle divided by total chemical loss term (in percent) for March from CSIRO model. Changes are calculated for EI_{NO_x} = 15 g NO_2/kg fuel: change in NO_x loss term, change in HO_x loss term, change in ClO_x loss term, and change in BrO_x loss term (not including $BrONO_2$ hydrolysis). Reactions involving bromine and chlorine molecules are classified as BrO_x. Reactions involving chlorine and nitrogen are classified as ClO_x. Reactions involving nitrogen and hydrogen are classified as NO_x.

NO_x perturbations. The NO_x catalysis reactions proceed in this region with less interference from the HO_x, ClO_x, and BrO_x reactions. The locations of large ozone depletions are not necessarily coincident with locations of large changes in the local photochemical terms. In the lower mid-latitude stratosphere, the models generally calculate a decrease in ozone (in percent) in spite of a small decrease in the local ozone removal rate. The ozone depletion that the models calculate in the lower mid-latitude stratosphere is the result of chemical losses which occurred at lower latitudes and higher altitudes and transport. The ozone-depleted air from the tropical middle stratosphere has then been transported downward and poleward, yielding the calculated ozone decreases in the area of the flight corridors.

2.5 Model Predictions of the Effects of HSCT Emissions on Climate Forcing

Potential HSCT climate effects result from the direct injection of CO_2, H_2O, soot, and sulfur. Indirect effects on climate are derived from the exhaust effects on ozone, cirrus formation, and background sulfate aerosol concentrations. The direct effect of CO_2 from HSCTs is expected to be small relative to that from fossil fuels because, at the present time, the projected HSCT fleet emissions of CO_2 are less than ~0.3% of the emissions from all fossil fuel combustion.

Regional climate changes that may follow from a increased climate forcing cannot be predicted at this time. A common approach to estimating the relative importance of various atmospheric changes to climate is to determine the difference in stratospheric radiative forcing at the tropopause. Lacis *et al.* [1990] showed that the radiative forcing due to changes in ozone is sensitive to the vertical distribution of the projected ozone changes, with a maximum forcing sensitivity per unit ozone occurring in the lower stratosphere and upper troposphere. Thus, the calculated changes in ozone shown in Section 2.4 have potential for affecting climate.

Rind and Lonergan [1995] used the low-resolution Goddard Institute for Space Studies (GISS) middle-atmosphere 3-D general circulation model (GCM) to predict the climate effects of the projected ozone changes calculated by the GSFC 2-D model. The GSFC model predicted ozone increases of up to 1% between 15 and 30 km in the tropics and decreases between 30 and 50 km, with a maximum decrease of 2.5% varying from 25 km at the poles to 35 km in the tropics for a Mach 2.4 fleet with EI_{NO_x} = 15 (similar to that shown in Figure 23). This profile change leads to a net positive forcing and, in the GISS model, produced a predicted global-average surface-temperature change of +0.025°C. Because the standard deviation of annual average temperatures in the GISS control run was 0.25°C to 0.34°C, depending on the length of integration, this predicted change is not statistically significant. The predicted surface temperature change was small, partly because the effect of the tropospheric ozone increase offset the effect of the stratospheric ozone decrease.

However, at high latitudes the projected 2015 ozone change that was used had smaller tropospheric increases. Thus the thermal forcing was more consistently negative and, combined with amplified climate feedbacks due to sea ice and dynamical changes, a relatively consistent reduction of a few tenths of a degree occurred for the surface air temperature. This value is still smaller than the natural interannual variability in either the model or surface observations; its significance will depend on model sensitivity and the ozone forcing used.

In the stratosphere, the ozone reductions predicted by most models, on the order of a few percent, resulted in *in situ* temperature reductions of a few tenths of a degree, while dynamical changes produced additional effects of up to ±1°C. The dynamical changes resulted from a decrease in vertical stability as the stratosphere cooled. Once again, these changes are smaller than the model or observed interannual variability [Rind and Lonergan, 1995; Shah *et al.*, 1995], although they were fairly consistent.

Another calculation by Rind and Lonergan [1995] was an idealized perturbation of H_2O (i.e., an increase of 0.2 parts per million by volume (ppmv) everywhere in the stratosphere). This calculation produced results that were inconsistent during a 50-year simulation. In one five-year average a warming of 0.06°C was found, while in a second a cooling of -0.07°C was found. Within the statistical fluctuations of their model, the resultant surface

temperature perturbation is not significant. They also tested the model sensitivity to changes in stratospheric H_2O by assuming a uniform increase from 3 to 6 ppmv. This calculation resulted in a consistent surface temperature warming of 0.24°C. It is not clear at this time whether longer simulation times would yield consistent perturbation predictions for the smaller perturbation in water vapor.

In the stratosphere, the increase in water vapor generally produced cooling of a few tenths of a degree, although dynamical changes associated with the decreased vertical stability and an increase in residual circulation of <5% produced some regions of greater effects. These changes are smaller than model or observed interannual variability [Rind and Lonergan, 1995; Shah *et al.*, 1995], but once again were somewhat persistent.

One interesting aspect of these perturbations, as highlighted by Rind and Lonergan [1995], is the fact that the climate sensitivity due to changes in the altitude distribution of radiatively important species can be different from the climate sensitivity derived from CO_2 experiments. The climate sensitivity is defined as the change in global-average surface temperature for a given radiative forcing at the tropopause. They found a reduced sensitivity relative to that calculated for a CO_2 forcing in both the ozone and H_2O perturbations. They traced the result to the altered response of high clouds in their model to the changes in dynamical stability in the case of ozone, and to the radiative forcing gradient in the case of H_2O perturbation. High clouds increase in CO_2 perturbations, thereby increasing their contribution to the greenhouse effect. In both the ozone and H_2O perturbations, high clouds either decreased (H_2O) or increased less than anticipated for a similar forcing by CO_2 (ozone), creating a smaller sensitivity to the same forcing. This result should be viewed with caution, because different models will respond differently to the various radiative perturbations (e.g., for typical GCMs, climate sensitivities due to a doubling of CO_2 vary between 1.5 and 4.5°C). However, it introduces the possibility that results may depend on the specific scenario introduced and that the results of different types of radiative perturbations may not be simply additive [compare Taylor and Penner, 1994]. Based on the results of Taylor and Penner [1994], it also may be important to sort out the effects of hemispheric differences in radiative forcing due to aircraft emissions.

The direct radiative and climatic effects of increased concentrations of sulfate aerosols and soot have not been assessed. However, the simulations of Weaver *et al.* [1995] for NO_y can be used to estimate their possible radiative effects. Weaver *et al.* [1995] used the 3-D GSFC chemical transport model (CTM) to simulate the distribution of NO_y for a Mach 2.4 scenario with EI of 5 g NO_2/kg fuel. The stratospheric residence time for both sulfate aerosols and soot should be similar to that calculated for NO_y, although small differences will occur because of the fall velocities of the aerosols. The concentration of sulfate or soot aerosol is then given by the ratio of EIs scaled by the appropriate molecular weights. For EIs of 0.4 g SO_2/kg fuel and 0.02 g soot/kg fuel, this scaling leads to maximum vertical column concentrations of 3×10^{-4} g m^{-2} for sulfate and 10^{-5} g m^{-2} for soot extending over a broad latitude belt from 40°N to 75°N in January. The numbers obtained by this simple scaling for sulfate are a factor of ~4 larger than those calculated by Weisenstein *et al.* [1995] in their 2-D model. Assuming specific extinction cross sections for visible light of 10 m^2 g^{-1} gives total optical depths for sulfate and soot of only 0.003 and 0.0001, respectively. These perturbations to aerosol optical depth are less than one-tenth and one one-hundredth, respectively, of the global-average perturbations due to tropospheric anthropogenic sulfate aerosols, and are much smaller than the peak optical depths for the Mt. Pinatubo volcanic aerosol which was +0.3. Thus, the radiative perturbations from sulfate and soot emissions are expected to be small if these estimates are accurate. Additional work is needed to define more precisely the expected sulfur and soot concentration changes and their calculated climatic impact, as well as their potential to act as cloud CN in the lower stratosphere/upper troposphere.

The final aircraft climate issue concerns the effect of H_2O emissions on possible contrail formation in the stratosphere. 2-D models predict an increase of approximately 0.8 ppmv H_2O at latitudes of maximum flight frequencies. Such loading might increase stratospheric water vapor to ~4-6 ppmv near 53-90 mbar. Using average temperatures of -56 to -58°C at these heights, saturation mixing ratios with respect to ice are 100 to 400 ppmv. Thus, in an average case the dry stratosphere would ensure that widespread

formation of contrails would not occur as a result of HSCT emissions. However, there remain questions about contrail formation, especially in winter when much lower temperatures can occur.

In summary, the climate changes which have been calculated from HSCT ozone and water vapor emissions tend to be small and less than model or observed interannual variability, but the *in situ* stratospheric responses tend to be consistent during the course of the simulation. Other effects (e.g., those due to sulfur and soot) are also likely to be small, but need to be quantified and tested.

The temperature changes shown above for aircraft effects on ozone and water vapor are equilibrium simulations, using estimated 2015 releases. Due to the heat capacity of the ocean, this equilibrium response would not be felt for some 30 years (by which time the aircraft perturbations would likely have changed). To provide a complete perspective of these results, aircraft-induced climate changes should be compared with those anticipated to occur by 2015 from other perturbations, particularly anthropogenic-induced trace-gas effects (primarily CO_2). According to IPCC [1995], with a doubled CO_2 sensitivity of some 1.5° to 4.5°C by 2015, surface temperature warming of a few tenths of a degree or more is likely and stratospheric cooling of similar or somewhat greater magnitude is possible [Rind *et al.*, 1990]. Hence the aircraft results which would have occurred by 2015 would likely be considerably smaller in comparison.

Note that neither the direct temperature effects of altered ozone nor the dynamically induced temperature changes were incorporated in assessment model photochemical calculations; neither were the model-calculated residual circulation changes. In addition, prospective changes in stratospheric temperatures or dynamics due to other anthropogenic perturbations (e.g., CO_2) by 2015 were not included. Sensitivity tests of the impact of these *in situ* changes should be made to incorporate in an iterative fashion potential climatic impacts and photochemical predictions.

3 ASSESSMENT UNCERTAINTIES

2-D model predictions for ozone changes in response to HSCT fleet operation are given in Chapter 2. Confidence in the construction quality of the models has increased since the NASA 1993 Interim Assessment Report [NASA 1993] by applying computational tests or "benchmarks" to the models, as described in Section 2.3. However, the degree to which the 2-D models adequately represent all of the qualitative and quantitative features of the atmosphere continues to be limited. This chapter defines the major areas of uncertainty associated with the quantitative assessment of HSCT impacts. These uncertainties are quantified where possible, either through formal propagation of errors in the model calculations or through model sensitivity studies. On account of the nonlinear nature of the atmospheric system, many of the uncertainties to be discussed in this chapter cannot be quantified at this time. Strategies to quantify those areas of uncertainty in the future are identified.

For the purposes of this chapter, the areas of uncertainty are organized around two major topics, the aircraft emissions which serve as input to the predictive models (Section 3.1) and the model representations of atmospheric processes (Section 3.2). The modeled processes include photochemistry, transport, and aerosol microphysics. The treatment of these processes in the models included in Chapter 2 ranges from very detailed (photochemistry) to highly parameterized (microphysics). A summary of the major uncertainties and their relationship to the overall confidence in the results of Chapter 2 is discussed in Section 3.3.

3.1 Aircraft Emissions

Future HSCT emissions cannot be forecast with great accuracy; hence, they contribute to the uncertainty of the overall assessment. Model results presented in Chapter 2 include inventories for aircraft-generated NO_x, H_2O, CO, and HCs (as CH_4). Measurable quantities of soot and SO_x are also emitted by aircraft but were not treated in those calculations. Input of the inventories into the models is achieved by simple dilution of the aircraft plume at the altitude of injection, with no chemical changes taking place, into a 1° longitude by 1° latitude by 1 km altitude grid. Further scaling of the exhaust composition is required when models employ larger grid sizes (e.g., zonal-average 2-D models), again with the same "frozen" chemistry assumption. Since HSCT engines have not been built, there are no direct observational constraints that can be placed on the estimated EIs of the important exhaust species, on potential chemical changes occurring on the model subgrid scale (i.e., in the aircraft plume/wake), or on the nature of the exhaust dilution process from subgrid to grid scale (e.g., degree of anisotropy, subsidence, etc.). An assessment of the model input quality requires that the uncertainties associated with each of these estimates or assumptions relating to aircraft exhaust and plume evolution be evaluated.

Uncertainties in the HSCT emission inventories derive from several sources. Inventory estimates for any of the exhaust species are affected by uncertainties in the total amounts of HSCT fuel burn and its geographic partitioning. As stated in Section 2.1, the flight routing assumed in this assessment represents an upper limit to the amount of emissions derived from a fleet of the specified size. As HSCT technology matures, better estimates of fuel consumption will be possible.

Emission inventory uncertainties associated with the individual exhaust species vary widely. NO_x emissions are subject to engineering tradeoffs in combustor design. Since initial assessments of HSCTs identified NO_x as having the largest potential impact on calculated ozone changes, the NO_x emission inventory has been treated parametrically in this assessment, with an EI range of a factor of 3 chosen to encompass both the HSCT design goal and the present state-of-the-art subsonic engine performance. Emission inventories for CO_2 and H_2O are directly related to the stoichiometric conversion of the fuel amounts. Because combustor efficiencies are greater than 99.9%, the uncertainty in CO_2 and H_2O due to this factor is <0.1%, far less than that associated with the total fuel consumption estimate used for the HSCT fleet. Thus, the uncertainty in CO_2 and H_2O emissions is approximately equal to the uncertainty in fuel consumption.

The effects of CO_2 emissions from an HSCT fleet are not considered here. Although emitted primarily into the stratosphere, CO_2 will become well mixed throughout the atmosphere, contributing to the overall greenhouse gas forcing of the climate. In contrast to NO_x, the CO emissions represent only a small (~10%) perturbation to ambient levels. Moreover,

the effect of additional CO on ozone levels is indirect, occurring only through repartitioning of HO_x. The degree of repartitioning resulting from increased CO is small relative to that arising from the NO_x perturbation. Hence, the uncertainty in CO emissions has a negligible effect on uncertainty in ozone response. The same reasoning applies to HC exhaust in the form of CH_4. The potential increase in CH_4 levels is essentially negligible relative to ambient levels, even assuming stoichiometric conversion of the HC fraction to CH_4.

Chemical composition studies of commercial and military subsonic engine exhaust [Spicer *et al.*, 1992, 1994] find that a significant fraction (>50%) of the HC exhaust at cruise conditions exists in forms other than CH_4. The NMHC fraction, if partitioned between a small number of species, might constitute significant perturbations to the ambient levels of the produced species. However, the experimental tests indicate that a myriad of NMHC species are produced in highly variable amounts, depending on engine type. Propagation of the uncertainties in NMHC emissions to calculated ozone response is difficult, owing to photochemical reactivity differences between the plethora of NMHC species. Based on the current understanding of HC chemistry, all NMHCs serve to produce ozone, to sequester chlorine into HCl, and to sequester nitrogen in the form of nitrites and nitrates. The latter pathway will reduce the aircraft-induced change in NO_x levels; however, the effect is negligible since aircraft NO_x emissions are, at a minimum, 50 times greater than the NMHC emissions. The effect of the first two pathways is more difficult to gauge since it involves a comparison of cycle efficiencies. A model sensitivity study to aircraft ethane emissions [Tie, 1994] indicates that changes in ozone are less than 0.1% for values of ethane slightly higher than levels considered possible by this assessment. The predicted change in ozone due to ethane emission increases under volcanically perturbed aerosol conditions to around 0.4%.

Soot and sulfur emissions from aircraft are, along with water vapor, the primary ingredients in particle formation; however, they are not included in the calculations described in Chapter 2. The impact of this omission on the assessment uncertainty is discussed in Section 3.3.

Omission of NO_x emission plume effects from the 2-D model input is supported by plume/wake model predictions of species in the near-field, which show no significant impact in that region. The near-field plume and wake has been modeled with $NO_x/SO_x/HO_x$ chemistry coupled to fluid mechanical calculations of the exhaust mixing and dynamics [Miake-Lye *et al.*, 1993, 1994; Quackenbush *et al.*, 1993]. Such calculations indicate that relatively small amounts of NO_y deposited at the point of wake break-up are in the form of HONO or HNO_3, the bulk remaining in the form of NO_x as emitted. Measurements in the wake of the ER-2 [Fahey *et al.*, 1995b], the Concorde [Fahey *et al.*, 1995a], and several commercial subsonic airliners [Arnold *et al.*, 1992] provide field experimental support for the modest conversion of emitted NO_x to other NO_y species.

Another omission from 2-D models is the descent of exhaust captured in the aircraft vortex wake, both through downward transport due to vortex motion and through radiative cooling due primarily to infrared emission of the exhaust water vapor. However, the degree of descent is expected to be less than a few hundred meters due to vortex descent and less than 1 km even for the maximum cooling rates occurring at mid- to high latitudes in the winter hemisphere [Rodriguez *et al.*, 1994]. *In situ* observations of the Concorde [Barrilleaux, 1995] and ER-2 [Fahey *et al.*, 1995b] aircraft exhaust are consistent with a small (<1 km) plume subsidence. As described in Section 2.4.2, lowering the injection altitude by 2 km results in calculated ozone changes that are ~0.2% and ~0.5% less negative for fleet EIs of 5 and 15, respectively. Since the subsidence is likely much less than 2 km, an upper limit on the uncertainty in predicted column ozone changes due to uncertainty in the injection altitude is, by linear extrapolation of the model results, reasonably set at 0.1%.

3.2 Model Representation of the Atmosphere

A primary goal of the global stratospheric models used in this assessment is to make accurate simulations of ozone, for both the historical, observed atmosphere and for future atmospheres. This goal can be achieved only by accurately representing the physical processes controlling atmospheric ozone in the models. The ability of the models to meet this

goal can be evaluated by comparison with existing and future observations and by attempts to reproduce measurements of past atmospheric changes. However, the evaluation of the 2-D predictive models using observations is not straightforward. A major difficulty is that a number of mechanisms in the model combine to determine ozone at any particular model location. Therefore, the possibility exists that the models predict ozone well, even though the relative contributions to the ozone value from the various model mechanisms are in error. In such a situation, the response of a model to a perturbation could differ significantly from the atmospheric response. A second difficulty in evaluation is that models are for an average, (i.e., typical) atmosphere, while measurements are taken under specific and perhaps different atmospheric conditions. The reasonable performance of a model in comparison with a number of different observations, each designed to test a specific model mechanism, will produce confidence that the models will be better suited to predict aircraft effects.

A systematic evaluation of 2-D models with measurements in connection with the AESA program has been carried out [Prather and Remsberg, 1993]. The models have since been revised and improved; current versions and their more complete variants (e.g., those including PSCs) need to be reexamined. There is now a much more extensive set of aircraft observations from the SPADE and ASHOE/MAESA campaigns, and a set of satellite observations from instruments on the Upper Atmosphere Research Satellite (UARS) and the Atmospheric Laboratory for Application and Science (ATLAS) payload on the Space Shuttle. This chapter will discuss some of the valuable comparisons that have been made in the past and describe some new comparisons for evaluation of model response to HSCT perturbations. An evaluation of the overall capabilities of the models by comparison with ozone observations follows. Subsequent discussion will treat the specific model components of transport, photochemistry, and particle formation.

3.2.1 Model Comparisons with Ozone Observations

3.2.1.1 Ozone Climatology

The Total Ozone Mapping Spectrometer (TOMS) provides a global picture of column ozone distribution. Figure 28, reproduced from WMO [1992], compares TOMS observations with several of the 2-D models included in this assessment report. Although the models have evolved since this comparison was made, it provides a useful illustration here. TOMS total ozone reaches a maximum in spring in both the Northern and Southern Hemispheres. The maximum is on the pole in the Northern Hemisphere and at ~60°S in the Southern Hemisphere. The magnitude of the Southern Hemisphere maximum is smaller than the Northern Hemisphere value by some 100 Dobson units (DU). The timing of the column ozone maxima varies by about a month amongst the models. The models locate the maxima at high latitudes in both hemispheres but do not consistently place the Northern Hemisphere maximum at the pole and the Southern Hemisphere maximum off the pole. Summertime mid- to high- latitude values of column ozone are relatively consistent among the models and agree fairly well with the TOMS observations. The models consistently underestimate the mid-latitude seasonal variability seen in TOMS column ozone. Equatorial values of column ozone in the models are typically within 10% of the TOMS values. However, the latitudinal extent of the low tropical values in the models is typically narrower than indicated by TOMS, leading to relatively weak latitudinal gradients in model column ozone compared to TOMS observations.

The general behavior of the calculated column ozone as a function of latitude suggests that the gross transport characteristics of the models are correct. The differences between the models and the observations suggest that there are significant transport uncertainties in the lower stratosphere. It should be noted that the usefulness of column ozone as a simple diagnostic of transport processes is somewhat limited because photochemistry still plays a significant role in determining column ozone.

Comparisons of observed and modeled profile ozone test different model features at various latitudes and altitudes. In the upper stratosphere, the comparison is a test of the overall effect of model photochemistry. In the lower stratosphere, ozone is sensitive to lower stratospheric transport but it is difficult to determine the specific cause of any disagreement. Comparisons of model profiles with Solar Backscatter Ultraviolet Spectrometer (SBUV) data indicate that models produce the correct shape of the mixing ratio profile in equatorial regions and at high

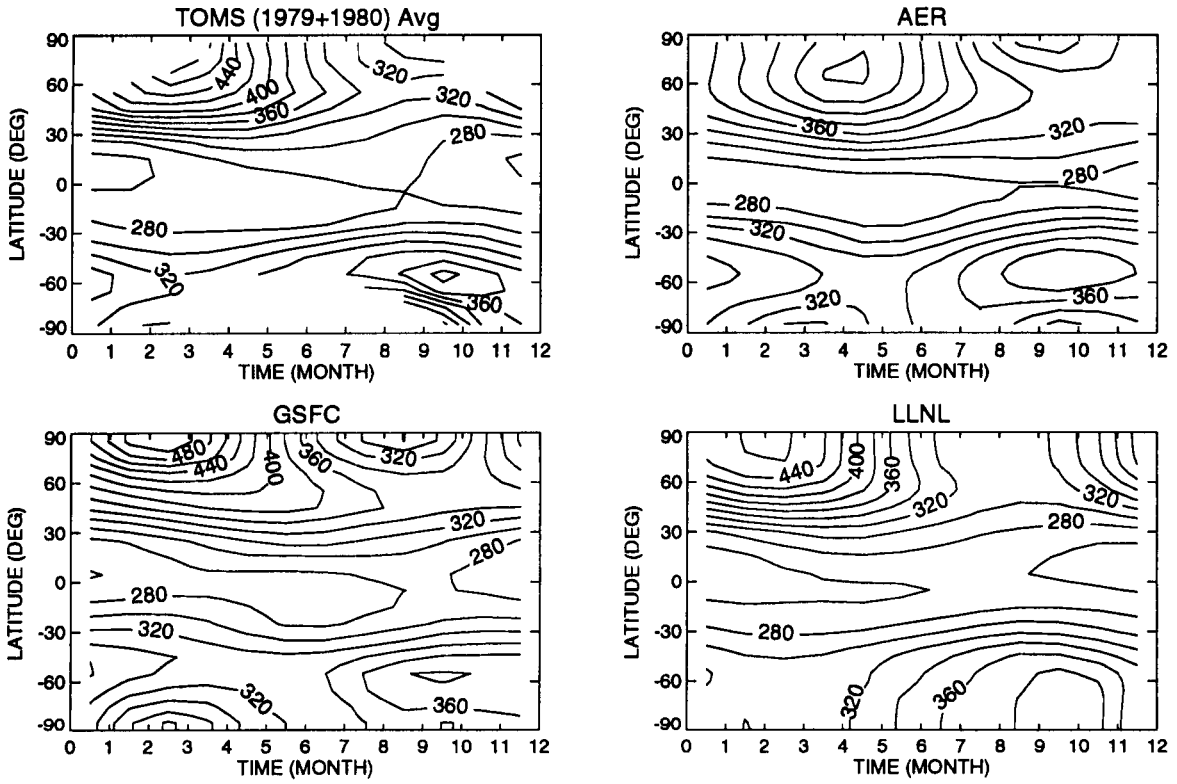

Figure 28. Column ozone abundances in Dobson units circa 1980 from TOMS observations as a function of latitude and season. Also shown are the results from three models used during the 1991 UNEP/WMO Scientific Assessment of Ozone Depletion; these models are not identical to the current versions of the same model. [WMO, 1992]

latitudes in the summer. The ozone peak in the models is a few kilometers too low in comparison to either SBUV or Stratospheric Aerosol and Gas Experiment (SAGE II) profiles. At higher latitudes in other seasons, the altitude of the modeled ozone peak tends to be ~5 km lower than observations suggest. Finally, models consistently underpredict ozone in the 35 to 50 km regions and overpredict ozone at low altitudes, especially in the equatorial regions. Recent work shows that the upper stratospheric ozone production and loss rates balance when measured values of the ozone and radical concentrations are used [Minschwaner *et al.*, 1993; Crutzen *et al.*, 1995; Dessler *et al.*, 1995a].

3.2.1.2 Ozone Trends: 1980-1990

Atmospheric ozone has been observed globally since the late 1970s. During the same time, stratospheric chlorine levels have been increasing and much of the change in ozone is thought to result from these chlorine increases. The observed ozone response to a well-defined perturbation can be compared to the calculated ozone response to test the predictive capability of the model, provided that increases in halogen levels are the sole cause. Although the HSCT fleet represents a NO_x and H_2O perturbation, the close connection between catalytic ozone loss cycles makes it difficult to argue that a model which fails to predict the atmospheric response to a chlorine perturbation can correctly predict the response to a NO_x perturbation.

Trends in column ozone have been estimated from TOMS observations and compared to model calculations [Stolarski *et al.*, 1991; Bojkov *et al.*, 1990, 1994; Randel and Cobb, 1994; Reinsel *et al.*, 1994]. Gas-phase models substantially underpredict the observed trends, while models including heterogeneous reactions on the sulfate aerosols do much better [Rodriguez *et al.*, 1991; Brasseur and Granier, 1992]. Figure 29, from Chapter 6 of WMO [1995] compares

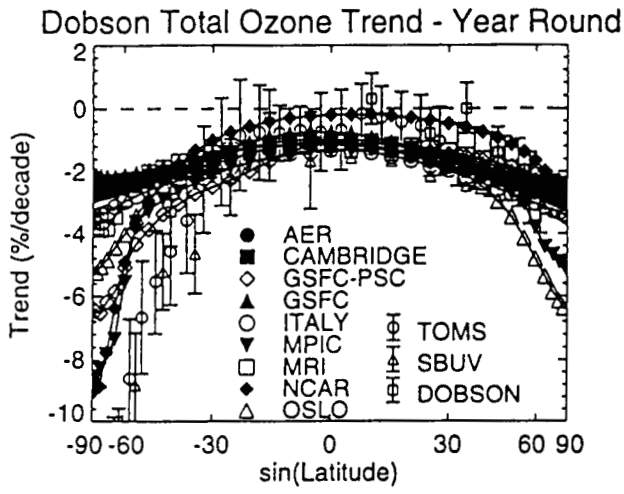

Figure 29. Model-calculated changes in column ozone between 1980 and 1990 compared to trends derived from observations. [WMO, 1995]

TOMS, SBUV, and Dobson station total ozone trends as a function of latitude with a number of 2-D models. The models are in reasonable agreement with the measurements in the tropics and lower mid-latitudes. At higher latitudes, the models tend to underestimate the observed trends significantly. In particular, the large Southern Hemisphere trend observed by the satellite measurements throughout the year is not captured by the models. Some of this discrepancy is due to the neglect of PSC processes in some of the models and a relatively poor model representation of the polar winter vortex in both hemispheres. There are also large discrepancies between the models and the observations in the Northern Hemisphere mid-latitudes, particularly in the late winter and spring. It is not known whether the discrepancy at these latitudes is due to neglected *in situ* chemistry or incorrect representations of lower stratospheric transport processes.

The above model calculations neglected the variability of the sulfate aerosol layer over the past decade, using a satellite-derived climatology instead. A recent study by Solomon *et al.*, [1995] finds that, if the temporal variations in the sulfate aerosol layer are included, then many of the features of the observed trend can be reproduced. However, the magnitude of the changes in this study was still underestimated by a factor of ~1.5 in comparison to TOMS trends. This could be due to an incorrect model formulation. The trends calculated from TOMS also have some uncertainty. For example, trends calculated from Dobson measurements are not as strongly negative as those from TOMS [WMO, 1992].

The models also can be evaluated by comparison with observed profile ozone trends such as those shown in Figure 3. This figure illustrates the March trends in profile ozone as a function of latitude and altitude for 1980 to 1990. Models predict peak fractional decreases to occur in the 40- to 45-km regions, with values similar to the satellite-derived trends. At ~25 km, SAGE II observations indicate a broad region of statistically insignificant trends extending from 50°S to 50°N. In the models, the width of this region generally extends from 30°S to 30°N, with trends increasing more rapidly toward higher latitudes in the models than in the SAGE II derived trends. The models generally fail to reproduce the very large decreases in low- to mid-latitude lower stratospheric ozone derived from the SAGE data. Trends in the mid-latitude lower stratosphere derived from ozonesonde measurements are less than half of the SAGE values at similar latitudes [Logan, 1994; Miller *et al.*, 1995; WMO, 1995]. However, the model-calculated trends at 15 km in the mid-latitudes are generally about half again as small as the sonde-derived trends. This underestimate of the lower stratospheric mid-latitude trends by the models is consistent with the results obtained from comparison to column ozone trends mentioned above. Thus, the overall pattern and location of ozone change are predicted, but the remaining discrepancies in the lower stratosphere are troubling since this region is critical to the HSCT problem. The reasons for the discrepancy between the models and the observations are not known.

3.2.2 ATMOSPHERIC TRANSPORT

The net impact of aircraft emissions is related to how fast the mid-latitude lower-stratosphere emissions are dispersed to other regions of the atmosphere. Much of the current emphasis is on how material crosses from mid-latitudes into the tropics where the pollutant can then be efficiently transported to the middle and upper stratosphere. Just as important, however, is transport from the lower stratosphere into the troposphere, which effectively cleanses the stratosphere. In addition, there is the issue of how aircraft emissions are transported into the wintertime polar vortex. Finally, there is the possibility of aircraft

emissions remaining in the corridors during times of weak winds, especially during the summer.

Transport of stratospheric air between mid-latitudes and either the tropics or the polar vortex is driven by episodic "wave" events. Similarly, the actual transport of lower stratospheric emissions into the troposphere is linked to large-scale "synoptic" wave activity. All of these wave processes are intrinsically 3-D and must be parameterized in the 2-D models. The 2-D wave parameterizations have focused primarily on stratospheric planetary waves.

3-D models explicitly resolve planetary and synoptic waves, and are adequately advanced to provide a useful tool for evaluating the transport characteristics of 2-D models. Generally, 3-D models require a parameterization of gravity waves on a smaller spatial scale than the model grids, and hence do not provide a direct evaluation of gravity-wave transport. Currently the most useful integrations are for a small number of reactive species or, more commonly, long-lived tracers with parameterized loss terms. The usual approach to the 3-D chemistry transport application is to first determine the 3-D wind and temperature fields and then to use these off-line to calculate the transport and chemical production and loss of constituents.

There are two approaches to obtaining 3-D wind fields. One is to use a self-deterministic GCM. The resulting winds are internally consistent solutions to the specified equations of motion. Even if the model were perfect, the chaotic nature of the weather would lead GCM integrations to depart from the behavior of the atmosphere and, at best, calculate a climatological-average state. Nevertheless, these models have been able to describe many of the averaged observations of long-lived chemicals in the stratosphere such as N_2O, ozone, and CO_2 [see e.g., Hall and Prather, 1993, 1995; Strahan *et al.*, 1994]. In addition to these chemical tracer tests, one needs to evaluate the GCM winds and temperatures with climatological averages and statistics. One problem with many GCMs is that the computed climatological-average state contains known but uncorrectable biases such as excessively cold temperatures at the winter pole that cause systematically biased winds. Unfortunately, chemical studies using GCMs are especially sensitive to the impact of temperature biases on aerosol processes.

The second approach is to use winds derived from a data assimilation system. In data assimilation, a GCM is run and observations are objectively melded into the model during the integration [Daley, 1991]. Data assimilation techniques have been used widely in numerical weather forecasts and are being actively extended to more general applications [e.g., Schubert *et al.*, 1993]. Through data assimilation vast amounts of routine meteorological observations are brought to bear on the transport simulation problem, and there is systematic comparison of winds and temperatures from the assimilation with radiosonde and aircraft observations. Data assimilation provides high-quality estimates of temperatures, extratropical horizontal winds, and other derived quantities that can be used to reduce the transport-related uncertainties in aircraft assessments made using off-line CTM calculations. While this approach cannot be used to evaluate feedbacks between changes in chemistry and climate for an assessment, when compared with self-deterministic GCMs, its strengths include relatively unbiased estimates of present-day temperature (no "cold pole"), proper representation of planetary- and synoptic-scale variability, proper location of climatological features (e.g., vortex, Aleutian anticyclone, storm tracks, etc.), timely representation of seasonal transitions, and representation of some important characteristics of the quasi-biennial oscillation (QBO). There are also weaknesses in this approach. The residual circulation is especially difficult to calculate because it is the difference of two large competing processes. In addition, the residual circulation is influenced by the data insertion process, which adds non-negligible forcing terms to the momentum and thermodynamic equations which impact the residual circulation. Winds in the tropics and subtropics are also highly uncertain because the temperature observations that dominate the input data for the assimilation do not effectively constrain the wind. Nevertheless, in 3-D models using assimilation winds agree well with ozone observations when integrated over yearly time scales [Douglass *et al.*, 1995]. Although the impact of errors in the residual circulation becomes more important with longer integrations, 3-D model integrations provide constraining information on all of the transport uncertainties discussed below. Such constraints have not been systematically incorporated into the 2-D models used in this assessment.

3.2.2.1 Model Comparisons with Tracer Observations

When results from the 1992 Models and Measurements Workshop were summarized [Prather and Remsberg, 1993], there were limited observations of stratospheric tracers capable of providing constraints on how well global-scale transport is represented in the 2-D models. Comparison of tracer distributions showed a range of agreement between observations and the various models. One consistent and significant area of disagreement was the tropical lower stratosphere. Simultaneous measurements of NO_y and ozone spanning the tropics and mid-latitudes in the lower stratosphere were available from the tropical 1987 Stratosphere-Troposphere Exchange Project (STEP) and Airborne Antarctic Ozone Experiment (AAOE) missions [Murphy *et al.*, 1993]. The difference in the NO_y/ozone ratio between the tropics and mid-latitudes was simulated by the 2-D models [Prather and Remsberg, 1993] and provides an indicator of the transport of mid-latitude air into the tropics both in the real atmosphere and in the models. The models tended to smooth out the tropical/extratropical difference in this ratio, suggesting that the subtropical transport barrier was not well represented in the models. Recently, a simulation of the effects of a stronger subtropical barrier on the NO_y/ozone ratio was calculated using a reduced horizontal eddy coefficient (K_{yy}) in the subtropics in the AER model [Donnelly *et al.*, 1995]; this steepened the gradient in NO_y/ozone across the subtropics and more closely simulated the observations.

Measurements in the 1960s and 1970s of carbon-14 (^{14}C) and strontium-90 that resulted from atmospheric weapons testing during the 1950s and 1960s [summarized by Johnston, 1989; Kinnison *et al.*, 1994] presented one of the few opportunities to evaluate transport in the models independent of chemistry. Due to the limited data set, however, definitive tests of model transport schemes cannot be made with ^{14}C. The comparisons that have been made serve to highlight potential model deficiencies. For instance, there have been several studies of bomb ^{14}C [e.g., Shia *et al.*, 1989, 1993; Jackman *et al.*, 1991; Kinnison *et al.*, 1994; Rasch *et al.*, 1994]. The 3-D calculation by Rasch shows the best agreement with observations. In particular, there is less pollutant in the upper stratosphere than in the 2-D calculations, which better agrees with observations. The physical reasons for this difference have not been determined. Although Plumb and Mahlman [1987] found good agreement between simulations with a GCM and a 2-D model derived from the same GCM, this approach has not yet been utilized in ^{14}C simulations. The studies of Jackman *et al.* [1991] and Rasch *et al.* [1994] seem to indicate that the 2-D models were, if anything, too slow in their overall transport when compared to 3-D models. On the other hand, a comparison by Kinnison *et al.* [1994] of 2-D calculations and observed ^{14}C years after the last major bomb tests indicated that the models tended to get a profile with altitude that was constant above ~25-30 km, while the data suggested a strong peak and falloff.

More recent data from the 1992 airborne SPADE mission has also been used to characterize the nature of atmospheric transport. Using a 1-D global diffuser model and observed CO_2 and N_2O correlations from the SPADE mission, Wofsy *et al.* [1994] deduced a more rapid transport of pollutants to the middle and upper stratosphere than is found in current 2-D models. Much of the character of these observations of CO_2 and N_2O were matched in a 3-D model [Hall and Prather, 1995], and these tests need to be examined with the current 2-D predictive models used here. On the other hand, as noted above, the 2-D models appear to exaggerate the upward transport of bomb ^{14}C. These comparisons, along with the NO_y/ozone ratios discussed above, suggest that the 2-D models used in this assessment are not global diffuser models. They may underestimate but do not neglect tropical isolation. The global diffuser model does not provide a good representation of stratospheric transport.

In the last several years, new observations of a variety of long-lived species have been obtained by instruments on aircraft, satellites, and balloons which hold the promise of providing important new tests of the representation of transport in models used for predicting HSCT effects. The global and seasonal coverage of CH_4, N_2O, CFCs, hydrofluoric acid (HF), and H_2O measurements from UARS will allow seasonal changes in stratospheric circulation to be deduced and will provide constraints for models. Correlations between the tracers N_2O, CFC-11, NO_y, ozone, CH_4, and H_2O measured by ATMOS and the ER-2 aircraft now span the tropics and extratropics and will allow a more thorough examination of model transport between the tropics and mid-latitudes. Initial analyses of the data suggest that trans-

port in the real atmosphere falls somewhere between the two conceptual models of the global diffuser and the tropical pipe and may be a strong function of altitude. Both the *in situ* and satellite data are consistent with estimates that approximately 20 to 45% of the air at 20 km in the tropics (equator ±7°) was transported from mid-latitudes while air above 20 km in the tropics is significantly more isolated (see Section 1.2.2) [Avallone and Prather, 1995; Minschwaner *et al.*, 1995]. However, a more thorough analysis of the data and systematic comparisons with model predictions are required before the transport barriers can be completely characterized. In addition, *in situ* observations of seasonally varying correlations between CO_2, H_2O, and N_2O will be needed to quantify vertical and quasi-horizontal transport rates in the lower stratosphere.

3.2.2.2 Dynamical Barriers: Tropical/Mid-Latitude Transport and Polar Vortices

The global diffuser and the tropical pipe are the extreme descriptions of mid-latitude transport into the tropics, and hence, transport of pollutants to the middle and upper stratosphere. Calculations with the AER model were made to test the sensitivity of the HSCT ozone perturbation to the inclusion of a pipe. They simulated the effects of a pipe on transport by reducing the K_{yy} in the subtropics at altitudes between 14 and 24 km to restrict transport between mid-latitudes and the tropics. The addition of the pipe resulted in a more positive calculated ozone response to the HSCT fleet, in the range of a few tenths of a percent to nearly 0.5%. Figure 30 shows the difference between the two model simulations. Note that while the tropics and Southern Hemisphere are distinctly different, Northern Hemisphere HSCT impacts are similar in the two cases.

As noted in Section 3.2.2.1, observations indicate that air in the tropics at 20 km consists of 25 to 40% air characteristic of mid-latitudes. Existing 2-D predictive models have yet to be diagnosed for this quantity, but their tropical NO_y/ozone ratio suggest that they exaggerate the exchange between mid-latitudes and the tropics. Agreement with observations improves in the AER model when a subtropical barrier is introduced.

Simulations using 3-D models also address the question of the subtropical barrier. Weaver *et al.* [1995] carried out a five-year calculation of the spread of

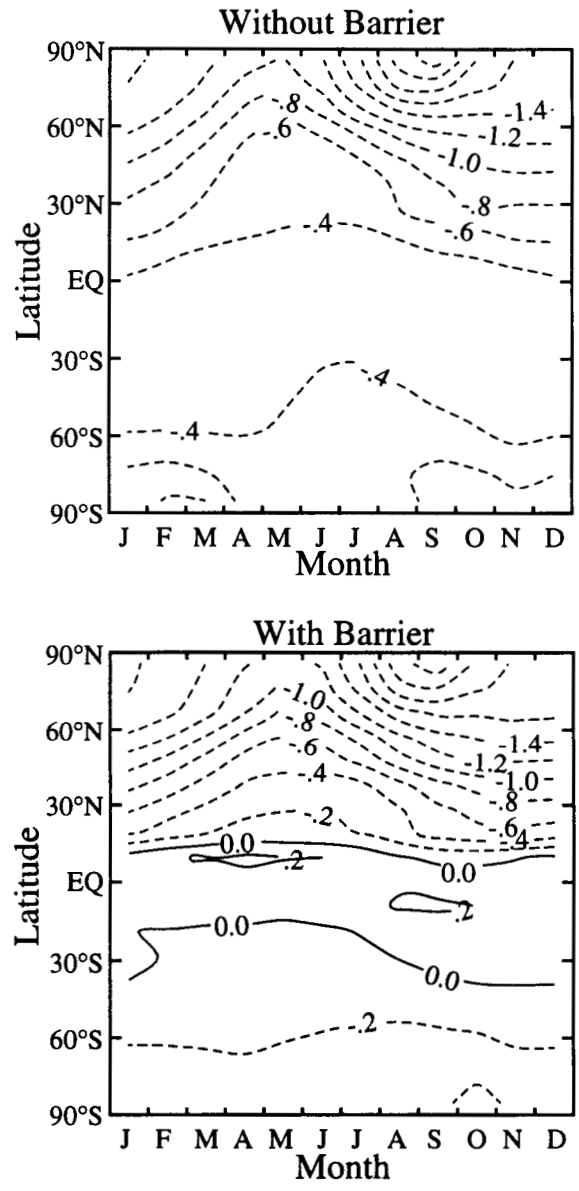

Figure 30. Calculation of the column ozone change as a function of month and latitude for the 2015 Mach 2.4 HSCT fleet with EI_{NO_x} = 15 g NO_2/kg fuel from the AER model; a) with "normal" dynamics, i.e., no reduction in eddy coefficients in subtropics, and b) with reduction of subtropical eddy coefficients by a factor of 10 to simulate effects of a subtropical barrier (or tropical pipe).

NO_y from a fleet of Mach 2.4 HSCTs using their 3-D CTM with winds from the GSFC assimilation. After five years, the zonal-average distribution of the NO_y perturbation compares reasonably with that calculated using the GSFC 2-D model (see Figure 31). However, the 3-D model does confine the aircraft pollutant to mid-latitudes more effectively than the 2-D model. In addition, as diagnosed with satellite

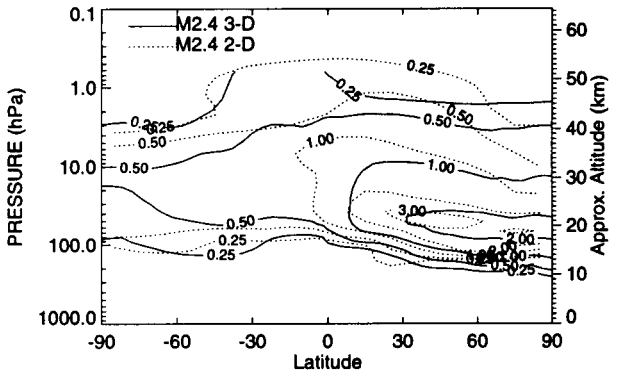

Figure 31. Comparison of 2-D and 3-D calculations for June of the added NO_y (in ppbv) from a fleet of Mach 2.4 HSCTs as a function of latitude and altitude (pressure). Contoured values have been scaled to an EI_{NO_x} = 15 g NO_2/kg fuel for comparison with other published figures. Dashed lines are for the 2-D calculation and solid lines are for the 3-D calculation. [Weaver *et al.*, 1995]

data, the winds used in the 3-D model overmix the subtropics with mid-latitudes in the lower stratosphere [Douglass *et al.*, 1995]. This adds more evidence that the current models incorporate more mid-latitude air into the tropics than actually occurs.

Most 2-D models used in the assessments also do not represent the observed isolation of the polar vortices, though more dynamically based transport parameterizations can simulate the isolation [Garcia *et al.*, 1992]. The implications of this model deficiency for the HSCT assessment have not been addressed.

3.2.2.3 Stratosphere-Troposphere Exchange and Residence Time of Emissions

The discussion above focused on the issue of how much pollutant gets into the upper stratosphere where ozone is more vulnerable to NO_x. Another important transport issue is stratosphere-troposphere exchange. The subject of stratosphere-troposphere exchange has a vast literature, as recently reviewed by Holton *et al.* [1995]. Movement of air into the troposphere is the primary mechanism for eliminating HSCT exhaust products from the stratosphere.

The simulation of stratosphere-troposphere exchange is discussed by Shia *et al.* [1993]. In 2-D predictive models, this exchange is accomplished through advection by the residual circulation and diffusive mixing across the tropopause. It has a tendency to occur at high latitudes rather than mid-latitudes, as found in 3-D models [e.g., Douglass *et al.*, 1993] and analyses of atmospheric data. Additionally, tropopause folding in some 2-D models is represented as diffusion that takes place along isentropes that are in the stratosphere at mid-latitudes and in the troposphere in the tropics. These models also misplace the stratosphere-troposphere exchange when compared with 3-D models, as indicated by large amounts of stratospheric material being transported into the tropical upper troposphere. This transport is discussed by Shia *et al.* [1993].

An important aspect of the differences in stratosphere-troposphere exchange for understanding HSCT effects is in the overall residence time. Jackman *et al.* [1991] did a sensitivity study of three different versions of the residual stream function. Their results confirmed that the build-up of pollutants in the lower stratosphere was directly related to the strength of the residual circulation. Comparisons of calculations with observations for total ozone and tracers N_2O and CH_4 can be used to determine whether a particular circulation is possible. The strongest circulation used by Jackman *et al.* [1991] was shown to be impossible within the framework of the model, i.e., constituent distributions calculated using the model with this circulation were very different from observations. The circulations that were considered possible each produced better qualitative comparisons with some observations. There is a significant difference in the maximum build-up of pollutants allowed using these circulations. Results show a significant sensitivity to the circulation, even when limited to "possible" by comparisons with long-lived species. This sensitivity is damped significantly when heterogeneous chemistry is included in the calculations.

In the Weaver *et al.* [1995] 3-D/2-D intercomparison discussed in 3.2.2.2, the calculated change of NO_y in the 3-D model is in general only slightly less than that in the 2-D model. Since the injection rates are the same, this indicates that the model residence times of the injected NO_y are almost equal (~13 months). Thus, while the stratosphere-troposphere exchange mechanisms in 2-D models are very different, the integrated effect on residence time appears to be similar. It is not clear how to reconcile this with the 2-D and 3-D model differences found in the ^{14}C transport studies described above.

3.2.2.4 Longitudinal Asymmetries and Corridor Effects

In addition to assumptions implicit in their transport parameterizations, 2-D models must assume zonally uniform sources whereas, in reality, emissions will be concentrated in localized corridors. This raises two issues of transport: how should these localized sources be mapped into 2-D, and what is the degree and significance of emission concentrations within the corridors?

The sensitivity of the assessment to specification of the 2-D source of emissions was addressed by Plumb *et al.* [1995]. In the first method, the 2-D source was specified as a simple zonal average of the 3-D source distribution (as is done in the assessments). In the second method, the potential vorticity/potential temperature mapping technique of Schoeberl *et al.* [1989] was used to map the 3-D source into pseudo-Lagrangian coordinates. The resulting zonally averaged source then included the effect of short-term transport processes that moved emissions away from initial locations. Only very small differences were found in predicted ozone loss using these 2-D source distributions, indicating that this issue is not one of significant uncertainty in the assessments.

The second 3-D issue concerns the possibility that some regions in the atmosphere will accumulate significantly more exhaust than would be expected using a zonal-mean model. In the study of Weaver *et al.* [1995], the largest zonal asymmetry in the perturbation is found in summer, when light winds fail to ventilate the corridors; this is in accord with results reported by Sparling *et al.* [1995]. In late summer during one of the extreme events, the maximum mixing ratio on the 54-mbar surface was only a factor of ~2 larger than the zonal mean at the same latitude. This suggests that the zonal averaging required for a 2-D calculation does not produce a large systematic error in the assessment calculations.

3.2.3 PHOTOCHEMISTRY

Knowledge of the chemical reaction rate coefficients has improved significantly in the last 20 years. Critical evaluations of the laboratory measurements of rate coefficients and estimates of uncertainty are made every two years by a NASA panel [see e.g., DeMore *et al., 1994*]. Major changes in the last two UNEP/WMO assessments occurred with the recognition of the importance of heterogeneous chemistry. The estimates of uncertainty by the NASA panel can be propagated through the 2-D model formulation. An example is described in Section 3.2.3.4.

Uncertainty in the gas-phase, heterogeneous, and photolytic processes can also be constrained by observations. Measurements of free radicals and longer-lived reservoir species made from aircraft, satellite, and balloon-borne platforms provide a test of the ability of photochemical process models to accurately partition the chemical families between reservoir and radicals. Provided that the photochemistry modules in the 2-D predictive models contain the full chemistry explored with the process models, knowledge gained in the observations/model intercomparison is transferred into the 2-D predictive models. However, such an evaluation does not directly test the distribution of free radicals in the 2-D predictive models. Since the concentrations of free radicals will also depend on the transport of the long-lived reservoirs, the distribution of ozone, and the temperature.

3.2.3.1 Middle and Upper Stratosphere Photochemistry

Observations from balloon, shuttle, and satellite-borne instrumentation have improved the understanding of processes that regulate the concentration of hydrogen, nitrogen, and chlorine radicals in the middle and upper stratosphere. Concentrations of hydrogen radicals in this region are primarily sensitive to the abundance of ozone, excited atomic oxygen ($O(^1D)$), H_2O, CH_4, HNO_3, and NO. Profiles of OH and HO_2 as a function of solar illumination have been measured by the Smithsonian Astrophysical Observatory Far Infrared Spectrometer (FIRS-2), Far Infrared Limb Observing Spectrometer (FILOS), and Stratospheric Limb Sounder (SLS) balloon-borne remote sensing instruments. These observations show good agreement (±30%) with theoretical profiles constrained by simultaneous measurements of the major precursors, as illustrated in Figure 32, for the range of altitudes (25 to 40 km) over which balloon-borne observations are available [Chance *et al.*, 1995; Pickett and Peterson, 1995]. A single *in situ* observation of OH and HO_2 between ~25 and 37 km shows broad agreement (±100%) with theory [Stimpfle *et al.*, 1990; Wennberg *et al.*, 1990]. These comparisons demonstrate that the primary sources

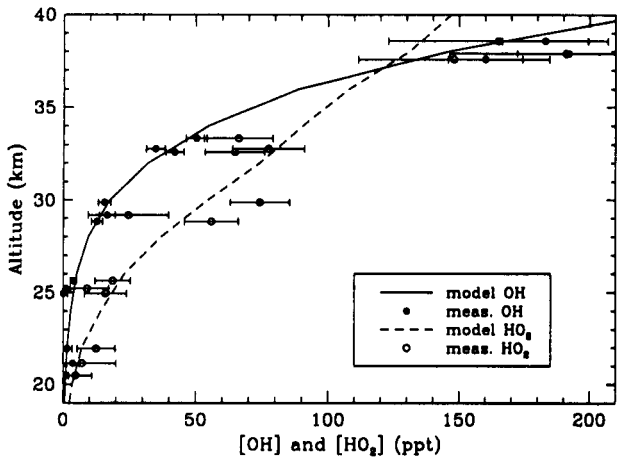

Figure 32. Measured and calculated OH and HO_2 at midday. Measurements were obtained by FIRS-2 near 34°N, on 26 and 27 September 1989. Error bars represent estimates of the 1-σ total accuracy of measurement, including uncertainties associated with molecular parameters, residuals from fits to the measured spectra, and intensity calibration of the spectra. Theoretical profiles appropriate for the local measurement time were found using a photochemical model [Salawitch *et al.*, 1994b] constrained by profiles of ozone, H_2O, and temperature measured by FIRS-2; profiles of NO_y, Cl_y, and CH_4 estimated from FIRS-2 measurements of N_2O; and sulfate aerosol surface area measured by SAGE II. [Adapted from Chance *et al.*, 1995]

and sinks of OH and HO_2 should be well represented by 2-D predictive models using recommended rates and cross sections [DeMore *et al.*, 1994], provided fields of precursors (ozone, H_2O, and CH_4) are calculated in a realistic manner. However, existing observations of hydrogen radicals in the middle and upper stratosphere are limited to mid-latitudes near equinox above altitudes of ~25 km. Observation of OH and HO_2 in the altitude range 20 to 25 km, for latitudes and seasons not yet sampled, are essential for testing 2-D predictive models.

Simultaneous measurements of radicals (NO and/or NO_2) and major reservoirs (HNO_3, or total NO_y), and ozone (which mediates the conversion efficiency of NO_x to HNO_3) guide our understanding of processes that regulate the abundance of NO_x gases. Concentration profiles of NO_y gases NO, NO_2, HNO_3, $ClONO_2$, N_2O_5, HNO_4, and ozone at sunrise and sunset have been obtained by ATMOS at a variety of latitudes and seasons throughout the middle stratosphere. Theoretical profiles of the partitioning of NO_y gases, constrained by simultaneous measurements of ozone, H_2O, and CH_4 from ATMOS and the surface area of sulfate aerosol from SAGE II, show good agreement with observations, as illustrated in Figure 9. These observations demonstrate the NO/NO_2 ratio is represented well by models. Furthermore, agreement between theory and observation for N_2O_5 suggests that the mechanism for conversion of NO_x to HNO_3 is well simulated by photochemical models. Similar levels of agreement between theory and observation of NO_y gases for altitudes between 25 and 40 km are demonstrated by balloon-borne measurements of NO, NO_2, HNO_3, and $ClNO_3$ by the JPL MkIV interferometer [Sen *et al.*, 1995] and measurements of NO_2, HNO_3, and ozone by the Balloon-borne Laser *In Situ* Sensor (BLISS) [Webster *et al.*, 1994]. These observations demonstrate that 2-D predictive models should calculate realistic fields of NO and NO_2 for aerosol conditions appropriate for near-background (i.e., non-volcanic) conditions, provided precursor fields (e.g., ozone, NO_y, Cl_y, H_2O, and CH_4) are calculated in a realistic manner.

There are limited measurements of NO_y gases in the middle stratosphere under conditions highly perturbed by volcanic aerosol. Measurements by ATMOS and the JPL MkIV interferometer are limited by the inability of their sun trackers to remain locked on the solar disk. Measurements of NO_2 by SAGE II are compromised by the high extinction associated with the volcanic aerosol. Ground-based measurements, however, reveal large decreases in column NO_2 and increases in column HNO_3 due to the Mt. Pinatubo aerosol over Lauder, NZ (47°S) [Koike *et al.*, 1994]. The magnitude of these changes is underestimated by nearly a factor of 2 by 2-D models [Koike *et al.*, 1994], suggesting possible missing sinks for NO_x at high surface area. However, balloon-borne *in situ* measurements within volcanic clouds of profiles of NO, NO_y, ozone, and surface area over Aire sur l' Adour, France (44°N, 0°W) on 20 October and 6 November 1992 [Kondo *et al.*, 1995], and of NO, NO_y, ClO, and ozone over Greenland (66°N) during March 1992 [Dessler *et al.*, 1993] reveal good agreement between observed and calculated NO_x. These observations suggest the major sink for NO_x in volcanic clouds is the heterogeneous hydrolysis of N_2O_5, and they appear to rule out a rapid rate for other sinks at temperatures higher than 200 K. Additional measurements of NO_y gases for volcanically perturbed conditions would be desir-

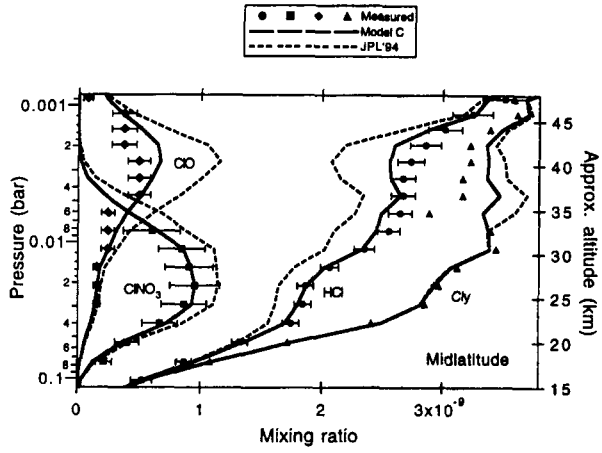

Figure 33. Partitioning of inorganic chlorine species in the stratosphere. The triangles represent the measured sum of HCl sunset + $ClNO_3$ sunset + ClO midmorning; lines labeled "Cl_y" represent the abundance of total inorganic chlorine necessary to match the measured sum of these gases. Differences at higher altitudes are due primarily to HOCl, not measured in this experiment, and $ClNO_3$, not retrieved by ATMOS above ~34 km. Model C (solid lines) uses rates for the reactions of Cl + CH_4 and OH + HCl from a reanalysis of laboratory data and allows for a 7% yield of HCl from the reaction of ClO + OH. [Adapted from Michelsen *et al.*, 1995]

able to further test the fidelity of 2-D predictive models and verify the chemical mechanism.

Significant discrepancy between theory and observation exists for inorganic chlorine in the middle and upper stratosphere. Figure 33 illustrates a comparison of theory and observations for mid-latitude halogen partitioning [Michelsen *et al.*, 1995]. HCl concentrations are underpredicted while $ClONO_2$ are overpredicted. Measurements of ClO by the Microwave Limb Sounder (MLS) are consistently lower than predicted in the upper stratosphere. This suggests that the production and loss mechanisms of HCl in the middle and upper stratosphere are not well quantified. The effects of this discrepancy on model predictions of HSCT impacts have not yet been evaluated.

Simultaneous measurements of hydrogen, nitrogen, and chlorine radicals show NO_x catalytic cycles dominate removal of ozone for altitudes between 24 and 38 km, as illustrated in Figure 34. At altitudes near 38 km, halogen cycles are less efficient sinks for ozone than calculated by models using accepted photochemistry [DeMore *et al.*, 1994], resulting in a balance between production and loss of ozone [Jucks *et al.*, 1995].

3.2.3.2 Lower Stratosphere Photochemistry

The photochemistry of the lower stratosphere is somewhat distinct from the higher altitudes because the sulfate aerosol layer and PSCs provide sufficient surface area for heterogeneous chemistry to play an important role in determining the concentrations of radicals. Observations from the NASA ER-2 aircraft have provided the bulk of the data sets that have been used to test the basic photochemistry of the lower stratosphere put forward from laboratory studies. These observations have motivated the choice of test cases used in the 2-D benchmark chemistry test discussed earlier in Section 2.3.

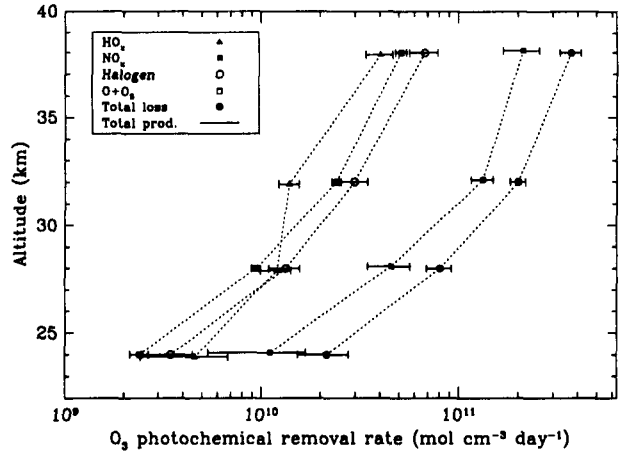

Figure 34. Production and loss of ozone in the middle stratosphere. Loss rates of ozone due to hydrogen radicals (closed triangles), nitrogen radicals (closed squares), halogen radicals (open circles), and the reaction of atomic O and ozone (open squares) inferred from calculated O, measurements of ozone, HO_2, OH, NO, NO_2, and ClO by the Far Infrared Spectrometer (FIRS-2) and the Balloon Microwave Limb Sounder (BMLS) near 34°N, on 26 and 27 September 1989. Error bars represent the 1-σ total accuracy of loss rates based on uncertainties associated with measurements of radicals, and the dotted lines connect individual measurements for convenience of interpretation. The production rate of ozone from photolysis of O_2, calculated using the Minschwaner *et al.* [1993] formulation for transmission in the O_2 Schumann-Runge region, is shown by the solid line. [Adapted from Jucks *et al.*, 1995]

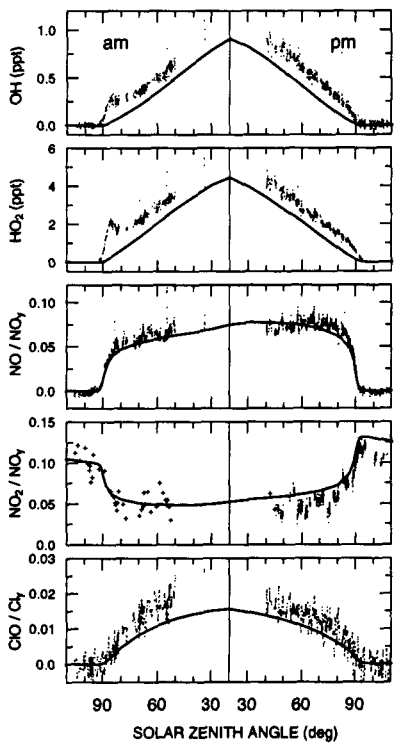

Figure 35. Diurnal variations of free radicals (OH, HO_2, NO, NO_2, and ClO) measured at 19 km, 37°N during SPADE. The lines are calculations using a photochemical model. [Adapted from Salawitch *et al.*, 1994b]

Detailed analysis of the SPADE data indicate that photochemical models using the existing kinetic data predict radical partitioning within ±40% [Salawitch *et al.*, 1994a, b; Cohen *et al.*, 1994; Stimpfle *et al.*, 1994; Jaeglé *et al.*, 1994]. Figure 35 shows the observed diurnal variation of the concentrations of free radical species from the SPADE data set. Also shown is the calculation from a photochemical model constrained with measured or directly inferred values of aerosol surface area, NO_y, ozone, temperature, pressure, and the ozone column. The agreement is generally better than expected from an error analysis of the measurements and models. The level of agreement shown in this figure is found consistently in analysis of all of the SPADE and most of the ASHOE/MAESA flights (except those with recent PSC processing or rapid latitudinal excursions) which include winter, spring, and fall observations over a large range in latitude and aerosol surface area loading. The Photochemistry of Ozone Loss in the Arctic Region in Summer (POLARIS) aircraft campaign, scheduled for summer 1997, is intended to fill the gap of summer observations when lower stratospheric NO_x concentrations are expected to be considerably higher.

In general, the photochemical model underpredicts the concentration of OH and HO_2. Most dramatically, the abrupt rise of OH and HO_2 at sunrise suggests that a nighttime process results in the accumulation of an easily photolyzed OH-containing molecule [Wennberg *et al.*, 1994]. Recent laboratory observations of the rapid hydrolysis of $BrONO_2$ on sulfate aerosols is a possible mechanism [Hanson and Ravishankara, 1995; Lary *et al.*, 1995]. Inclusion of this process at the rate suggested by Hanson and Ravishankara improves the agreement between the model and measurement of OH throughout the day, particularly at high solar zenith angle. However, because this reaction is assumed to produce HNO_3, the predicted NO_x concentrations fall below the observations [R. Salawitch, personal communication]. Because this reaction leads to enhanced concentrations of HO_x and depresses NO_x, it can impact the HSCT assessment. A sensitivity study has been performed within the 2-D model formulation. For a base case scenario (500 aircraft; 3.0 ppbv Cl_y; EI_{NO_x} = 15; UNEP aerosol), the LLNL/UI 2-D model predicts that global ozone change is reduced from -0.66 to -0.49% when the process is included. Similarly, the CSIRO model predicts the change to be reduced from -0.44 to -0.33%.

Measured noontime OH concentrations are also higher than expected, although the differences are not beyond the uncertainty in the measurements. Nevertheless, it has been suggested in laboratory studies, [Ball and Hancock, 1995], atmospheric measurements [Müller *et al.*, 1995], and modeling work [Michelsen *et al.*, 1994] that the DeMore *et al.* [1994] formulation of the $O(^1D)$ yields from ozone photolysis is not adequate. Addition of a larger yield of $O(^1D)$ from ozone in the 310- to 315-nm range improves the agreement of the model with OH measurements [Salawitch *et al.*, 1994a, b]. Although a sensitivity study to predict how this affects HSCT impact predictions has not been conducted, its inclusion should affect model predictions. The increase in HO_x, particularly in the lower stratosphere, will further shift the photochemistry towards a HO_x-dominated lower stratosphere.

Observations of the NO/NO_y ratio in the lower stratosphere are generally in good agreement with

the photochemical model. However, during the SPADE measurements, measured NO_2 concentrations were considerably lower than predicted based on simultaneous measurements of NO, ClO, and ozone [Jaeglé *et al.*, 1994]. NO_2 measurements during ASHOE/MAESA suggest a much smaller discrepancy on the order of 15% [Gao *et al.*, 1995]. This problem deserves further attention because it will impact the HSCT assessment. As mentioned earlier, addition of the $BrONO_2$ hydrolysis tends to lead to underprediction of the observed NO_x/NO_y ratio. This could arise from an error in measured surface area or the formulation of the N_2O_5 hydrolysis reaction on sulfate aerosol, which dominates the heterogeneous conversion of NO_x to NO_y. Variations in the laboratory measurements for this process are uncertain up to a factor of 2. Additionally, the rate of this reaction is very dependent on the N_2O_5 formation rate which depends on the concentration of ozone and the temperature - areas of known deficiencies in the 2-D models.

Aircraft *in situ* observations of HCl in the Southern Hemisphere in 1994 by the Aircraft Laser Infrared Absorption Spectrometer (ALIAS) instrument, obtained for near-background sulfate aerosol loading, agree well with model calculations (HCl/Cl_y ~0.8). Measurements of the HCl/Cl_y fraction in the Northern Hemisphere have evolved upward from 0.35 in 1991/2 to 0.45 in 1993 to 0.6 in 1994, compared to model values close to 0.8. For the 1993 and 1994 data from both hemispheres, the measured HCl/Cl_y fraction shows a possible dependence on aerosol particle surface area, suggesting an unidentified heterogeneous loss of HCl or Cl_y that follows the evolution with time of the Mt. Pinatubo aerosol. From an ATMOS/ER-2 intercomparison in November 1994 in the Northern Hemisphere, the ATMOS and ALIAS measurements of HCl/Cl_y agree within their respective uncertainties, although the ALIAS measurements are systematically lower by ~10% at higher HCl mixing ratios, and up to 40% at lower mixing ratios where precision is poor [Chang *et al.*, 1995]. UARS measurements in 1992 and 1993 also indicate that models overpredict the HCl/Cl_y ratio at 550K, but not by as much as indicated by the ALIAS observations [Dessler *et al.*, 1995b].

Observations of ClO/Cl_y are in good agreement with model calculations [Stimpfle *et al.*, 1994]. The observed diurnal behavior of ClO indicates that it is strongly linked with photolysis of $ClONO_2$; however, the inferred fraction $ClONO_2/Cl_y$ = 0.06 to 0.24 is in apparent conflict with the 1993 aircraft measurements of HCl.

As discussed in Section 3.2.4, the aerosol chemistry in the polar regions remains quite uncertain. As changes in our knowledge of the aerosol microphysics have occurred, laboratory investigations have been made of the rates of heterogeneous processes on various surfaces that are identified as potentially important. These studies demonstrate that, largely independent of the nature of the surface (e.g., liquid ternary mixture, NAT, sulfuric acid tetrahydrate (SAT)), the reaction of HCl with $ClONO_2$ becomes very efficient at low temperatures found in the winter polar regions (<195 K). This suggests that, with respect to the activation of chlorine, simulation of this chemistry in the 2-D models will be much more sensitive to the temperature and water than to the formulation of the microphysics (see Section 3.2.4).

Recognition of the various model/observation discrepancies has led to speculation about possible missing chemistry in the models. Missing chemistry includes photochemical mechanisms that are not in the computer models, and errors in reaction rate constants and photolysis rates. These errors may occur in the absolute values or in the dependencies on pressure, temperature, and the presence of other trace-gas constituents. For missing chemistry to be significant for this assessment, it must have chemical impacts comparable to known gas-phase and heterogeneous chemistry and its inclusion in the models must change the calculated effects of stratospheric aircraft. Assessing the uncertainties associated with missing chemistry is difficult, as evidenced by the surprising discovery of the Antarctic ozone hole and by the N_2O_5 hydrolysis on sulfate aerosol that has widely altered the predicted impact of aircraft on the lower stratosphere.

In addition to disagreements between model results and observations, the search for missing chemistry usually is motivated by new laboratory results. As laboratory gas-phase measurements have improved and become more consistent, much of the emphasis has shifted to photolysis rates and heterogeneous chemistry. To date, no systematic assessment has been made of the uncertainties associated with missing chemistry.

For a few instances, such as the HO_x catalytic reactions, the possibility of missing chemistry has been constrained by observations [Cohen *et al.*, 1994]. *In situ* measurements of the HO_2/OH ratio appear to agree to better than implied by propagation of the quoted uncertainties in the measurements and the key reaction rate constants. Because the HO_x catalytic cycle that destroys ozone is responsible for about one half of the total ozone loss at mid-latitudes, the constraints on missing HO_x chemistry provide important bounds on the overall uncertainty.

Iodine chemistry has been suggested, and has received considerable attention, as a contributor to ozone loss in the lower stratosphere [Solomon *et al.*, 1994]. However, observations of the iodine monoxide (IO) column abundance suggest that the inorganic iodine concentration in the lower stratosphere is lower than the 1 pptv assumed for the calculations [P. Wennberg, personal communication]. In addition, recent measurements of the reaction rate constant for the proposed rate-limiting reaction that destroys ozone, $IO + ClO \rightarrow I + Cl + O_2$, is three times slower than had been assumed [Gilles *et al.*, 1995] and the $IO + BrO \rightarrow I + Br + O_2$ reaction is about as fast as assumed [Laszlo *et al.*, 1995a, b]. Ongoing studies will better define iodine's role in lower stratospheric ozone loss. However, if this or any other halogen reaction is significant, then any increase in NO_x from aircraft exhaust very likely will lead to a decrease in local ozone destruction due to increased control of the halogens by the added NO_x, provided that the interaction of the "missing" halogen oxide family with NO_x is similar to that of ClO_x and BrO_x.

3.2.3.3 Upper Troposphere Photochemistry

Changes in tropospheric ozone due to HSCT NO_x emissions as predicted by various models are highly variable and uncertain. The uncertainty is mostly due to the lack of understanding of the distribution and budget of NO_x in the troposphere, particularly in the upper and middle troposphere. The largest *in situ* source of NO_x in the upper and middle troposphere is from lightning. Yet neither the magnitude and altitude distribution are understood [Fehsenfeld and Liu, 1993]. In addition, the convective transport of NO_x emitted near the surface is important to the NO_x budget in the free troposphere but is extremely difficult to evaluate. These near-surface sources are more than two orders of magnitude greater than the predicted NO_x emissions from HSCTs in the troposphere. A small fraction of the near-surface NO_x transported to the upper troposphere can overwhelm the contribution of the NO_x from HSCTs.

Because the column density of ozone in the troposphere is only ~10% of the total column density, even with large uncertainty, the predicted changes in tropospheric ozone due to HSCT NO_x emissions have negligible impact on the total ozone column density. The same thing cannot be said about the effect of NO_x emissions from subsonic aircraft because the emissions are significantly greater than those from HSCTs. Their effect on tropospheric ozone and climate will be addressed in a separate but coordinated NASA research program, the Subsonic Assessment (SASS) element of the Atmospheric Effects of Aviation Project (AEAP).

3.2.3.4 Propagation of Errors Due to Uncertainty in Rate Coefficients

One aspect of the predictive uncertainty that is amenable to a direct numerical estimate involves the reaction rate coefficients. Assuming that the chemical model is complete, the estimated uncertainties from the JPL evaluation [DeMore *et al.*, 1994] have been propagated through a typical 2-D model calculation [Stolarski and Considine, 1995]. Some preliminary results are shown in Figures 36 and 37. Figure 36 shows the calculated 1-σ uncertainties on the calculated column ozone change due to a Mach 2.4 HSCT fleet with $EI_{NO_x} = 15$ as a function of latitude and time of year. The results show 0.5 to 0.8% uncertainties in the Southern Hemisphere, where the perturbation is due mainly to ozone-depleted air transported to the upper stratosphere (see Figure 23). In the Northern Hemisphere, the uncertainty rises rapidly to 1% and then more gradually to 1.5 to 2% near the pole. The larger Northern Hemispheric uncertainty in the column prediction is the result of larger uncertainties on the lower stratospheric perturbation, as shown in Figure 37. The smaller uncertainties in the upper stratosphere occur where the change in ozone is due primarily to an increase in the NO_x catalytic cycle. In the lower stratosphere, the increased catalysis by NO_x is balanced by interference and a subsequent decrease in the catalytic cycles due to ClO_x and HO_x. These processes, whose absolute uncertainties add together, result in the larger overall uncertainty. The next step in this analysis is to identify and remove from consideration

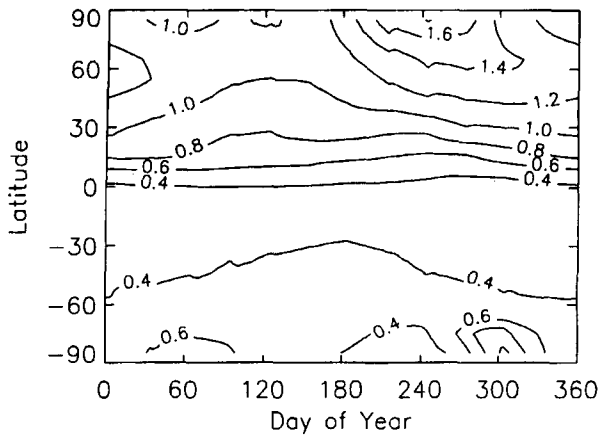

Figure 36. Calculated 1-σ uncertainty in column ozone change (in percent) for a Mach 2.4 HSCT fleet with EI_{NO_X} = 15 g NO_2/kg fuel from the GSFC model Monte Carlo error analysis as a function of season and latitude.

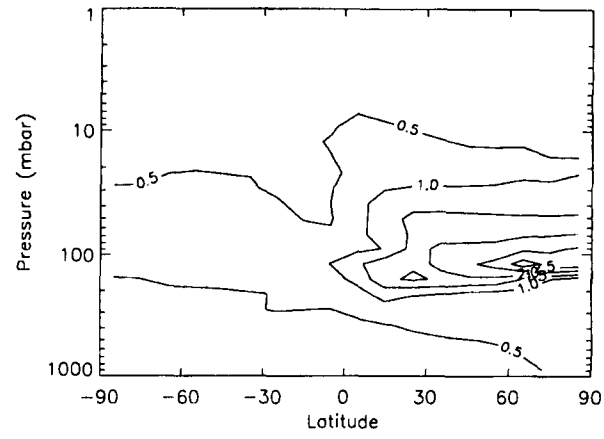

Figure 37. Calculated 1-σ uncertainty in ozone concentration (in percent) for a Mach 2.4 HSCT fleet with EI_{NO_X} = 15 g NO_2/kg fuel from the GSFC model Monte Carlo error analysis as a function of altitude and latitude for the month of March.

those model results that predict values of key species which are outside the range of measured concentrations, thereby narrowing the uncertainties.

3.2.4 AEROSOL AND PARTICLE MICROPHYSICS

3.2.4.1 Aerosol Formation Processes

The 2-D HSCT predictive models include sulfate aerosols prescribed by the UNEP surface area distribution [WMO, 1992], which represents an average derived from satellite observations in 1989, prior to the Mt. Pinatubo eruption. Since the variability due to volcanic sulfur injection or PSC formation is not considered, the evolution and transformations of particles are not complete in the models. This omission is particularly important for low-temperature regions at high latitudes where both particle microphysics and heterogeneous chemical reactivity have large temperature dependencies. Separate sensitivity studies that include a parameterization for PSCs, variations in sulfate aerosols due to volcanoes, and HSCT particle formation are discussed in Sections 3.2.4.5 through 3.2.4.7.

The composition and abundance of aerosols in the stratosphere are controlled by the vapor densities of H_2SO_4, HNO_3, and H_2O that condense into particles according to their temperature-dependent ternary phase diagram. In most of the low- and mid-latitude stratosphere at temperatures above 200 K, supercooled liquid H_2SO_4/H_2O particles form the ambient aerosol layer observed between 10 and 30 km. At lower temperatures (<200 K), HNO_3 condensation forms ternary particles that become Type I PSCs composed largely of HNO_3 and H_2O at temperatures below 192 to 195 K [McCormick *et al.*, 1982; Steele *et al.*, 1983]. At still lower temperatures (<190 K), H_2O condensation forms Type II ice clouds. A complete model of stratospheric aerosols requires a detailed microphysical formulation of the formation and evolution of all these particles [see e.g., Turco *et al.*, 1989].

Such a model would include sources and sinks of gaseous sulfur species. Primary stratospheric sources are transport of carbonyl sulfide (OCS) from the troposphere and episodic volcanic injections of SO_2. In the stratosphere, all these species are oxidized to H_2SO_4. Microphysical models must account for the competition between nucleation of new H_2SO_4 particles and accommodation on preexisting particles. In this context, the aircraft exhaust plume forms a special case where high acid and water vapor levels favor binary nucleation of new particles. Models also include the effects of coagulation on aerosol concentration and surface. Finally, the primary loss mechanism is transport via sedimentation to the troposphere.

In situ and remote observations of PSCs [for example, Dye *et al.*, 1992; Browell *et al.*, 1993; Toon and

Tolbert, 1995] show considerable variability that is consistent with the complex ternary phase diagram. These PSCs are often composed of liquid and solid phases that are distinct from the most stable thermodynamic phase, presumed to be crystalline NAT [Hanson and Mauersberger, 1988]. For temperatures above 195 K, H_2O condenses onto particles consistent with supercooled liquid sulfate composition in range of 50-80 weight percent [Steele and Hamill, 1981]. At temperatures of ~192 K, HNO_3 and H_2O can condense to form a ternary liquid solution whose composition depends on the overall HNO_3/H_2SO_4 ratio in the air [Molina *et al.*, 1993; Tabazadeh *et al.*, 1994]. The existence of supercooled liquid particles [Dye *et al.*, 1992; Drdla *et al.*, 1994; Carslaw *et al.*, 1994] is consistent with much laboratory and theoretical work which predicts significant barriers to freezing of both binary H_2SO_4·H_2O and ternary H_2SO_4·HNO_3·H_2O liquid particles [Song, 1994; Koop *et al.*, 1995; Anthony *et al.*, 1995; MacKenzie *et al.*, 1995; Murphy and Gary, 1995]. Moreover, other laboratory studies show multiple metastable solid phases are possible upon freezing [Worsnop *et al.*, 1993; Marti and Mauersberger, 1993; Fox *et al.*, 1995].

Original models that identified Type I PSCs as NAT with a temperature threshold of ~195 K cannot explain Type I PSC appearance between 191 and 192 K [Dye *et al.*, 1992; Kawa *et al.*, 1992; Drdla *et al.*, 1994; Carslaw *et al.*, 1994]. These complexities raise questions about the validity of relating temperature and global PSC probabilities, such as those catalogued by Poole and Pitts [1994], to heterogeneous chemical processes such as those controlling chlorine activation which have steep dependence on aerosol temperature, composition, and phase [see e.g., Hanson and Ravishankara, 1993; Hanson *et al.*, 1994].

Overall, uncertainties in aerosol microphysics increase at high latitudes, and low temperatures must be combined with steeply temperature-dependent microphysical and heterogeneous reaction processes to predict effects on photochemistry. This is particularly true for microphysical aerosol processes for which there is significant conceptual uncertainty. Most importantly, mechanisms of denitrification likely depend on transformations between liquid and solid metastable phases. More study is needed to evaluate the microphysical implications of adding HSCT plume sulfate particles to background aerosol distributions on these PSC/denitrification processes.

3.2.4.2 Denitrification and Dehydration

Field experiments have shown that heterogeneous chemical processes during polar winter in both the Antarctic and Arctic yield very high levels of active chlorine, yet widespread ozone depletion has occurred to date only over Antarctica. This is thought to be due to the fact that the springtime Antarctic stratosphere is substantially denitrified, its NO_x content being irreversibly reduced over large areas by some 90% relative to both prewinter and extra-vortex values [Crutzen and Arnold, 1986; Solomon *et al.*, 1986a; McElroy *et al.*, 1986, Fahey *et al.*, 1990]. Denitrification has also been observed in the Arctic, but only to a much smaller degree and in localized "patches." The springtime Antarctic (but not the Arctic) stratosphere is also substantially dehydrated, its H_2O content over large areas being less than half that of prewinter and extra-vortex values.

The presence or absence of NO_x is crucial to determining the amount of chlorine-catalyzed ozone destruction. If sufficient NO_x is present in polar springtime, chlorine radicals are converted quickly to the reservoir $ClONO_2$ and more slowly to the reservoir HCl. If there is substantial denitrification, the reservoirs remain depleted, and ozone destruction can proceed rapidly until nearly all the ozone is destroyed or until the polar vortex breaks down.

Denitrification and dehydration are caused by the precipitation of large PSC particles that contain condensed HNO_3 and H_2O, respectively. Microphysical models of Type 2 (ice) PSC formation can produce particles that are large enough and precipitate fast enough to explain observed dehydration levels. Widespread dehydration occurs in the Antarctic, but not in the Arctic, because Antarctic stratospheric temperatures often fall below the frost point for extended periods of time [Fahey *et al.*, 1990]. However, the mechanism by which denitrification occurs remains largely a mystery. It is difficult to explain observed levels of denitrification through "direct" microphysical models of either Type 1 or Type 2 PSC formation [see e.g., Salawitch *et al.*, 1988; Toon *et al.*, 1990]. Type 1 PSC models generally produce particles that contain substantial amounts of condensed HNO_3, but which are too numerous and hence too small to precipitate at rates re-

quired to explain observed denitrification levels. Models assuming that Type 2 PSCs nucleate directly on preexisting Type 1 PSCs can produce precipitating particles, but the particles contain too little HNO_3 to account for observed denitrification levels. Other denitrification schemes have been proposed, such as the independent scavenging and irreversible removal of gas phase HNO_3 by falling Type 2 particles [Wofsy *et al.*, 1990], but these are supported by limited observations [Deshler *et al.*, 1994; Peter *et al.*, 1994].

A concern with the projected HSCT fleet is whether NO_x, H_2O, and/or particulate emissions from the fleet might increase PSC formation in the Arctic. PSC formation could produce more widespread denitrification and/or dehydration and hence trigger widespread Arctic ozone destruction. This is even more of a concern if ambient temperatures in the lower stratosphere in the HSCT era are lower than at present, as predicted by global climate models. Even without HSCT emissions, lower temperatures alone would increase the extent of PSC formation in the Arctic. There have been attempts to represent PSC microphysical processes in 2-D predictive models (see Section 3.2.4.6). However, since the basic mechanism for denitrification is unknown, one must conclude that the impact of HSCT emissions on Arctic PSC formation and denitrification cannot be predicted confidently. Understanding the mechanisms controlling denitrification will probably require detailed, process-oriented field measurements of temperature, HNO_3, H_2O, and particle size and composition. Since it is problematic to predict when and where denitrification will occur in the Arctic, the Antarctic appears to be the best place to collect the required observations.

3.2.4.3 Plume/Wake Aerosol Processing

Input for the HSCT fleet emission 2-D predictive models is achieved by simple dilution of the aircraft plume at the altitude of injection, with no chemical changes taking place, into a 1° longitude by 1° latitude by 1 km altitude grid. Omission of plume effects from the model input is supported by plume/wake model predictions for NO_y gas-phase species which show no significant conversion from NO_x to other NO_y species in that regime. However, near-field processing of SO_x emissions and near-field aerosol formation may not be similarly dismissed (see Section 3.1). Model results demonstrate that a large number of small particles can form via binary homogeneous nucleation of sulfur compounds [Miake-Lye *et al.*, 1994; NASA, 1993; Kärcher, 1995; Zhao and Turco, 1995; Brown *et al.*, 1995]. This has been confirmed by measurements in the Concorde plume which show that large numbers of small, persistent particles are rapidly formed in the engine or in the plume [Fahey *et al.*, 1995a].

Comparison of the particle mass measured in the Concorde exhaust with EI_{SO_2} inferred from fuel analysis [Fahey *et al.*, 1995a] indicates that at least 12 to 45% of the sulfur emitted from the aircraft is in the form of small particles less than one hour after emission. This result is consistent with earlier studies of plumes behind a stratospheric SR-71 aircraft [Hofmann and Rosen, 1978] and subsonic jets [Pitchford *et al.*, 1991; Whitefield and Hagen, 1995]. However, these results conflict with the plume chemistry model that predicted only 1% of the sulfur being converted to particles, based on OH-limited oxidation of SO_2 to H_2SO_4 [Miake-Lye *et al.*, 1994; Brown *et al.*, 1995]. Measurements of OH in the Concorde exhaust support the plume model contention [Fahey *et al.*, 1995a]. Therefore, the Concorde particulate measurements apparently indicate a rapid conversion of SO_2 to small sulfate particles via some unknown process. Together with the observation of small numbers of sulfate particles in an ER-2 plume encounter [Fahey *et al.*, 1995b], these results show that current understanding of plume chemistry and particle formation processes is not capable of predicting particle emission rates for different stratospheric aircraft.

The potential impact of HSCT-produced sulfate aerosols on ozone (see Section 3.2.4.5) raises the possibility of the need to reduce sulfur levels in the fuel. The sulfur content of jet fuel is currently ~0.04% by weight (EI_{SO_2} = 0.8), much less than the current maximum specification of 0.3%, and is expected to diminish in the future [Hadaller and Momenthy, 1989, 1993]. One other unknown is whether soot plays any role in the particle formation process (see Section 3.2.4.7). The Concorde plume encounter showed that one third of the particles had an involatile core (larger than 10 nm in diameter) that is most likely derived from soot emitted from the aircraft. It is clear that prediction of plume particle emissions from stratospheric aircraft plumes requires further modeling and field study of near-field aircraft chemical and microphysical processes.

3.2.4.4 Sensitivity of HSCT Ozone Perturbations to Ambient Sulfate Aerosol Loading

Injection of SO_2 from major volcanic eruptions over the past 20 years has caused episodic stratospheric sulfate aerosol mass loading increases of more than a factor of 10 [McCormick *et al.*, 1995]. These perturbations remain significant for three or more years; post-eruption total stratospheric aerosol mass decreases with a 1/e-folding time of approximately one year. It is difficult to define the true nonvolcanic (background) aerosol level because of the frequency of major eruptions, their lingering influence [Thomason *et al.*, 1995], and the possibility of a positive temporal trend linked to increasing subsonic aircraft emissions [Hofmann, 1990].

Fahey *et al.* [1993] presented ER-2 data illustrating the impact of heterogeneous processing by sulfate aerosols on mid-latitude NO_y chemistry. The observed NO_x/NO_y ratio decreased by a factor of 2 or less as aerosol surface areas increased from 0.5-5 $\mu m^2\ cm^{-3}$ to ~20 $\mu m^2\ cm^{-3}$. This result indicates a nonlinear dependence of the NO_y partitioning into reactive and reservoir species on surface area. The ratio of NO_x to NO_y should approach a low, constant value at surface areas of 5 to 10 times the nonvolcanic background.

Model calculations of the sensitivity of HSCT-induced chemical perturbations to ambient sulfate surface area have been performed by Weisenstein *et al.* [1993], Considine *et al.* [1995], Tie *et al.* [1994], and Ramaroson and Louisnard [1994]. The first two of these studies used the surface area distribution given in WMO [1992] to represent ambient conditions, and multiplied this distribution by a factor of 4 to represent the median aerosol loading observed over the past two volcanically active decades. Thomason and Poole [1995] show that the WMO distribution is very similar to the lowest 10-percentile SAGE II surface area distribution over the last decade, while the decadal median is, on the average, a factor of 2 to 3 higher than the 10-percentile distribution. Results of the Weisenstein *et al.* [1993] (Figure 38) and Considine *et al.* [1995] studies are similar, indicating that ozone depletion due to HSCT emissions is reduced as the ambient sulfate aerosol surface area is increased. It must be noted that these calculations assume that the ambient aerosol surface area is not affected by the HSCT emissions of sulfate or soot. The Tie *et al.* [1994] model included explicit sulfate aerosol microphysics to simulate the global distribution of aerosols produced by an eruption such as El Chichón. They found that during the post-volcanic period, the injection of NO_x from the HSCT fleet would actually increase the ozone column by interfering with the catalytic destruction of ozone by ClO_x.

3.2.4.5 Sensitivity of HSCT Ozone Perturbations to Fleet Sulfur Emissions

An important issue for a full assessment of the proposed HSCT fleet is whether the sulfur present in the aircraft exhaust could lead to sulfate aerosol surface area increases large enough to impact ozone. Sensitivity studies addressing this issue, including explicit sulfur chemistry and microphysics, have been performed by Bekki and Pyle [1993], Pitari *et al.* [1993], and Tie *et al.* [1994]. Using $EI_{SO_2} = 1$, two of these studies predict surface area increases of 20 to 50% relative to the nonvolcanic background, with a small decrease in calculated ozone depletion due to the HSCT emissions. Bekki and Pyle [1993] predict a doubling of aerosol surface area in the northern lower stratosphere due to HSCT flights, probably because they assumed an EI for sulfur of 2 g/kg fuel. As would be expected, they also show a more substantial reduction in the sensitivity of ozone to the HSCT NO_x emissions, accompanied by an increased sensitivity of ozone to chlorine. These studies all assumed that the sulfur was emitted by the engines as SO_2 so that it would condense onto preexisting particles.

A recent study by Weisenstein *et al.* [1995] used a 2-D model with coupled sulfur chemistry and aerosol microphysics to examine the combined effects of NO_x, sulfur, and water vapor emitted by HSCTs. The results are summarized in Table 5. Of particular interest are the results in the last row, where all the sulfur is assumed to be emitted as small particles or to form small particles rapidly in the aircraft wake. The impact of small particles on the calculations depends in a complicated way on EI_{NO_x} and background chlorine. For $EI_{NO_x} = 5$ g/kg fuel, the calculation of ozone change is more negative when small particles are formed; the perturbation is as large or larger than that for the $EI_{NO_x} = 15$ g/kg fuel case. Inclusion of the reaction of $BrONO_2$ with water on aerosols increased the effect of the small particles.

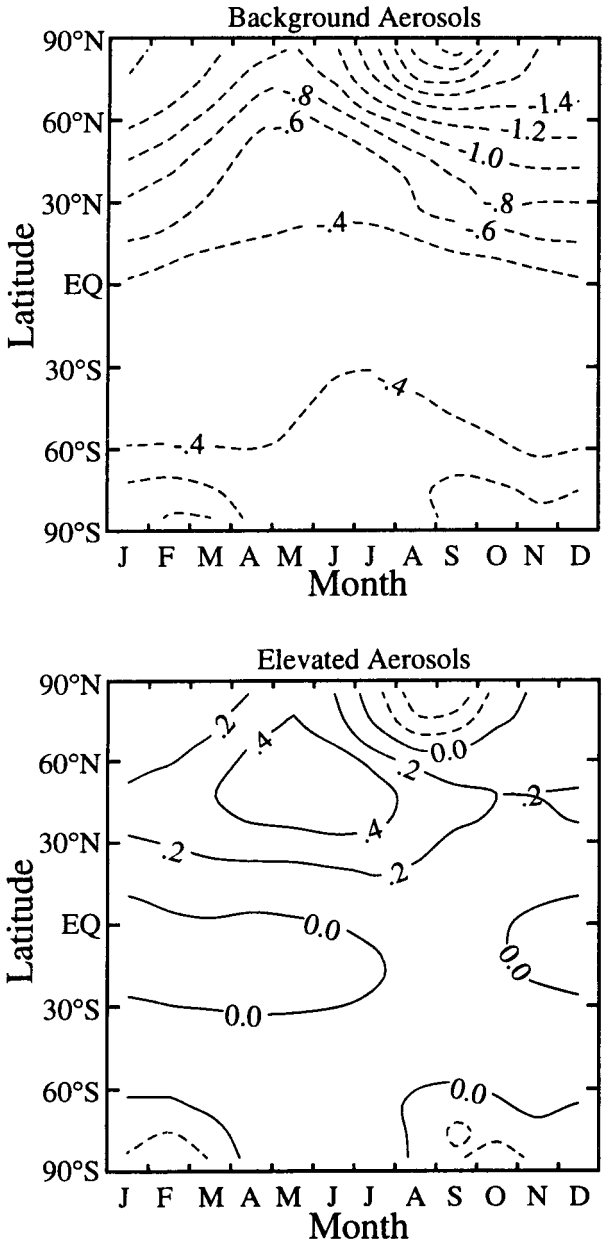

Figure 38. Calculated change in column amount of ozone as a function of month and latitude for a Mach 2.4 HSCT fleet with EI_{NO_x} = 15 g NO_2/kg fuel from the AER model; a) aerosols held fixed at background as defined in WMO [1992], and b) aerosols fixed at four times background (approach discussed in Weisenstein *et al.* [1993]).

This occurs because the increased surface area changes the mid-latitude chlorine partitioning in the model. It is important to note that the Weisenstein *et al.* [1995] calculation represents the extreme case. This calculation assumed that all of the emitted sulfur formed persistent small particles, thus maximizing the perturbation in surface area. (See Section 3.2.4.3 for discussion of uncertainty regarding this point.) Another assumption was that the perturbation was added to a nonvolcanic aerosol background produced by photolysis of tropospheric source gases only. If the stratospheric sulfate layer were already perturbed by volcanic activity, then saturation of the N_2O_5 hydrolysis reaction should reduce the sensitivity to aerosol surface area added by the HSCT. Thus, more attention must be given to the role of HSCT exhaust products on changing the background aerosol surface area in a future stratosphere containing lower amounts of chlorine.

3.2.4.6 Sensitivity of HSCT Ozone Perturbations to Inclusion of PSCs

Heterogeneous reactions on PSCs cause dramatic chemical perturbations in the polar regions, and there is concern that HSCT exhaust products might lead to an increase in PSC occurrence or to changes in their microphysical characteristics which would ultimately affect ozone. The models used for the basic HSCT perturbation calculations do not include PSCs, because of microphysical uncertainties and also because of fundamental limitations in the 2-D representation. For example, data from the Stratospheric Aerosol Measurement (SAM II) show that PSC sighting probability is not zonally symmetric, especially in the Arctic, with higher probabilities occurring in lower-temperature regions [Poole and Pitts, 1994]. Likewise, it is difficult for 2-D models to treat variations in sunlight experienced by a PSC-processed air parcel as it moves around the polar vortex when the vortex is displaced or elongated. Finally, it is difficult for these models to predict the transport (or lack thereof) to lower latitudes of air parcels that have been chemically processed by PSCs in the polar vortices.

Nonetheless, several groups have used 2-D models that include simplified representations of PSC processes to investigate the impact of HSCT emissions on stratospheric ozone [Pitari *et al.*, 1993; Considine *et al.*, 1994; Tie *et al.*, 1994]. All the models assumed that Type 1 PSCs form as NAT, but they incorporated different representations of the cloud particles and temperature excursions. Pitari *et al.* [1993] included an explicit particle microphysics code with PSC nucleation delayed until reasonable levels of vapor supersaturation were reached. The temperature at each model grid point was treated statistically

Table 5. Calculated change in annual average ozone column at 57°N due to emissions of a Mach 2.4 HSCT fleet including the effects of NO_x, H_2O, and sulfur. Results shown are for EI_{SO_2} = 0.4 g per kg fuel burned and EI_{NO_x} = 5 and 15. All calculations have been done for background inorganic chlorine amounts of 3 ppbv and 2 ppbv. [Adapted from Weisenstein *et al.*, 1995]

SO_2 Emission (EI_{SO_2} = 0.4)	Aerosol Surface Area Change	EI_{NO_x} = 5		EI_{NO_x} = 15	
		3 ppbv	2 ppbv	3 ppbv	2 ppbv
UNEP aerosols [a]	0%	-0.4%	-0.6%	-1.1%	-1.6%
0% SO_2 as particles	30%	-0.5%	-0.6%	-0.7%	-1.1%
10% SO_2 as particles	50%	-0.7%	-0.7%	-0.7%	-1.0%
100% SO_2 as particles	150%	-1.0%	-0.8%	-0.8%	-0.9%

[a] UNEP aerosol refers to an atmosphere with a background stratospheric aerosol amount equivalent to a relatively clean period between major volcanic eruptions. None of these scenarios included the effects of polar stratospheric cloud chemistry. [WMO, 1992]

by assuming a normal distribution, with a mean temperature equal to the monthly zonal average value and a standard deviation derived from global-atmospheric circulation statistics from 1958 to 1983. PSC condensation probabilities calculated using this approach appear to be somewhat lower than the climatological SAM II data. Considine *et al.* [1994] represented grid-point temperatures by empirical probability distributions derived from National Meteorological Center (NMC) data for the period January 1989 to May 1992. This model also required modest supercoolings before PSCs were allowed to form. PSC particle surface areas were determined by allowing HNO_3 and H_2O to condense onto log-normal distributions with fixed-mode radii of 1 μm for Type 1 PSCs and 10 μm for Type 2 PSCs, and a geometric standard deviation of 1.8 for both cloud types. Cloud formation probabilities calculated by Considine *et al.* [1994] agreed fairly well with the SAM II data.

Both the Pitari *et al.* [1993] and the Considine *et al.* [1994] studies found that inclusion of PSCs generally reduced the sensitivity of model ozone to HSCT emissions. For example, Pitari *et al.* [1993] found that HSCT-induced Northern Hemisphere mid-latitude ozone depletion decreased from 1.5% to 0.5% when the PSC formulation was included in the model. This decrease is due primarily to enhanced NO_y removal by the PSCs, which shortens the residence time of the NO_x emitted by the HSCT fleet. However, the NO_y removal rates computed in these models may be artificially large due to their simplified particle microphysics representations. Both studies noted an important exception to this reduced sensitivity in Antarctic spring, when larger PSC surface areas caused by the HSCT emissions extend the duration of PSCs into late October and November. This results in an extended time period in which the chlorine catalytic cycle operates efficiently and, thus, leads to more ozone loss than in model runs excluding PSCs. Other calculations used Type 1 PSC mode radii of 0.5 μm and 2 μm (a crude test of NO_y removal rates); these yielded global ozone depletions that differed only slightly from that of the standard run. The second sensitivity study used both 1980 and 1990 atmospheric chlorine amounts (~2.0 and ~3.5 ppbv, respectively). With inclusion of the PSC parameterization, the higher chlorine level reduces the sensitivity of ozone to HSCT emissions, with the exception again of the Southern Hemisphere high-latitude spring, where more ozone depletion was predicted to occur.

The 2-D model study by Tie *et al.* [1994] allowed PSCs to form at temperatures several degrees K above their thermodynamic thresholds to account for the fact that zonal-mean temperatures are somewhat higher than those where PSCs are most likely to form. This study did not include a microphysics representation, but instead prescribed time constants for the pertinent heterogeneous reactions and for NO_y

and water vapor removal. PSC-formation temperatures were raised by an additional 1 K to account for HSCT-induced increases in HNO_3 and H_2O vapor. Tie *et al.* [1994] found a substantial (6%) reduction in ozone column abundance at high northern latitudes in late winter and early spring, but this result is highly uncertain due to the simplicity of their PSC representation parameterization.

Pitari and Visconti [1994] used their 2-D model to evaluate the effect of an HSCT fleet in an atmosphere where the CO_2 concentration was increased from 335 to 500 ppmv. The lower temperatures in this atmosphere led to a large enhancement in NAT surface areas in the Arctic and, hence, to more NO_y removal and a reduced effect of the added NO_x from an HSCT fleet. They also used a 3-D circulation model to calculate a change in the transport rates in a CO_2-perturbed atmosphere. They found that the stratospheric residence time of HSCT emissions was 15% shorter than in an atmosphere with the present amount of CO_2. This leads to less buildup and, consequently, smaller perturbations in NO_x concentrations.

All these sensitivity studies indicate that including the effects of PSCs may be important for improving the accuracy of the 2-D predictive models. The representation of PSC formation in the 2-D models by statistical temperature fluctuations about the zonal-mean values reasonably matches observed PSC occurrences, but the photochemical results have not been tested against atmospheric observations. Fundamentally, the 2-D representation, and the relatively simple microphysical assumptions included within it, contrast with the complex and variable behavior inferred from the laboratory studies and field observation of PSCs. Thus, confidence in the ultimate results of the models - ozone depletion resulting from HSCT emissions - would increase with a more accurate treatment of PSC microphysics, including an assessment of uncertainties in particle composition and denitrification mechanisms.

3.2.4.7 Impact of Soot on Aerosols

Although an extensive database exists for conventional aircraft soot emissions, it is comprised of "smoke number" data, an industry-standard measure that can be related to total mass but not to particle size or density. Since the atmospheric effects of particles depend on their effective surface area and reactivity, the total soot mass is not particularly useful and does not effectively constrain atmospheric model usage of soot emissions. In addition, the plume evolution of the soot particles is highly uncertain, involving competition between nucleation, gas-to-particle condensational growth, and coagulation. In view of these uncertainties and the lack of laboratory data on direct gas/soot interactions, soot is not considered explicitly in the assessment model scenarios.

Recent experimental data have been collected from ground-based jet engine tests and *in situ* plume encounters [Hagen *et al.*, 1993; Whitefield *et al.*, 1993; Whitefield and Hagen, 1995; Pitchford *et al.*, 1991; Baumgardner and Cooper, 1994; Schumann *et al.*, 1995; Fahey *et al.*, 1995a, b]. The general conclusions of such tests are that nascent soot emissions follow a log-normal size distribution with a peak around 0.05 μm. Total number densities are on the order of 10^6 cm^{-3}, resulting in soot EIs on the order of 0.01 g/kg fuel. Latitude surveys of soot abundance in the lower stratosphere and upper troposphere also have been made using wire impactors exposed at altitude [Pueschel *et al.*, 1992; Blake and Kato, 1995]. These show that the latitudinal distribution of soot at 10 to 11 km altitude between 90°N and 45°S covaries with commercial air traffic fuel use. Lower stratospheric soot measurements in the 40°N to 60°N latitude band range from 0.25 to 3.35 ng m^{-3}, averaging ~2 ng m^{-3}, while those in the Southern Hemisphere range from 0 to 0.6 ng m^{-3}, with an average of 0.1 ng m^{-3}.

Collectively, these measurements suggest that HSCT soot emissions could possibly increase the natural stratospheric soot background by a factor of 2 to 3. It should be noted that the natural stratospheric soot mass loading is only ~1% of that of stratospheric sulfate. However, under the extreme assumption that all of the emitted soot particles become activated as CN for H_2O and H_2SO_4, the resulting sulfate aerosol surface area will rival that of the ambient background. Potential CN activation is particularly important in the near-field region behind the aircraft. It is also possible that HSCT-emitted soot particles will serve as nuclei for cirrus cloud formation and potentially alter cirrus properties or formation mechanisms.

3.3 Analysis of Uncertainties

In Chapter 2, a number of 2-D models were used to predict the impact of a fleet of HSCTs on ozone. For

a Mach 2.4 fleet of 500 airplanes with an assumed EI_{NO_x} = 5 g/kg fuel, the models calculated a perturbation to the total column amount of ozone averaged over the Northern Hemisphere which ranged from +0.1% to -0.3%. These calculations were made with models using the reaction rates and photolysis cross sections recommended in the 1994 JPL kinetics review [DeMore *et al.*, 1994]. Results of similar calculations with the same models for higher EIs of NO_x (10 and 15 g/kg fuel) and for cruise altitudes of 1 km above and 2 km below the nominal Mach 2.4 cruise altitude are summarized in Chapter 2.

The calculations are uncertain for a number of reasons discussed above. These uncertainties can be classified in two ways: those which may be evaluated directly through parametric studies in an existing model (e.g., the impact of uncertainties in input reaction rate coefficients), and those for which we do not have sufficient information to do this completely (e.g., model representation of transport and the effect of PSCs). The first class of uncertainties are quantifiable at a specified confidence level; the second class is not yet quantifiable, but still affects the overall confidence of the prediction. The results of parametric studies, which have been completed as a Transport uncertainties have proven to be more difficult to quantify. Although there has not been a single comprehensive study of the sensitivity of the prediction of HSCT effects to dynamical uncertainties, there have been systematic efforts to evaluate some individual uncertainties as they have been identified.

Stratosphere-troposphere exchange is very important for the fate of exhaust emissions in the lower stratosphere, because it determines where and how fast the polluted air exits to the upper troposphere. The scale and type of dynamical processes which are responsible are either too small (e.g., tropopause folds near jet streams) or longitudinally dependent (e.g., the upward extension of monsoonal circulations) to be represented in 2-D models. Such uncertainties will be difficult to quantify because even state-of-the-art 3-D models have not been tested against observations in this regard. For the current assessment, the five 2-D models show very little difference in the total perturbed amount of NO_y (range from 3.5 to 4.3 x 10^{15} molecules cm^{-2} in the global-average column). The 3-D model described in Section 3.2.2 calculated perturbed NO_y within this same range. These calculations are consistent with a part of this assessment report, are summarized here. Where parametric studies are incomplete or unavailable, the processes which lead to uncertainty in the models are identified for future work.

The uncertainties in gas-phase reaction rate coefficients have been propagated through one of the 2-D predictive models using the Monte Carlo approach. This resulted in an uncertainty of approximately 1% (1 σ) averaged over the Northern Hemisphere. Inclusion of uncertainties in the input cross sections for photolysis and heterogeneous reactions would increase the range of calculated values. Comparing the results for many model cases for the current atmosphere with atmospheric measurements of key radical concentrations narrows the range for the calculated ozone change because not all of the model cases are consistent with these measurements.

The effect of $BrONO_2$ hydrolysis, while absent from the suite of 2-D predictive models, has been evaluated and makes the predicted perturbation less negative by a few tenths of a percent. This is consistent with our understanding of the role of this reaction in converting NO_x to HNO_3 in low-temperature stratospheric regions.
stratospheric residence time for aircraft exhaust of 13 to 16 months.

A further test was to use dynamical inputs from the GSFC model in the AER model. The resulting perturbation to ozone was less negative than the AER value, but more negative than the GSFC value. This indicates that a significant portion of the difference between the models is due to the representation of dynamics. However, the differences were not due to the total steady-state accumulation of HSCT pollutants. Rather, the dynamics in the separate 2-D models create differences in constituents such as ozone and NO_y that are affected by transport in the model base atmosphere and differences in transport of pollutants to higher altitudes.

The question of the effect of the zonal asymmetry of the pollutant source has been investigated using a 3-D calculation. The maximum accumulations in flight corridors differ from the zonal mean by only a factor of 2. Since the photochemistry is expected to be linear over this range, the uncertainty in the 2-D calculation introduced by the "corridor effect" is small compared with other uncertainties.

The transport between the tropics and mid-latitudes is poorly represented in current 2-D models. The importance of the tropical pipe concept was tested through arbitrary restriction of subtropical diffusion coefficients in the AER model. This produced a calculated perturbation which was slightly more positive than the result for AER in Chapter 2 (see Table 4). This is qualitatively consistent with the idea that the barrier restricts the transport of aircraft effluent from mid-latitudes to the tropics, allowing efficient transport to high altitudes where NO_x catalysis of ozone destruction is rapid. However, the assumed altitude dependence of the barrier suggests that this study does not represent the extreme case because of competing effects. The existence of a barrier to transport between the tropics and mid-latitudes reduces the amount of exhaust gases which can be transported to high altitudes. The worst-case scenario for ozone depletion would be a leaky barrier in the lower stratosphere, allowing exhaust gases from the mid-latitudes to reach the tropics, and a stronger barrier above, effectively confining the gases and allowing them to reach high altitudes. This case should be evaluated.

As discussed in Section 3.2.4.6, the 2-D models used in this assessment do not include the effects of PSCs. The important processes are inherently difficult to represent in a 2-D framework. Several groups have used models which attempt to overcome these difficulties, such as the nonuniform distribution of winter temperature with longitude. Over most of the globe, the model response is generally less negative because models with PSCs have more chlorine-catalyzed ozone destruction which is damped by addition of NO_x. At high-latitude spring, the model response is more negative due to increased persistence of PSCs as a result of more HNO_3 and H_2O. The formation of PSCs is a strong function of temperature, H_2O, and HNO_3, and the chemical response is nonlinear both as a result of the threshold process and model sensitivity to sedimentation of PSC particles, which permanently remove NO_y. Calculations to date do not represent the range of possible answers for the impact of PSCs on the HSCT perturbation. However, it should be noted that the importance of chlorine-catalyzed ozone destruction resulting from PSC processes will decrease as chlorine from man-made gases decreases during the next century.

A recent study [Weisenstein *et al.*, 1995] considered the impact of sulfur in the exhaust on the stratospheric sulfate particle surface area. The impact depends critically on the form of the sulfur in the exhaust. If small particles are formed, as indicated in the ER-2 measurements of the Concorde plume [Fahey *et al.*, 1995a], then the increase in sulfate surface area is maximized. Under the extreme condition of small particles forming from all of the available sulfur in the fuel and being emitted into a nonvolcanically perturbed stratosphere, the calculated ozone change for the HSCT perturbation is ~-1%. The impact of the production of small particles on calculated ozone change depended on both EI_{NO_x} and background chlorine amount.

If the range of the parametric sensitivity tests is taken as an estimate of uncertainty and these results are combined, the overall uncertainty due to the processes not included in the basic scenarios is equal to or greater than the reaction-rate uncertainty. For all of the uncertainties, the model results must be constrained by observations. For example, the extreme condition of the tropical pipe must produce tracer distributions which are compatible with UARS and ER-2 observations. This may reduce the estimates of uncertainties, and is an approach which should be pursued in the future.

The Monte Carlo uncertainty propagation showed that the maximum uncertainty is in the high-latitude lower stratosphere. This is true without any consideration of PSCs. The uncertainty at high latitudes is significantly larger when considering that condensibles from aircraft exhaust could change the PSC formation probability. Of particular concern is the possibility that the increase in HNO_3 and H_2O could change the conditions in the Arctic to be more like the Antarctic, in which the total NO_y levels are significantly reduced during Antarctic spring through processes associated with PSC formation that are not well understood. Since this loss of NO_y is responsible for allowing the chlorine-catalyzed ozone destruction to proceed unchecked during the Antarctic spring, it is important to improve understanding of the possible role of the aircraft effluent in producing conditions that would lead to large-scale permanent removal of NO_y from the Arctic lower stratosphere.

The evaluations described above were all for a projected 2015 atmosphere with low levels of sulfate area and two different values of chlorine concentration (3 ppbv and 2 ppbv). The 2015 atmosphere itself is not certain. The sulfate surface area may be

affected by future (unpredictable) volcanic eruptions. Atmospheric CO_2 is increasing, which may lead to changes in the atmospheric temperature structure and to the atmospheric circulation. The effects of these conditions may be evaluated with sensitivity studies.

Not all of the processes are included in this uncertainty estimate, and including better estimates for processes such as the effect of PSCs may lead to a higher estimate of overall uncertainty. However, there will be a higher level of confidence in the uncertainty estimate when all identified processes are included realistically.

4 SUMMARY

This report is an assessment of the potential atmospheric effects of a proposed fleet of HSCT aircraft based on the current scientific understanding of the atmosphere. Recent advances in that understanding allow us to make more definitive statements about potential HSCT effects than were possible in past assessments. The assessment consists of three parts. The first is a description of how recent advances have improved our understanding of the stratosphere and how it works. Second is a set of calculations of the potential impacts of an HSCT fleet. These calculations were made by 2-D atmospheric models that attempt to include all of the latest advances in understanding for the important processes controlling ozone. The last is a discussion of the shortcomings in our understanding and in the model representations of atmospheric processes. These shortcomings lead to a discussion of the uncertainties inherent in our predictions. These uncertainties can be only partially quantified.

4.1 Plume Measurements

The evolution of the exhaust plume in the atmosphere and conversions of the exhaust components have been addressed with new *in situ* aircraft exhaust sampling experiments and modeling of engine processes and the dilution of exhaust gases in the atmosphere. Measurements of NO_y species, CN, and CO_2 were recently made in the exhaust of the Concorde supersonic aircraft and the NASA ER-2 subsonic aircraft while in flight. The EIs were calculated independently of plume dynamics because measurements of CO_2 provide a measure of fuel burned. The measured EI of NO_x, expressed as grams of equivalent NO_2 per kilogram of fuel burned, is in excellent agreement with earlier results deduced from altitude chamber measurements of exhaust from the Concorde engine as part of CIAP. These results suggest that the methodology developed to calculate the EI of NO_x at cruise from altitude chamber data will be appropriate to evaluate new HSCT engines.

Observations show that NO_x is the most abundant NO_y species in both supersonic and subsonic aircraft plumes. The presence of only a small percentage of HNO_3 and HONO is in agreement with observations of HO_x in the plume and theoretical model calculations.

The large number of detectable particles in the Concorde plume conflicts with the results of plume models that predict the formation of a large number of much smaller sulfate particles and a smaller fractional conversion of SO_x to condensed sulfate. These results indicate that current understanding of plume chemistry and particle formation processes is not complete. If new HSCT aircraft produce particles at a rate comparable to the Concorde, significant increases in particle number and surface area could occur in the lower stratosphere of the Northern Hemisphere. Including these increases in predictive models could change calculated ozone and climate impacts from an HSCT fleet.

4.2 Predicted Changes

Five 2-D photochemical models were used to calculate the impact of an HSCT fleet for a variety of cases including sensitivity tests for the EI of NO_x, cruise altitude, background atmospheric chlorine amount, and fleet size. Individual models were used to test sensitivity to a variety of effects not included in these basic predictive calculations. Conditions include a baseline fleet of 500 Mach 2.4 aircraft burning 8.2×10^{10} kg of fuel per year in an atmosphere with a background stratospheric aerosol amount equivalent to a relatively clean period between major volcanic eruptions. The models do not include the formation or reactivity of PSC particles.

For a fleet of 500 Mach 2.4 HSCTs with EI_{NO_x} = 5 g NO_2/kg fuel, the model-calculated effect of the emission of NO_x and H_2O on the total column amount of ozone in the Northern Hemisphere ranged from -0.3% to +0.1%. The calculated total ozone change generally increases with increasing emission index for NO_x. At EI_{NO_x} = 15 g NO_2/kg fuel, the range of average values from the five models was -1.0% to -0.02%. The calculated total ozone change depends on the cruise altitude of the aircraft. For the case of 500 HSCTs with EI_{NO_x} = 5 g NO_2/kg fuel, increasing the assumed fleet altitude by 1 km results in a model range for the perturbation of -0.5% to +0.02% averaged over the Northern Hemisphere. Decreasing the cruise altitude by 2 km (approximately equivalent to a Mach 2.0 fleet) resulted in a calculated range of -0.06% to +0.1%.

For an assumed fleet size doubling to approximately 1000 aircraft, the calculated perturbation of the average total ozone over the Northern Hemisphere for EI_{NO_x} = 5 ranged from -0.7% to +0.03%. At EI_{NO_x}= 15 g NO_2/kg fuel, the range was from -2.7% to -0.6%.

Reduction of the assumed background chlorine amount from 3 ppbv (projected 2015 concentration) to 2 ppbv (projected 2050 concentration) makes the calculated HSCT perturbation of Northern Hemispheric total ozone somewhat more negative; a range of -0.4% to +0.02% for EI_{NO_x}= 5 g NO_2/kg fuel.

The calculated changes in ozone result from a decrease in the middle and upper stratosphere and an increase in the lower stratosphere and troposphere. The time required for photochemistry and transport to effect these ozone changes precludes large ozone changes near the assumed HSCT flight corridors. The EI_{NO_x} values reflect those expected for future HSCT combustors (5 g NO_2/kg fuel) and those closer to current engines (15 g NO_2/kg fuel).

Four of the five models used in the calculations were tested against two benchmarks, one for photolysis rates and one for chemistry. These indicate mostly minor differences, implying that the range in model results follows, at least in part, from differences in the 2-D representation of dynamics. The chemistry benchmark tested the model chemistry integrators against a photochemical steady-state model that has been used in detailed comparisons with atmospheric measurements of key radicals involved in the chemistry of stratospheric ozone.

When the background aerosol surface area used in the models is increased by a factor of 4 (roughly equivalent to the median amount in the stratosphere over the last 2 decades), the calculated perturbation to total ozone is less negative by a few tenths of a percent. Variations in future stratospheric aerosol levels, primarily due to the frequency of large volcanic eruptions, are a source of uncertainty in HSCT ozone impact predictions.

Sulfur emitted by a fleet of HSCTs can increase the sulfate aerosol surface area throughout the lower stratosphere. Although the increase in surface area decreases the impact of NO_x emissions, it also increases ozone loss due to the existing chlorine and hydrogen radicals in the stratosphere. If the sulfur emitted by HSCTs immediately forms small particles in the plume, then the global increase in sulfate surface area is maximized.

A model that included aerosol processes was used to calculate ozone changes when 100% of the sulfur (EI_{SO_2} = 0.4 g sulfur/kg fuel) from an HSCT fleet was emitted as small particles into a volcanically unperturbed stratosphere. The change in total column ozone from the injection of small particles depended in a complex way on EI_{NO_x} and background chlorine amount. For EI_{NO_x} = 5 g/kg fuel, the calculated ozone depletion increased when small particles were formed; the overall perturbation became as large or larger than that for the EI_{NO_x} = 15 g/kg fuel case. Inclusion of the reaction of $BrONO_2$ with water on aerosols increased the effect of the small particles.

The model results for ozone change in the basic scenarios vary more widely when heterogeneous reactions on PSCs are included. This results from uncertainty in PSC microphysical processes and from ambiguity in how to best represent such processes in a 2-D model.

A GCM was used to calculate the global surface air temperature and stratospheric temperature responses to predicted changes in ozone and water vapor from a fleet of HSCTs with EI_{NO_x}= 15 g NO_2/kg fuel. Since the resulting changes in temperature are smaller than the climatic fluctuations in the model, they likely would not be detectable in the atmosphere.

Climate effects due to sulfur and soot emissions, while likely to be small, have yet to be evaluated. Formation of persistent contrails from HSCTs is expected to be infrequent.

4.3 Model/Measurement Comparisons

Atmospheric observations can provide tests of our understanding of the photochemical and transport processes responsible for controlling the distribution of ozone and the potential impact of HSCTs. Laboratory measurements define the formulation of chemistry in models. Subsets of this formulation are tested by comparing the model predictions against a sufficiently complete set of atmospheric observations. Although constraints on transport formulations in 2-D models are less direct, observations of

the distribution of and the correlations between long-lived gases provide a test of these formulations. An extensive series of 2-D model tests, conducted in 1992 [Prather and Remsberg, 1993], led to improvements in the models and an understanding of the differences among them. Comparisons to observations made since that time are ongoing, as are further model improvements.

Models reproduce the basic features of the ozone column and vertical profile. Consistent with observations, the models suggest that ozone concentrations should have decreased in the past decade. However, the predicted changes are smaller than those measured by a factor of 1.5 to 2, particularly in the lower stratosphere. Inclusion of a realistic representation of the temporal changes in stratospheric sulfate aerosol in a model improves the agreement with the observed trends, but the predicted changes are still smaller than observed. These differences suggest that important uncertainties remain in the ozone changes calculated for an HSCT fleet.

Model simulations reproduce some, but not all, of the basic features of the distribution of long-lived trace gases in the stratosphere. Since trace gases are the sources of the free radicals that catalyze ozone removal, model-measurement differences reflect inaccuracies in the model transport formulation and affect comparisons of reactive species calculations with measurements.

Important regions for simulation of atmospheric transport are those with high spatial gradients in long-lived species such as N_2O, NO_y, or ozone. Examples are the regions in the stratosphere between the tropics and subtropics and at the edge of the polar vortices in winter. Aircraft and satellite observations have increased the level of understanding of the gradients and the barriers to transport that create them. In general, the 2-D models used to predict HSCT effects exhibit weak gradients, suggesting that they have too much mixing across these barriers.

Observations of HO_x, NO_x, ClO_x, and BrO_x in the stratosphere allow direct evaluation of the photochemical destruction cycles of ozone. Above 25 km altitude, observations of HO_x and NO_x free radicals agree with photochemical models to within ~40% when the models are constrained by observed abundances of long-lived chemical species, temperature, aerosol surface area, and overhead ozone column. Observations of ClO at these altitudes are up to a factor of 2 lower than model predictions. Below 20 km, midday observations of HO_x, NO_x, ClO_x, and BrO_x also generally agree with similarly constrained models to within ~40%. However, HO_x observations exceed model calculations by more than a factor of 3 near sunrise and sunset, times when HO_x concentrations are small. Incorporation of the reaction of $BrONO_2$ with H_2O on sulfate aerosols reduces this discrepancy but increases the discrepancy in other species. Between about 20 and 25 km, observations of HO_x and ClO_x radicals are not available to provide a rigorous test of models.

The observations and modeling of NO_x, HO_x, and ClO_x free radicals in the lower stratosphere agree in showing that the concentrations of HO_x and ClO_x depend on NO_x radicals. When the NO_x concentration is low, such as observed in the lower stratosphere of the Northern Hemisphere during the fall of 1992 and spring of 1993, the HO_x and ClO_x/BrO_x reactions dominate the local ozone loss rates. Thus, according to model calculations, when NO_x from HSCTs is added to these regions, reductions in HO_x and ClO_x/BrO_x abundances generally result in reductions in local ozone loss rates.

Observations show that PSCs occur during the Antarctic winter and spring and Arctic winter. Heterogeneous reactions on these PSC surfaces activate large fractions of the available chlorine that can then destroy ozone in the presence of sunlight. Widespread ozone destruction does occur in the Antarctic because sedimenting PSC particles also denitrify the stratosphere and alter the buffering of ClO_x by NO_x. The proper inclusion of PSC processes in the 2-D predictive models would reduce an important uncertainty in the HSCT impact results.

4.4 Uncertainties

Several classes of uncertainty are associated with predictions of HSCT impacts made with 2-D models as shown in Table 1. Uncertainties in some model parameters can be readily quantified and evaluated directly with the models. Other sources of uncertainty have been identified but not yet quantified. Finally, uncertainty from the possibility of missing processes or major errors in understanding cannot be quantified, but only discussed in terms of the overall confidence in the assessment.

The only quantified uncertainty in this assessment is that due to uncertainties in gas-phase reaction rate coefficients. These have been propagated through a model to give an estimated uncertainty of ~1% (1-σ) in the calculated ozone column perturbation in the Northern Hemisphere. Uncertainties in heterogeneous chemical reactions and photolysis rates will increase the overall chemical uncertainty. Constraining these results with atmospheric observations will reduce the uncertainty.

A number of parametric sensitivity tests were performed for processes not included in the basic assessment scenarios. If the combined range of these tests is taken as an estimate of uncertainty, the overall uncertainty due to the processes not included in the basic scenarios is equal to or greater than the reaction-rate uncertainty.

Uncertainties in microphysics include both the formation of numerous small particles in the HSCT exhaust plume and the possibility of increased denitrification in polar regions due to increases in condensible gases from the HSCT exhaust. Although the numerous small particles in the HSCT plume can indirectly affect ozone loss rates, the particle formation process is poorly understood and the uncertainties are large. Although the likelihood of a significant increase in Arctic denitrification and in polar ozone loss through chlorine and bromine chemistry is small, the implications of such processes for this assessment are large.

Uncertainties in model transport remain important and difficult to quantify. Observations of seasonally varying and short- and long-lived tracers provide diagnoses of the degree of mixing and rates of transport between tropical and mid-latitude regions of the stratosphere, as well as providing information on residence times for stratospheric trace species.

The impact of ozone and water vapor from HSCTs on climate was calculated to be within the climatic fluctuations of the model used. Thus, the expected perturbation and its uncertainty are difficult to quantify.

The possibility of missing processes in the models creates an unquantifiable uncertainty in the HSCT assessment. However, the probability that important processes have been overlooked decreases as we continue to explore HSCT perturbations with models and continue to challenge these models with atmospheric measurements.

4.5 Reducing Uncertainties

Future efforts to reduce the overall assessment uncertainty are expected to focus on the major unquantified uncertainties and attempts to quantify them. The primary methodology for improving our predictive capability continues to involve testing model representations of the atmosphere through comparison with observational data. Substantial progress in that direction will be realized in the near term by systematic comparisons with recent data from UARS, ATLAS on the Space Shuttle, and ER-2 aircraft, as well as a host of balloon platforms. Specific additional strategies for addressing the major uncertainties identified in this assessment are listed below in no specific order of priority:

- Extension of the observational database for long-lived tracers and radicals to include a number of seasonal cycles and undersampled regions of the atmosphere, notably the summer high latitudes and tropics.

- Systematic development of 3-D chemical-transport models for testing transport formulations and zonal-symmetry assumptions in 2-D predictive models.

- Inclusion of standardized descriptions of particle formation and evolution in 2-D predictive models and comparison with global aerosol distributions derived from existing satellite and aircraft data.

- Further characterization, through laboratory and atmospheric observations, of the composition and temporal evolution of aircraft exhaust aerosols in the wake/plume regime, and of the composition and microphysics of PSCs.

APPENDICES

APPENDIX A

CHANGES TO THE 2-D PREDICTIVE MODELS SINCE THE 1993 NASA INTERIM ASSESSMENT OF THE ATMOSPHERIC EFFECTS OF STRATOSPHERIC AIRCRAFT

AER

Malcolm Ko, Debra Weisenstein, Jose Rodriguez, and N. D. Sze
Atmospheric and Environmental Research, Inc.

1) The vertical resolution has been increased by a factor of 3, from 3.5 km to 1.2 km.

2) Temperatures are now the National Meteorological Center (NMC) 8-year climatology which was used as the standard in the 1993 Models and Measurements Workshop [Prather and Remsberg, 1993]. Tropopause heights are computed monthly based on temperature gradients.

3) The AER code for calculation of photolysis rates has been replaced by the code of Michael Prather, which was used as the standard in the 1995 intercomparison exercise.

4) The AER model now calculates water (H_2O) concentrations in the stratosphere. Tropospheric values of H_2O are based on assumed relative humidities.

5) The reactions rates have been updated to DeMore *et al.* [1994]. The species nitrous acid (HONO) and bromine chloride (BrCl) have been added to the model, along with a number of reactions. Sticking coefficients from Hanson and Ravishankara [1994] are now used for the reactions

$$HCl + ClONO_2 \rightarrow HNO_3 + Cl_2,$$
$$ClONO_2 + H_2O \rightarrow HNO_3 + HOCl, \text{ and}$$
$$HOCl + HCl \rightarrow H_2O + Cl_2 \text{ on sulfate aerosols.}$$

CAMED

J. S. Kinnersley, R. S. Harwood, Y. V. Roberts, and J. A. Pyle
University of Cambridge/University of Edinburgh

The model has been improved since Kinnersley and Harwood [1993] in the following ways, as documented in Kinnersley [1996]. A spectrum of gravity waves is emitted from the tropopause which help to produce realistic stratospheric and mesospheric winds and temperatures; in particular, a tropical-winter mesospheric jet and a good semiannual oscillation. The three planetary waves now interact with each other, leading to improved behavior [Kinnersley, 1995], and the troposphere has been made more interactive. The chemistry has been updated with the JPL-94 rates [DeMore *et al.*, 1994] and some more reactions have been included. Heterogeneous chemistry now incorporates Hanson and Mauersberger [1988] Type 1 polar stratospheric cloud (PSC) onset and surface area calculations with Tabazadeh and Turco [1993] reaction probabilities in the calculation of PSC reaction rates. The radiation scheme now includes a treatment of multiple scattering from air molecules.

CSIRO

Keith Ryan, Lakshman Randeniya, Peter Vohralik, and Ian Plumb
Division of Applied Physics
Commonwealth Scientific and Industrial Research Organization, Australia

This model did not participate in the 1993 Atmospheric Effects of Stratospheric Aircraft (AESA) Interim Assessment or the 1992 Models and Measurement Workshop. A description of the model is provided below.

Introduction

The model domain extends from 90°S to 90°N and from the ground to 80 km. Model grid cells are 2 km by 5 degrees and are centered at 87.5°S, 82.5°S, ..., 87.5°N latitude and 1, 3, ..., 79 km altitude (log-pressure vertical coordinates, $z^* = 16 \cdot \log_{10}(1000/p)$), where z* is in km and p is in mbar. Diabatic residual circulation together with appropriate diffusion terms provide the dynamics transport. The chemistry module is family-based and employs full diurnal averaging methods. Long-lived species are transported over 10-day intervals using a transport time step of 0.25 days. After each 10-day transport interval, solar fluxes are updated, diurnal averaging is done to calculate diurnal coefficients, and 24-hour-average concentrations of equilibrium species are determined (including the partitioning of transported family totals). The CSIRO model uses a 360-day year, with updating of solar fluxes, diurnal coefficients, and equilibrium species carried out every 10 days.

Transport

Derivation of Residual Circulation

Residual circulation velocities for the model are calculated from heating rates and observed temperatures using a full solution of the energy conservation equation as described by Solomon *et al.* [1986b] together with continuity. Temperatures from the ground to 60 km are 8-year zonal- and monthly-mean NMC values obtained from the 1992 Models and Measurements database [Prather and Remsberg, 1993]. From 60 to 80 km, temperatures are from the Middle Atmosphere Program (MAP) database [Barnett and Corney, 1985]. Radiative heating rates from the ground to 60 km are as calculated by Rosenfield [1987] and obtained from the 1992 Models and Measurements database [Prather and Remsberg, 1993]. Above 60 km, because of the breakdown of local thermodynamic equilibrium (LTE) assumptions, cooling rates are calculated using a Newtonian cooling approximation with coefficients from Holton and Wehrbein [1980] and heating rates are calculated using parameterizations developed by Strobel [1978] and Schoeberl and Strobel [1978]. In the troposphere, latent and sensible heating rates are added to the radiative heating rates to obtain net heating rates. Sensible and latent heating rates are obtained from Dopplick [1974].

Advection

For a given model run, vertical velocities are calculated for the 12 months of the year at the beginning of the run. Both vertical velocities and temperatures are interpolated to the beginning of each 10-day transport interval. Horizontal velocities are then computed from the vertical velocities using continuity, small mass-conservation correction factors are applied to correct for departures from mass conservation (<1%) due to the process-splitting algorithm used to integrate the continuity equation, and horizontal eddy diffusion coefficients (K_{yy}) are derived for the current set of horizontal velocities.

Advection is implemented using the variable-order Bott scheme [Bott, 1989]. This method, which is a high-order implementation of the upwind scheme, is conservative and positive-definite and produces only small numerical diffusion. The 1995 AESA assessment results were obtained using the second-order version of the scheme.

Diffusion

Stratospheric eddy diffusion coefficients are computed self-consistently with the residual circulation using the method of Jackman *et al.* [1988], namely:

$$K_{yy} = 0.25 \cdot R_e \cdot v \cdot \tan(\text{latitude})$$

where R_e denotes the radius of the Earth. Where the calculated values fall outside the range $2 \times 10^5 < K_{yy} < 30 \times 10^5$ $m^2 s^{-1}$, they are reset to these limiting values. Stratospheric K_{yy} values between the poles and 80°N or S are set to 2×10^5 $m^2 s^{-1}$. Tropospheric K_{yy} values are set to 10.0×10^5 $m^2 s^{-1}$. Off-diagonal components of the diffusion tensor are included by assuming that diffusion occurs predominantly along isentropes [e.g., Jackman *et al.*, 1988].

Vertical eddy diffusion coefficient (K_{zz}) values are set to 4 $m^2 s^{-1}$ in the troposphere, 0.25 $m^2 s^{-1}$ between 21 and 42 km, and 0.1 $m^2 s^{-1}$ throughout the remainder of the stratosphere.

Tropopause Height

The CSIRO model uses an annually averaged zonal-mean tropopause height distribution obtained by averaging daily NMC tropopause data for the period 1983-1993. Tropopause heights used by the CSIRO model for latitudes 87.5°S, 82.5°S, ... , 82.5°N, 87.5°N, using the log-pressure coordinates defined above (i.e., z* values in km) are:

Latitude	z*	Latitude	z*	Latitude	z*
87.5°S	9.57	27.5°S	14.64	32.5°N	12.94
82.5°S	9.54	22.5°S	15.24	37.5°N	11.68
77.5°S	9.50	17.5°S	15.48	42.5°N	10.70
72.5°S	9.49	12.5°S	15.60	47.5°N	10.00
67.5°S	9.44	7.5°S	15.65	52.5°N	9.53
62.5°S	9.39	2.5°S	15.66	57.5°N	9.23
57.5°S	9.47	2.5°N	15.64	62.5°N	9.02
52.5°S	9.78	7.5°N	15.63	67.5°N	8.82
47.5°S	10.32	12.5°N	15.59	72.5°N	8.63
42.5°S	11.06	17.5°N	15.47	77.5°N	8.47
37.5°S	12.07	22.5°N	15.14	82.5°N	8.37
32.5°S	13.43	27.5°N	14.29	87.5°N	8.33

Treatment of H_2O

Stratospheric H_2O is determined by transporting H_2O in the stratosphere with a lower boundary condition of 3 parts per million by volume (ppmv) at the tropopause. Tropospheric H_2O is set to values determined by the Oort climatology where available [Oort, 1983] and the Stratospheric Aerosol and Gas Experiment (SAGE II) otherwise [Prather and Remsberg, 1993].

Emission Scenarios

Subsonic and high-speed civil transport (HSCT) emissions for nitrogen oxides (NO_x) (as odd nitrogen, NO_y), carbon monoxide (CO), hydrocarbon (HC) (as methane, CH_4) and H_2O (using EI_{H_2O} = 1230 gm H_2O/kg fuel) are calculated using the data files supplied by the National Aeronautics and Space Administration (NASA) for the CSIRO grid.

Additional Tropospheric NO_y Source

An upper tropospheric source of NO_y in included in the model. This NO_y source is included between 30°S and 30°N and from 4 to 12 km (model levels at 5, 7, 9, and 11 km), and between 25°S and 25°N from 12 to 14 km (model level at 13 km). The NO_y source strength used is 1100 cm^{-3} s^{-1}, corresponding to a total source of approximately 2 Mt N yr^{-1}.

Rainout and Surface Deposition

Rainout rates are included for transported family totals NO_y, inorganic chlorine (Cl_y), and inorganic bromine (Br_y), and for equilibrium species H_2O_2, formaldehyde (CH_2O), and methyl peroxide (CH_3OOH) for model grid cells below 10 km which are also more than 3 km below the tropopause. Rainout rates for individual members of NO_y, Cl_y, and Br_y are not explicitly included when partitioning these family totals. Rainout rates for model levels at z = 1, 3, 5, 7, and 9 km are 3.74 x 10^{-6}, 3.98 x 10^{-6}, 2.96 x 10^{-6}, 1.38 x 10^{-6}, and 0.42 x10^{-6} s^{-1}, respectively. In addition to these rainout processes, the following surface deposition rates are included: 6.7 x 10^{-6} s^{-1} for NO_y, hydroxyl radical (OH), hydroperoxy radical; (HO_2), hydrogen peroxide (H_2O_2), formyl radical (HCO), methyl radical (CH_3); and 3.3 x 10^{-8} s^{-1} for CH_2O. (Surface deposition is not applied to odd oxygen (O_x), Cl_y, Br_y, atomic hydrogen (H), and CO as these species are held fixed at the ground by the model.)

Surface Boundary Conditions

All surface boundary conditions are independent of latitude and time. At the surface (CSIRO model level at z* = 1 km), the boundary conditions are:

- Molecular hydrogen (H_2) = 0.515 ppmv
- CO = 0.1 ppmv
- O_x = 20 ppbv
- NO_y = flux of 6 x 10^9 cm^{-2} s^{-1}
- Cl_y = 80 pptv
- Br_y = 0.5 pptv
- CFC-114 = CFC-115 =
- Other surface mixing ratios as specified by NASA for the Cl_y = 2 ppbv and Cl_y = 3 ppbv atmospheres:

Species	Cl_y = 3 ppbv	Cl_y = 2 ppbv
CO_2	412 ppmv	412 ppmv
CH_4	1994 ppbv	1994 ppbv
N_2O	330 ppbv	330 ppbv
$CFCl_3$	220 pptv	120 pptv
CF_2Cl_2	470 pptv	350 pptv
CFC-113	80 pptv	60 pptv
CCl_4	70 pptv	35 pptv
HCFC-22	250 pptv	15 pptv
CH_3CCl_3 *	11 pptv	0
halon-1301	1.4 pptv	0.9 pptv
halon-1211	1.1 pptv	0.2 pptv
CH_3Cl	600 pptv	600 pptv
CH_3Br	15 pptv	15 pptv

*(including HCFC-141b)

Solar Radiation

The solar radiation module includes fully interactive, multiple scattering calculations and allows for the curvature of the Earth. The method of Meier *et al.* [1982] is employed to account for the effects of multiple scattering, while the spherical atmosphere treatment uses ray-tracing techniques. The model uses 158 wavelengths from 175 to 850 nm, as defined in WMO [1986]. Photodissociation cross sections were taken from DeMore *et al.* [1994], except for J(HOBr), which was taken from Orlando and Burkholder [1995].

Chemistry

Species and Family Definitions

Transported families are defined as follows:

$O_x = O + O(^1D) + O_3$
$NO_y = N + NO + NO_2 + NO_3 + HONO + HNO_3 + HNO_4 + 2N_2O_5 + ClONO_2 + BrONO_2$
$Cl_y = Cl + 2Cl_2 + ClO + ClO_2 + OClO + 2Cl_2O_2 + HOCl + HCl + ClONO_2$
$Br_y = Br + BrO + HOBr + HBr + BrONO_2$

Other species included in the CSIRO model are:

Fixed Species: N_2, O_2, CO_2

Transported Species: N_2O, CH_4, CO, H_2O, H_2, $CFCl_3$, CF_2Cl_2, CFC-113, CFC-114, CFC-115, CCl_4, HCFC-22, CH_3CCl_3, CH_3Cl, halon-1301, halon-1211, CH_3Br

Equilibrium species: H, OH, HO_2, H_2O_2, HCO, CH_2O, CH_3, CH_3O, CH_3O_2, CH_3OOH

Rate Coefficients

Cross sections and other reaction-rate parameters are taken from DeMore *et al.* [1994], except for J(HOBr) (as noted above).

The sulfate aerosol loading is fixed at background levels as defined in Chapter 8 of WMO [1992]. Sulfate aerosol reaction rates are calculated using $\gamma(N_2O_5 + H_2O) = 0.1$ and $\gamma(ClONO_2 + H_2O)$, as defined by Hanson *et al.* [1994]. For the additional runs which include bromine nitrate ($BrONO_2$) hydrolysis, it was assumed that $\gamma(BrONO_2 + H_2O) = 0.4$.

Solution Method

A typical simulation is carried out using a number of consecutive five-year model runs. During the first year, diurnal averaging is carried out every 10 days for all model grid cells which are not in polar night to determine diurnal coefficients for all reactions. The same diurnal coefficients are then used for the remaining four years of the five-year run when partitioning the transported families and calculating other equilibrium species concentrations. Transported species are held constant during the diurnal integration, and the 24-hour variation of all equilibrium species is obtained as a by-product.

Equilibrium Chemistry

24-hour-average rate coefficients are obtained using the diurnal coefficients and calculated noon photo-rate coefficients. These 24-hour-average rate coefficients are used to solve the coupled set of steady-state equations $d\mathbf{C}/dt = 0$ for all 24-hour-average equilibrium species concentrations (including transported family members). For each transported family, one of the steady-state equations $d\mathbf{C}/dt = 0$ is replaced by an equation to ensure that the family total concentration equals the sum of its member's concentrations. An iterative Newton-Raphson algorithm is used to solve the coupled system of equations.

GSFC

Charles H. Jackman, David B. Considine, and Eric L. Fleming
NASA/Goddard Space Flight Center

1) A look-up table is now used for the photolytic source term (PST) and $J(O_2)$ generated by R. Kawa (GSFC) using a radiation code developed by D. Anderson and co-workers at the Johns Hopkins Applied Physics Laboratory [Anderson and Meier, 1979; Anderson and Lloyd, 1990]. The PST table is a function of wavelength, solar zenith angle, and column ozone and is given on the pressure grid of the GSFC two-dimensional (2-D) model. The PST is computed for the particular wavelength, solar zenith angle, column ozone, and pressure of interest and is multiplied by the solar irradiance at the top of the model to compute the reduced flux at the point of interest.

2) Sticking coefficients from Hanson and Ravishankara [1994] are now used for the reactions

$$HCl + ClONO_2 \rightarrow HNO_3 + Cl_2,$$
$$ClONO_2 + H_2O \rightarrow HNO_3 + HOCl, \text{ and}$$
$$HOCl + HCl \rightarrow H_2O + Cl_2 \text{ on sulfate aerosols.}$$

3) H_2O is now transported above 400 mbar rather than fixed over the entire model domain. H_2O is set to the Oort [1983] climatology below 400 mbar. A detailed description of our treatment of H_2O is given in Fleming *et al.* [1995].

4) The reactions rates have been updated to DeMore *et al.* [1994].

5) Several minor modifications have been made in the model treatment of the photochemistry of the NO_y, Cl_y, and Br_y families.

6) A parameterization and treatment of Type 1 and 2 PSCs was formulated and used in the GSFC 2-D model. This PSC treatment is described in detail in Considine *et al.* [1994]. PSCs were not included in the base supersonic transport plane assessments; however, sensitivity studies were run for some of these assessments with PSCs included.

LLNL/UI

D. E. Kinnison, P.S. Connell, K. E. Grant, D. A. Rotman, and L. Li
Lawrence Livermore National Laboratory
K. O. Patten and D. J. Wuebbles
University of Illinois

Since the NASA Models and Measurement Workshop [Prather and Remsberg, 1993], the LLNL 2-D chemical radiative transport (CRT) model has been improved and refined, with combined support of AESA, the NASA Atmospheric Chemistry Modeling and Analysis Program (ACMAP), and the Department of Energy. The grid resolution of the model has been increased from 3 km (pressure altitude) by ~10 degrees in latitude to 1.5 km and 5 degrees in latitude. The vertical extent of the model is extended from 60 to ~85 km to allow for the breaking of planetary and gravity waves, which is important to the interactive calculation of the dynamics of the residual circulation.

The treatment of dynamical processes has been revised to take the 2-D model a major step closer to having fully interactive, complete derivation of dynamics and temperature fields. In past studies, an interim approach to planetary-wave parameterization using climatological temperature fields, based on the Newman method [Newman *et al.*, 1988], was used in the 2-D model to calculate K_{yy}. A significant additional step has been the development of a first-principle treatment of planetary waves (both wave number 1 and 2), based on the groundbreaking work of Garcia [1991] and Garcia *et al.* [1992]. This improvement, along with gravity-wave effects following Lindzen [1981], have been implemented and are currently being used in the LLNL 2-D CRT assessment. These additions have greatly improved the dynamical representation of long-lived tracers (e.g., N_2O) when compared to satellite data (e.g., the Upper Atmosphere Research Satellite).

We have updated our treatment of reaction on sulfate aerosols as presented in Hanson *et al.* [1994]. Hydrolysis of chlorine nitrate ($ClONO_2$) and dinitrogen pentoxide (N_2O_5) on the surface of stratospheric sulfate aerosol is included. In addition, $BrONO_2$ hydrolysis is included as a sensitivity study. The LLNL 2-D CRT model can also represent heterogeneous chemical processes to account for PSCs. Here, polar heterogeneous chemistry is represented with climatological fields of PSC frequencies. This first-order, linearized approach cannot capture the actual situation of processing, recovery, and reprocessing that must occur, but is probably adequate to represent the effect of polar processing on the global zonally averaged stratosphere. Several sensitivity studies were completed with this version of the LLNL 2-D CRT.

APPENDIX B

REFERENCES

Anderson, D. E., Jr., and S. A. Lloyd, Polar twilight UV-visible radiation field: Perturbations due to multiple scattering, ozone depletion, stratospheric clouds, and surface albedo, *J. Geophys. Res.*, *95*, 7429-7434, 1990.

Anderson, D. E., Jr., and R. R. Meier, Effects of anisotropic multiple scattering on solar radiation in the troposphere and stratosphere, *Appl. Optics*, *18*, 1955-1960, 1979.

Anderson, J. G., Presentation to the Subcommittee on Space and Aeronautics, Committee on Science, U. S. House of Representatives, March 1995.

Anthony, S. E., R. T. Tisdale, R. S. Disselkamp, M. A. Tolbert, and J. C. Wilson, FTIR studies of low temperature sulfuric acid aerosols, *Geophys. Res. Lett., 22,* 1105-1108, 1995.

Arnold, F., J. Scheid, Th. Stilp, H. Schlager, M. E. Reinhardt, Measurements of jet aircraft emissions at cruise altitude I: The odd nitrogen gases NO, NO_2, HNO_2, and HNO_3, *Geophys. Res. Lett.*, *19*, 2421-2424, 1992.

Avallone, L. M., and M. J. Prather, Photochemical evolution of ozone in the lower tropical stratosphere, submitted to *J. Geophys. Res.*, 1995.

Ball, S. M., and G. Hancock, The relative quantum yields of $O_2(a^1\Delta_g)$ from the photolysis of ozone at 227K, *Geophys. Res. Lett.*, *22*, 1213-1216, 1995.

Barnett, J. J., and M. Corney, A middle atmosphere temperature reference model from satellite measurements, *Adv. Space Res.*, *5*, 125-134, 1985.

Barrilleaux, J., Background and logistics of the ER-2/Concorde encounter, presentation at Atmospheric Effects of Aviation Project Annual Meeting, Virginia Beach, VA, 23-28 April 1995.

Baughcum, S. L., and S. C. Henderson, *Aircraft Emission Inventories Projected in Year 2015 for a High Speed Civil Transport (HSCT) Universal Airline Network,* NASA Contractor Report 4659, Washington, DC, 1995.

Baughcum, S. L., S. C. Henderson, P. S. Hertel, D. R. Maggiora, and C. A. Oncina, *Stratospheric Emissions Effects Database Development,* NASA Contractor Report 4592, Washington, DC, 1994.

Baumgardner, D, and W. A. Cooper, *Impact of Emissions from Aircraft and Spacecraft upon the Atmosphere,* Proceedings of an International Scientific Colloquium, Cologne, Germany, April 18-20, 1994, U. Schumann and D. Wurzel, Editors, 106-112, 1994.

Bekki, S., and J. A. Pyle, Potential impact of combined NO_x and SO_x emissions from future high speed civil transport aircraft on stratospheric aerosols and ozone, *Geophys. Res. Lett., 20,* 723-726, 1993.

Blake, D. F., and K. Kato, Latitudinal distribution of black carbon soot in the upper troposphere and lower stratosphere, *J. Geophys. Res., 100,* 7195-7202, 1995.

Boering, K. A., B. C. Daube, Jr., S. C. Wofsy, M. Loewenstein, J. R. Podolske, and E. R. Keim, Tracer-tracer relationships and lower stratospheric dynamics: CO_2 and N_2O correlations during SPADE, *Geophys. Res. Lett.*, *21*, 2567-2570, 1994.

Boering, K. A., E. J. Hintsa, S. C. Wofsy, J. G. Anderson, B. C. Daube, A. E. Dessler, M. Loewenstein, M. P. McCormick, J. R. Podolske, E. M. Weinstock, and G. K. Yue, Measurements of stratospheric carbon dioxide and water vapor at northern mid-latitudes: Implications for troposphere-to-stratosphere transport, *Geophys. Res. Lett.*, in press, 1995.

Bojkov, R. D., L. Bishop, W. J. Hill, G. C. Reinsel, and G. C. Tiao, A statistical trend analysis of revised Dobson total ozone data over Northern Hemisphere, *J. Geophys. Res., 95,* 9785-9807, 1990.

Bojkov, R. D., V. E. Fioletov, and A. M. Shalamjansky, Total ozone changes over Eurasia since 1973 based on reevaluated filter ozonometer data, *J. Geophys. Res., 99,* 22985-22999, 1994.

Bojkov, R. D., and V. E. Fioletov, Estimating the global ozone characteristics during the last 30 years, *J. Geophys. Res., 100,* 16537-16551, 1995.

Bott, A., A positive definite advection scheme obtained by nonlinear renormalization of the advective fluxes, *Mon. Weath. Rev., 117,* 1006-1015, 1989.

Brasseur, G. P., and C. Granier, Mt. Pinatubo aerosols, chlorofluorocarbons, and ozone depletion, *Science, 257,* 1239-1242, 1992.

Briegleb, B. P., Delta-Eddington approximation for solar radiation in the NCAR Community Climate Model, *J. Geophys. Res., 97,* 7603-7612, 1992a.

Briegleb, B. P., Longwave band model for thermal radiation in climate studies, *J. Geophys. Res., 97,* 11475-11485, 1992b.

Browell, E. V., C. F. Butler, M. A. Fenn, W. B. Grant, S. Ismail, M. R. Schoeberl, O. B. Toon, M. Loewenstein, and J. R. Podolske, Ozone and aerosol changes during the 1991-1992 Airborne Arctic Stratospheric Expedition, *Science, 261,* 1155-1158, 1993.

Brown, R. C., R. C. Miake-Lye, M. R. Anderson, C. E. Kolb, and T. J. Resch, Aerosol dynamics in near field aircraft plumes, submitted to *J. Geophys. Res.*, 1995.

CAEP, Committee on Aviation Environmental Protection, Second Meeting, Montreal, 2-13 December 1991, International Civil Aviation Organization, Doc. 9592, CAEP/2, 1992.

Carslaw, K. S., B. P. Luo, S. L. Clegg, Th. Peter, P. Brimblecombe, and P. J. Crutzen, Stratospheric aerosol growth and HNO_3 gas phase depletion from coupled HNO_3 and water uptake by liquid particles, *Geophys. Res. Lett., 21,* 2479-2482, 1994.

Chance, K. V., W. A. Traub, D. G. Johnson, K. W. Jucks, P. Ciarpallini, R. A. Stachnik, R. J. Salawitch, and H. A. Michelsen, Simultaneous measurements of stratospheric HO_x, NO_x, and Cl_x: Comparison with a photochemical model, submitted to *J. Geophys. Res.*, 1995.

Chang, A. Y., R. J. Salawitch, H. A. Michelsen, M. R. Gunson, M. C. Abrams, R. Zander, C. P. Rinsland, C. R. Webster, R. D. May, J. W. Elkins, G. S. Dutton, C. M. Volk, R. M. Stimpfle, M. Loewenstein K. R. Chan, M. M. Abbas, A. Goldman, F. W. Irion, G. L. Manney, M. J. Newchurch, and G. P. Stiller, A comparison of measurements from ATMOS and instruments aboard the ER-2 aircraft: Halogenated gases transport, submitted to *Geophys. Res. Lett.*, 1995.

CIAP Monograph 2, *Propulsion Effluents in the Stratosphere,* Climate Impact Assessment Program, DOT-TST-75-52, U.S. Department of Transportation, Washington, DC, 1975.

Cohen, R. C., P. O. Wennberg, R. M. Stimpfle, J. Koplow, J. G. Anderson, D. W. Fahey, E. L. Woodbridge, E. R. Keim, R. Gao, M. H. Proffitt, M. Loewenstein, and K. R. Chan, Are models of

catalytic removal of O_3 by HO_x accurate? Constraints from *in situ* measurements of the OH to HO_2, *Geophys. Res. Lett., 21,* 2539-2542, 1994.

Considine, D. B., A. R. Douglas, and C. H. Jackman, Effects of a polar stratospheric cloud parameterization on ozone depletion due to stratospheric aircraft in a two-dimensional model, *J. Geophys. Res., 99,* 18879-18894, 1994.

Considine, D. B., A. R. Douglas, and C. H. Jackman, Sensitivity of two-dimensional model predictions of ozone response to stratospheric aircraft: An update, *J. Geophys. Res., 100,* 3075-3090, 1995.

Crutzen, P. J., and F. Arnold, Nitric acid cloud formation in the cold Antarctic stratosphere: A major cause for the springtime 'ozone hole,' *Nature, 324,* 651-655, 1986.

Crutzen, P. J., J.-U. Gross, C. Brühl, R. Müller, and J. M. Russell III, A reevaluation of the ozone budget with HALOE UARS data: No evidence for the ozone deficit, *Science, 268,* 705-708, 1995.

Dahlback, A., and K. Stamnes, A new spherical model for computing the radiation field available for photolysis and heating at twilight, *Planet. Space Sci., 39,* 671-683, 1991.

Daley, R., *Atmospheric Data Analysis,* Cambridge University Press, Cambridge, England, 1991.

DeMore, W. B., D. M. Golden, R. F. Hampson, C. J. Howard, C. E. Kolb, M. J. Kurylo, M. J. Molina, A. R. Ravishankara, and S. P. Sander, *Chemical Kinetics and Photochemical Data for use in Stratospheric Modeling, Evaluation Number 11,* JPL Publication 94-26, Jet Propulsion Laboratory, 1994.

Deshler, T., Th. Peter, R. Müller, and P. Crutzen, The lifetime of leewave-induced ice particles in the Arctic stratosphere, *Geophys. Res. Lett., 21,* 1327-1330, 1994.

Dessler, A. E., R. M. Stimpfle, B. C. Daube, R. J. Salawitch, E. M. Weinstock, D. M. Juda, J. D. Burley, J. W. Munger, S. C. Wofsy, J. G. Anderson, M. P. McCormic, and W. P. Chu, Balloon-borne measurements of ClO, NO, and O_3 in a volcanic cloud: An analysis of heterogeneous chemistry between 20 and 30 km., *Geophys. Res. Lett., 20,* 2527-2530, 1993.

Dessler, A. E., S. R. Kawa, D. B. Considine, J. B. Kumer, J. W. Waters, L. Froidevaux, and J. M. Russell III, UARS measurements of ClO and NO_2 at 40 and 46 km and implications for the 'ozone deficit', to be submitted to *Geophys. Res. Lett.,* 1995a.

Dessler, A. E., D. B. Considine, G. A. Morris, M. R. Schoeberl, J. M. Russell III, A. E. Roche, J. B. Kumer, J. L. Mergenthaler, J. W. Waters, J. C. Gille, and G. K. Yue, Correlated observations of HCl and $ClONO_2$ from UARS and implications for stratospheric chlorine partitioning, *Geophys. Res. Lett., 22,* 1721-1724, 1995b.

Donnelly, S. G., L. A. DelNegro, D. W. Fahey, R. S. Gao, R. C. Wamsley, E. L. Woodbridge, K. H. Rosenlof, M. H. Proffitt, M. K. W. Ko, D. K. Weisenstein, C. Scott, C. Nevison, S. Solomon, and K. R. Chan, *In situ* observations of NO_y, O_3, and the NO_y/O_3 ratio in the lower stratosphere: Latitude distributions, seasonal variations, and comparison with 2-D model calculations, to be submitted to *J. Geophys. Res.*, 1995.

Dopplick, T. G., Radiative heating of the global atmosphere, *J. Atmos. Sci., 29,* 1278-1294, 1972.

Dopplick, T. G., The heat budget, in *The General Circulation of the Tropical Atmosphere and Interactions with Extratropical Latitudes, vol. 2,* R. E. Newell, J. W. Kidson, D. G. Vincent, and C. J. Boer, Editors, MIT Press, 27-94, 1974.

Dopplick, T. G., Radiative heating of the global atmosphere: Corrigendum, *J. Atmos. Sci., 36,* 1812-1817, 1979.

Douglass, A. R., M. A. Carroll, W. B. DeMore, J. R. Holton, I. S. A. Isaksen, and H. S. Johnston, *The Atmospheric Effects of Stratospheric Aircraft: A Current Consensus,* NASA Reference Publication 1251, 1991.

Douglass, A. R., R. B. Rood, C. J. Weaver, M. C. Cerniglia, K. F. Brueske, Implications of three-dimensional tracer studies for two-dimensional assessments of the impact of supersonic aircraft on stratospheric ozone, *J. Geophys. Res., 98,* 8949-8963, 1993.

Douglass, A. R., C. J. Weaver, R. B. Rood, and L. Coy, A three-dimensional simulation of the ozone annual cycle using winds from a data assimilation system, submitted to *J. Geophys. Res.,* 1995.

Drdla, K., A. Tabazadeh, R. P. Turco, M. Z. Jacobson, J. E. Dye, C. Twohy, and D. Baumgardner, Analysis of the physical state of one Arctic polar stratospheric cloud based on observations, *Geophys. Res. Lett., 21,* 2475-2478, 1994.

Dunkerton, T. J., On the mean meridional mass motions of the stratosphere and mesosphere, *J. Atmos. Sci., 35,* 2324-2333, 1978.

Dye, J. E., D. Baumgardner, B. Gandrud, S. R. Kawa, K. K. Kelly, M. Loewenstein, G. V. Ferry, K. R. Chan, and B. L. Gary, Particle size distributions in Arctic polar stratospheric clouds, growth and freezing of sulfuric acid droplets, and implications for cloud formation, *J. Geophys. Res., 97,* 8015-8034, 1992.

Ehhalt, D. H., E. P. Roeth, and U. Schmidt, On the temporal variance of stratospheric trace gas concentrations, *J. Atmos. Chem., 1,* 27-51, 1983.

Fahey, D. W., D. M. Murphy, K. K. Kelly, M. K. W. Ko, M. H. Proffitt, C. S. Eubank, G. V. Ferry, M. Loewenstein, and K. R. Chan, Measurements of nitric oxide and total reactive odd-nitrogen in the Antarctic stratosphere: Observations and chemical implications, *J. Geophys. Res., 94,* 16665-16681, 1989.

Fahey, D. W., K. K. Kelly, S. R. Kawa, M. Loewenstein, A. F. Tuck, K. R. Chan, and L. E. Heidt, Observations of denitrification and dehydration in the winter polar stratospheres, *Nature, 344,* 321-324, 1990.

Fahey, D. W., S. R. Kawa, E. L. Woodbridge, P. Tin, J. C. Wilson, H. H. Jonsson, J. E. Dye, D. Baumgardner, S. Borrmann, D. W. Toohey, L. M. Avallone, M. H. Proffitt, J. Margitan, M. Loewenstein, J. R. Podolske, R. J. Salawitch, S. C. Wofsy, M. K. W. Ko, D. E. Anderson, M. R. Schoeberl, and K. R. Chan, *In situ* measurements constraining the role of sulphate aerosols in mid-latitude ozone depletion, *Nature, 363,* 509-514, 1993.

Fahey, D. W., E. R. Keim, K. A. Boering, C. A. Brock, J. C. Wilson, S. Anthony, T. F. Hanisco, P. O. Wennberg, R. C. Miake-Lye, R. J. Salawitch, N. Louisnard, E. L. Woodbridge, R. S. Gao, S. G. Donnelly, R. C. Wamsley, L. A. Del Negro, B. C. Daube, S. C. Wofsy, C. R. Webster, R. D. May, K. K. Kelly, M. Loewenstein, J. R. Podolske, and K. R. Chan, Emission measurements of the Concorde supersonic aircraft in the lower stratosphere, *Science, 270,* 70-74, 1995a.

Fahey, D. W., E. R. Keim, E. L. Woodbridge, R. S. Gao, K. A. Boering, B. C. Daube, S. C. Wofsy, R. P. Lohmann, E. J. Hintsa, A. E. Dessler, C. R. Webster, R. D. May, C. A. Brock, J. C. Wilson, R. C. Miake-Lye, R. C. Brown, J. M. Rodriguez, M. Loewenstein, M. H. Proffitt, R. M. Stimpfle, S. W. Bowen, and K. R. Chan, *In situ* observations in aircraft exhaust plumes in the lower stratosphere at midlatitudes, *J. Geophys. Res., 100,* 3065-3074, 1995b.

Fehsenfeld, F. C., and S. C. Liu, Tropospheric ozone: Distribution and sources, in *Global Atmospheric Chemical Change*, C. N. Hewitt and W. T. Sturges, Editors, Elsevier Applied Science, London and New York, 169-231, 1993.

Fleming, E. L., S. Chandra, C. H. Jackman, D. B. Considine, and A. R. Douglass, The middle atmospheric response to short- and long-term solar UV variations: Analysis of observations and 2-D model results, *J. Atmos. Terr. Phys.*, *57*, 333-365, 1995.

Fox, L. E., D. R. Worsnop, M. S. Zahniser, and S. C. Wofsy, Metastable phases in polar stratospheric aerosols, *Science*, *267*, 351-355, 1995.

Froidevaux, L., J. W. Waters, W. G. Read, L. S. Elson, D. A. Flower, and R. F. Jarnot, Global ozone observations from the UARS MLS: An overview of zonal-mean results, *J. Atmos. Sci.*, *51*, 2846-2866, 1994.

Gao, R. S., D. W. Fahey, R. J. Salawitch, S. A. Lloyd, D. E. Anderson, R. DeMajistre, R. T. McElroy, E. L. Woodbridge, R. C. Wamsley, S. G. Donnelly, L. A. Del Negro, M. H. Proffitt, R. M. Stimpfle, D. W. Kohn, J. E. Dye, J. C. Wilson, and K. R. Chan, Partitioning of the reactive nitrogen reservoir in lower stratosphere of the Southern Hemisphere: Observations and modeling, manuscript in preparation, 1995.

Garcia, R. R., Parameterization of planetary wave breaking in the middle atmosphere, *J. Atmos. Sci.*, *48*, 1405-1419, 1991.

Garcia, R. R., F. Stordal, S. Solomon, and J. F. Kiehl, A new numerical model of the middle atmosphere, 1. Dynamics and transport of tropospheric source gases, *J. Geophys. Res.*, 97, 12967-12991, 1992.

Gilles, K. M., A. Turnipseed, J. B. Burkholder, and A. R. Ravishankara, Iodine in the lower stratosphere: Laboratory studies of relevant reactions, paper presented at the International Conference on Ozone in the Lower Stratosphere, Halkidiki, Greece, 1995.

Graedel, T. E., Statement before Subcommittee on Technology, Environment, and Aviation, Committee on Science, Space, and Technology, U.S. House of Representatives, February 10, 1994.

Hadaller, O. J., and A. M. Momenthy, *The Characteristics of Future Fuels*, Boeing Publication D6-54940, 1989.

Hadaller, O. J., and A. M. Momenthy, Characteristics of future aviation fuels, in *Transportation and Global Climate Change*, D. L. Greene and D. J. Santini, Editors, American Council for an Energy-Efficient Economy, Washington, DC, 1993.

Hagen, D. E., P. D. Whitefield, M. B. Trueblood, and H. V. Lilenfeld, Particulates and aerosols characterized in real time from harsh environments using the UMR mobile aerosol sampling system (MASS), American Institute of Aeronautics and Astronautics (AIAA) Paper 93-2344, 1993.

Hall, T. M., and M. J. Prather, Simulations of the trend and annual cycle in stratospheric CO_2, *J. Geophys. Res.*, *98*, 10573-10581, 1993.

Hall, T. M., and M. J. Prather, Seasonal evolution of N_2O, O_3, and CO_2: Three dimensional simulations of stratospheric correlations, *J. Geophys. Res.*, *100*, 16699-16720, 1995.

Hanisco, T. F., P. O. Wennberg, R. C. Cohen, J. G. Anderson, D. W. Fahey, E. R. Keim, R. S. Gao, R. C. Wamsley, S. D. Donnelly, L. A. Del Negro, R. J. Salawitch, K. K. Kelly, and M. H. Proffitt, *In situ* measurements of HOx in super- and subsonic aircraft exhaust plumes, manuscript in preparation, 1995.

Hanson, D. R., and K. Mauersberger, Laboratory studies of the nitric acid trihydrate: Implications for the south polar stratosphere, *Geophys. Res. Lett., 15,* 855-858, 1988.

Hanson, D. R., and A. R. Ravishankara, Reaction of $ClONO_2$ + HCl on NAT, NAD, and frozen sulfuric acid and the hydrolysis of N_2O_5 and $ClONO_2$ on frozen sulfuric acid, *J. Geophys. Res., 98, D12,* 22931-22936, 1993.

Hanson, D. R., and A. R. Ravishankara, Reactive uptake of $ClONO_2$ onto sulfuric acid due to reaction with HCl and H_2O, *J. Phys. Chem., 98,* 5728-5735, 1994.

Hanson, D. R., and A. R. Ravishankara, Heterogeneous chemistry of bromine species in sulfuric acid under stratospheric conditions, *Geophys. Res. Lett., 22,* 385-388, 1995.

Hanson, D. R., A. R. Ravishankara, and S. Solomon, Heterogeneous reactions in sulfuric acid aerosols: A framework for model calculations, *J. Geophys. Res., 99,* 3615-3629, 1994.

Haynes, P. H., C. J. Marks, M. E. McIntyre, T. G. Shepherd, and K. P. Shine, On the 'downward control' of extratropical diabatic circulations by eddy-induced mean zonal forces, *J. Atmos. Sci., 48,* 651-678, 1991.

Hofmann, D. J., Increase in the stratospheric background sulfuric acid aerosol mass in the past 10 years, *Science, 248,* 996-1000, 1990.

Hofmann, D. J., and J. M. Rosen, Balloon observations of a particle layer injected by a stratospheric aircraft at 23 km, *Geophys. Res. Lett., 5,* 511-514, 1978.

Hofmann, D. J., and S. Solomon, Ozone destruction through heterogeneous chemistry following the eruption of El Chichón, *J. Geophys. Res., 94,* 5029-5041, 1989.

Hofmann, D. J., S. J. Oltmans, W. D. Komhyr, J. M. Harris, J. A. Lathrop, A. O. Langford, T. Deshler, B. J. Johnson, A. Torres, and W. A. Matthews, Ozone loss in the lower stratosphere over the United States in 1992-1993: Evidence for heterogeneous chemistry on the Pinatubo aerosol, *Geophys. Res. Lett., 21,* 65-68, 1994.

Holton, J. R., A dynamically-based transport parameterization for one-dimensional photochemical models of the stratosphere, *J. Geophys. Res., 91,* 2681-2686, 1986.

Holton, J. R., and W. M. Wehrbein, A numerical model of the zonal mean circulation of the middle atmosphere, *Pure Appl. Geophys., 118,* 284-306, 1980.

Holton, J. R., P. H. Haynes, M. E. McIntyre, A. R. Douglass, R. B. Rood, and L. Pfister, Stratosphere-Troposphere exchange, manuscript in preparation, 1995.

ICAO, *ICAO Engine Exhaust Emissions Databank,* First Edition, ICAO Doc. 9646-AN/943, International Civil Aviation Organization, 1995.

IPCC, Intergovernmental Panel on Climate Change, *Climate Change: The Supplementary Report to the IPCC Scientific Assessment,* Edited by J. T. Houghton, B. A. Callander, and S. K. Varney, Cambridge University Press, Cambridge, UK, 1992.

IPCC, Intergovernmental Panel on Climate Change, *Climate Change, Radiative Forcing of Climate Change, and an Evaluation of the IPCC IS92 Emission Scenarios,* Edited by J. T. Houghton, L. G. M. Filho, J. Bruce, H. Lee, B. A. Callander, E. Haites, N. Harris, and K. Maskell, Cambridge University Press, Cambridge, UK, 1995.

Jackman, C. H., P. A. Newman, P. D. Guthrie, and M. R. Schoeberl, Effect of computed horizontal diffusion coefficients on two-dimensional N_2O model distributions, *J. Geophys. Res., 93,* 5213-5219, 1988.

Jackman, C. H., A. R. Douglass, K. F. Brueske, and S. A. Klein, The influence of dynamics on two-dimensional model results: Simulations of ^{14}C and stratospheric aircraft NO_x injections, *J. Geophys. Res., 96,* 22559-22572, 1991.

Jaeglé, L., C. R. Webster, R. D. May, D. W. Fahey, E. L. Woodbridge, E. R. Keim, R. S. Gao, M. H. Proffitt, R. M. Stimpfle, P. O. Wennberg, R. J. Salawitch, S. C. Wofsy, and L. Pfister, *In-Situ* measurements of the NO_2/NO ratio for testing atmospheric photochemical models, Geophys. *Res. Let., 21,* 2555-2558, 1994.

Johnston H. S., Reduction of stratospheric ozone by nitrogen oxide catalysts from supersonic transport exhaust, *Science, 173,* 517-522, 1971.

Johnston, H. S., Evaluation of excess carbon-14 and strontium-90 data for suitability to test two-dimensional stratospheric models, *J. Geophys. Res.*, 94, 18485-18493, 1989.

Johnston, H. S., M. J. Prather, and R. T. Watson, *The Atmospheric Effects of Stratospheric Aircraft: A Topical Review,* NASA Reference Publication 1250, 1991.

Jucks, K. W., D. G. Johnson, K. V. Chance, W. A. Traub, R. J. Salawitch, and R. A. Stachnik, Ozone production and loss rate measurements in the middle stratosphere, submitted to *Science,* 1995.

Kärcher, B., A trajectory box model for aircraft exhaust plumes, *J. Geophys. Res., 100,* 18835-18844, 1995.

Kawa, R. S., D. W. Fahey, K. K. Kelly, J. E. Dye, D. Baumgardner, B. W. Gandrud, M. Loewenstein, G. V. Ferry, and K. R. Chan, The Arctic polar stratospheric cloud aerosol: Aircraft measurements of reactive nitrogen, total water, and particles, *J. Geophys. Res., 97,* 7925-7938, 1992.

Kerr, J. B., D. I. Wardle, and D. W. Tarasick, Record low ozone values over Canada in early 1993, *Geophys. Res. Lett., 20,* 1979-1982, 1993.

Kinnersley, J. S., A realistic three-component planetary wave model, with a wave breaking parameterisation, *Q. J. Roy. Met. Soc., 121,* 853-881, 1995.

Kinnersley, J. S., The Climatology of the stratospheric `THIN AIR;' model, to be submitted to *Q. J. Roy. Met. Soc.*, 1996.

Kinnersley, J. S., and Harwood R. S., An isentropic two-dimensional model with an interactive parameterisation of dynamical and chemical planetary-wave fluxes, *Q. J. Roy. Met. Soc.*, 119, 1167-1193, 1993.

Kinnison, D., H. S. Johnston, and D. J. Wuebbles, Model study of atmospheric transport using carbon 14 and strontium 90 as inert tracers, *J. Geophys. Res., 99,* 20647-20664, 1994.

Koike, M., N. B. Jones, W. A. Matthews, P. V. Johnston, R. L. McKenzie, D. Kinnison, and J. M. Rodriguez, Impact of Pinatubo aerosols on the partitioning between NO_2 and HNO_3, *Geophys. Res. Lett., 21,* 597-600, 1994.

Kondo, Y., T. Sugita, R. J. Salawitch, M. Koike, P. Aimedieu, and T. Deshler, The effect of Pinatubo aerosols on stratospheric NO, to be submitted, to *J. Geophys. Res.*, 1995.

Koop, T., U. M. Biermann, W. Raber, B. P. Luo, P. J. Crutzen, and Th. Peter, Do stratospheric aerosol droplets freeze above the ice frost point?, *Geophys. Res. Lett., 22,* 917-920, 1995.

Lacis, A. A., D. J. Wuebbles, and J. A. Logan, 1990: Radiative forcing of climate by changes in the vertical distribution of ozone, *J. Geophys. Res., 95,* 9971-9981, 1990.

Landau, Z. H., M. Metwally, R. Van Alstyne, and C. A. Ward, *Jet Aircraft Engine Exhaust Emissions Database Development -- Year 1990 and 2015 Scenarios*, NASA Contractor Report 4613, Washington, DC, 1994.

Lary, D. J., M. P. Chipperfield, and R. Toumi, Atmospheric heterogeneous bromine chemistry, *J. Geophys. Res.*, in press, 1995.

Laszlo, B., R. E. Huie, and M. J. Kurylo, Absorption cross sections, kinetics of formation and self-reaction of the IO radical produced via the laser photolysis of N_2O/I_2 mixtures, *J. Phys. Chem., 99,* 11701-117XX, 1995a.

Laszlo, B., R. E. Huie, M. J. Kurylo, and A. W. Miziolek, Kinetic studies of the reactions of BrO and IO radicals, submitted to *J. Geophys. Res.*, 1995b.

Lindzen, R. S., Turbulence and stress owing to gravity wave and tidal breakdown, *J. Geophys. Res., 86,* 9707-9714, 1981.

Logan, J. A., Trends in the vertical distribution of ozone: An analysis of ozonesonde data, *J. Geophys. Res., 99,* 25553-25585, 1994.

MacKenzie, A. R., M. Kulmala, A. Laaksonen, and T. Vesala, On the theories of type 1 polar stratospheric cloud formation, *J. Geophys. Res., 100,* 11275-11288, 1995.

Mahlman, J. D., H. Levy II, and W. J. Moxim, Three-dimensional simulations of stratospheric N_2O: Predictions for other trace constituents, *J. Geophys. Res., 91,* 2687-2707, 1986.

Marti, J. J., and K. Mauersberger, Laboratory simulations of PSC particle formation, *Geophys. Res. Lett., 20,* 359-362, 1993.

McCormick, M. P., H. M. Steele, P. Hamill, W. P. Chu, and T. J. Swissler, Polar stratospheric cloud sightings by SAM II, *J. Atmos. Sci., 39,* 1387-1397, 1982.

McCormick, M. P., E. W. Chiou, L. R. McMaster, W. P. Chu, J. C. Larsen, D. Rind, and S. Oltmans, Annual variations of water vapor in the stratosphere and upper troposphere observed by the Stratospheric Aerosol and Gas Experiment II, *J. Geophys. Res., 98,* 4867-4874, 1993.

McCormick, M. P., L. W. Thomason, and C. R. Trepte, Atmospheric effects of the Mt. Pinatubo eruption, *Nature, 373,* 399-404, 1995.

McElroy, M. B., R. J. Salawitch, and S. C. Wofsy, Antarctic ozone: Chemical mechanisms for the spring decrease, *Geophys. Res. Lett., 13,* 1296-1299, 1986.

McElroy, M. B., R. J. Salawitch, and K. Minschwaner, The changing stratosphere, *Planet. Space Sci., 40,* 373-401, 1992.

Meier, R. R., D. E. Anderson, Jr., and M. Nicolet, Radiation field in the troposphere and stratosphere from 240-1000 nm, 1. General analysis, *Planet. Space Sci., 30,* 923-933, 1982.

Metwally, M., *HSCT Simulated Airlines Scenario Year 2015 with Mach 1.6, Mach 2.0, and Mach 2.4 Configurations,* NASA Contractor Report, manuscript in preparation, 1995.

Miake-Lye, R. C., J. A. Matulaitis, F. H. Krause, W. J. Dodds, M. Albers, J. Hurmouziadis, K. L. Hasel, R. P. Lohmann, C. Stander, J. H. Gerstle, and G. L. Hamilton, High speed civil transport aircraft

emissions, in *The Atmospheric Effects of Stratospheric Aircraft: A First Program Report,* NASA Reference Publication 1272, 1992.

Miake-Lye, R. C., M. Martinez-Sanchez, R. C. Brown, and C. E. Kolb, Plume and wake dynamics, mixing, and chemistry behind a high speed civil transport aircraft, *J. Aircraft, 30,* 467-479, 1993.

Miake-Lye, R. C., M. Martinez-Sanchez, R. C. Brown, and C. E. Kolb, Calculations of condensation and chemistry in an aircraft contrail, in *Impact of Emissions from Aircraft and Spacecraft upon the Atmosphere,* Proceedings of an International Scientific Colloquium, Cologne, Germany, April 18-20, 1994, U. Schumann and D. Wurzel, Editors, 106-112, 1994.

Michelsen, H. A., R. J. Salawitch, P. O. Wennberg, and J. G. Anderson, Temperature and wavelength dependence of the quantum yield of $O(^1D)$ from O_3 photolysis, *Geophys. Res. Lett., 21,* 2227-2230, 1994.

Michelsen, H. A., R. J. Salawitch, M. R. Gunson, C. Aellig, N. Kaempfer, M. M. Abbas, M. C. Abrams, T. L. Brown, A. Y. Chang, A. Goldman, F. W. Irion, M. J. Newchurch, C. P. Rinsland, G. P. Stiller, and R. Zander, Stratospheric chlorine partitioning: Constraints from shuttle-borne measurements of HCl, $ClNO_3$, and ClO, submitted to *Geophys. Res. Lett.,* 1995.

Miller, A. J., G. C. Tiao, G. C. Reinsel, D. Wuebbles, L. Bishop, J. Kerr, R. M. Nagatani, J. J. deLuisi, and C. L. Mateer, Comparisons of observed ozone trends in the stratosphere though examination of Umkehr and balloon ozonesonde data, *J. Geophys. Res., 100,* 11209-11218, 1995.

Minschwaner, K., R. J. Salawitch, and M. B. McElroy, Absorption of solar radiation by O_2: Implications for O_3 and lifetimes of N_2O, $CFCl_3$, and CF_2Cl_2, *J. Geophys. Res., 98,* 10543-10561, 1993.

Minschwaner, K., A. E. Dessler, J. W. Elkins, C. M. Volk, D. W. Fahey, M. Loewenstein, J. R. Podolske, A. E. Roche, and K. R. Chan, The bulk properties of isentropic mixing into the tropics in the lower stratosphere, submitted to *J. Geophys. Res.,* 1995.

Molina, M. J., T.-L. Tso, L. T. Molina, and F. C.-Y. Wang, Antarctic stratospheric chemistry of chlorine nitrate, hydrogen chloride, and ice: Release of active chlorine, *Science, 238,* 1253-1257, 1987.

Molina, M. J., R. Zhang, P. J. Wooldridge, J. R. McMahon, J. E. Kim, H. Y. Chang, and K. D. Beyer, Physical chemistry of the $H_2SO_4/HNO_3/H_2O$ system: Implications for polar stratospheric clouds, *Science, 261,* 1418-1423, 1993.

Mote, P. W., Reconsideration of the cause of dry air in the southern middle-latitude stratosphere, *Geophys. Res. Lett., 22,* 2025-2028, 1995.

Mote, P. W., K. H. Rosenlof, M. E. McIntyre, E. S. Carr, K. H. Kinnersley, H. C. Pumphrey, R. S. Harwood, J. R. Holton, J. M. Russell III, J. W. Waters, and J. C. Gille, An atmospheric tape-recorder; The imprint of tropical tropopause temperatures on stratospheric water vapor, submitted to J. *Geophys. Res.,* 1995.

Mozurkewich, M., and J. G. Calvert, Reaction probabilities of N_2O_5 on aqueous aerosols, *J. Geophys. Res., 93,* 15889-15896, 1988.

Müller, M., A. Kraus, and A. Hofzumahaus, $O_3 \rightarrow O^1D$ photolysis frequencies determined from spectroradiometric measurements of solar actinic UV-radiation: Comparison with chemical actinometer measurements, *Geophys. Res. Lett., 22,* 679-682, 1995.

Murgatroyd, R. J., and F. Singleton, Possible meridional circulation in the stratosphere and mesosphere, *Q. J. Meteorol. Soc., 87,* 125-135, 1961.

Murphy, D. M., D. W. Fahey, M. H. Proffitt, S. C. Liu, K. R. Chan, C. S. Eubank, S. R. Kawa, and K. K. Kelly, Reactive nitrogen and its correlation with ozone in the lower stratosphere and upper troposphere, *J. Geophys. Res.*, 98, 8751-8733, 1993.

Murphy, D. M., and Gary, B. L., Mesoscale temperature fluctuations and polar stratospheric clouds, *J. Atmos. Sci., 52,* 1753-1760, 1995.

NASA, National Aeronautics and Space Administration, *The Atmospheric Effects of Stratospheric Aircraft: Interim Assessment Report of the NASA High-Speed Research Program,* NASA Reference Publication 1333, 1993.

Newman, P. A., M. R. Schoeberl, R. A. Plumb, and J. E. Rosenfield, Mixing rates calculated from potential vorticity, *J. Geophys. Res., 93,* 5221-5240, 1988.

NRC, National Research Council, *Atmospheric Effects of Stratospheric Aircraft, An Evaluation of NASA's Interim Assessment,* National Academy Press, Washington, DC, 1994.

Orlando, J. J., and J. B. Burkholder, Gas-phase UV/visible absorption spectra of HOBr and Br_2O, *J. Phys. Chem., 99,* 1143-1150, 1995.

Oort, A. H., Global Atmospheric Circulation Statistics, 1958-1983, NOAA Prof. Paper 14, U. S. Dept. of Commerce, Rockville, MD, 1983.

Peter, Th., R. Müller, P. J. Crutzen, and T. Deshler, The lifetime of leewave-induced ice particles in the Arctic stratosphere: II. Stabilization due to NAT-coating, *Geophys. Res. Lett., 21,* 1331-1334, 1994.

Pickett, H. M., and D. B. Peterson, Comparison of measured stratospheric OH with prediction, submitted to *Geophys. Res. Lett.,* 1995.

Pitari, G., L. Ricciardulli, and G. Visconti, High-speed civil transport impact: Role of sulfate, nitric acid trihydrate, and ice aerosols studied with a two-dimensional model including aerosol physics, *J. Geophys. Res., 98,* 23141-23164, 1993.

Pitari, G., and G. Visconti, Possible effects of CO_2 increase on the high-speed civil transport impact on ozone, *J. Geophys. Res., 99,* 16879-16896, 1994.

Pitchford, M., J. G. Hudson, and J. Hallett, Size and critical supersaturation for condensation of jet engine exhaust particles, *J. Geophys. Res., 96,* 20787-20793, 1991.

Plumb, R. A., A "tropical pipe" model of stratospheric transport, submitted to *J. Geophys. Res.,* 1995.

Plumb, R. A., and M. K. W. Ko, Interrelationships between mixing ratios of long lived stratospheric constituents, *J. Geophys. Res., 97,* 10145-10156, 1992.

Plumb, R. A., and J. D. Mahlman, The zonally averaged transport characteristics of the GFDL general circulation/tracer model, *J. Atmos. Sci., 44,* 298-327, 1987.

Plumb, R. A., M. K. W. Ko, and R.-L. Shia, Representation of localized aircraft NO_y emissions in a two-dimensional model of stratospheric ozone, *J. Geophys. Res.,* 100, 20901-20911, 1995.

Poole, L. R., and M. C. Pitts, Polar stratospheric cloud climatology based on Stratospheric Aerosol Measurement II observations from 1978 to 1989, *J. Geophys. Res., 99,* 13083-13089, 1994.

Prather, M. J. and E. E. Remsberg, Editors, *The Atmospheric Effects of Stratospheric Aircraft: Report of the 1992 Models and Measurements Workshop,* NASA Reference Publication 1292, Vol. I-III, 1993.

Prather, M. J., and H. L. Wesoky, Editors, *The Atmospheric Effects of Stratospheric Aircraft: A First Program Report,* NASA Reference Publication 1272, Washington, DC, 1992.

Pueschel, R. F., D. F. Blake, K. G. Snetsinger, A. D. A. Hansen, S. Verma, and K. Kato, Black carbon (soot) aerosol in the lower stratosphere and upper troposphere, *Geophys. Res. Lett., 19,* 1659-1662, 1992.

Quackenbush, T. R., M. E. Teske, and A. J. Bilanin, Computation of wake/exhaust mixing downstream of advanced transport aircraft, American Institute of Aeronautics and Astronautics (AIAA) 24th Fluid Dynamics Conference, Orlando, FL, 6-9 July 1993.

Ramaroson, R., and N. Louisnard, Potential effects on ozone of future supersonic aircraft: 2-D simulation, *Annae Geophysicae, 12,* 986-995, 1994.

Randel, W. J., and J. B. Cobb, Coherent variations of monthly mean total ozone and lower stratospheric temperature, *J. Geophys. Res., 99,* 5433-5447, 1994.

Randel, W. J., J. C. Gille, A. E. Roche, J. B. Kumer, J. L. Mergenthaler, J. W. Waters, E. F. Fishbein, and W. A. Lahoz, Stratospheric transport from the tropics to middle latitudes by planetary-wave mixing, *Nature, 365,* 533-535, 1993.

Rasch, P. J., X. X. Tie, B. A. Boville, and D. L. Williamson, A three-dimensional transport model for the middle atmosphere, *J. Geophys. Res., 99,* 999-1017, 1994.

Reed, R. J., and K. E. German, A contribution to the problem of stratospheric diffusion by large-scale mixing, *Mon. Weath. Rev., 93,* 313-321, 1965.

Reinsel, G. C., G. C. Tiao, D. J. Wuebbles, J. B. Kerr, A. J. Miller, R. M. Nagatani, L. Bishop, and L. H. Ying, Seasonal trend analysis of published ground-based and TOMS total ozone data through 1991, *J. Geophys. Res., 99,* 5449-5464, 1994.

Rind, D., and P. Lonergan, Modeled impacts of stratospheric ozone and water vapor perturbations with implications for high-speed civil transport aircraft, *J. Geophys. Res., 100,* 7381-7396, 1995.

Rind, D., R. Suozzo, N. K. Balachandran, and M. J. Prather, 1990: Climate change and the middle atmosphere. I. The doubled CO_2 climate, *J. Atmos. Sci., 47,* 475-494, 1990.

Rodriguez, J. M., M. K. W. Ko, and N. D. Sze, Role of heterogeneous conversion of N_2O_5 on sulphate aerosols in global ozone losses, *Nature, 352,* 134-137, 1991.

Rodriguez, J. M., R.-L. Shia, M. K. W. Ko, C. W. Heisey, D. K. Weisenstein, R. C. Miake-Lye, and C. E. Kolb, Subsidence of aircraft engine exhaust in the stratosphere: Implications for calculated ozone depletions, *Geophys. Res. Lett., 21,* 69-72, 1994.

Rosenfield, J. E., M. R. Schoeberl, and M. A. Geller, A computation of the stratospheric diabatic residual circulation using an accurate radiative transfer model, *J. Atmos. Sci., 44,* 859-876, 1987.

Salawitch, R. J., S. C. Wofsy, and M. B. McElroy, Influence of polar stratospheric clouds on the depletion of Antarctic ozone, *Geophys. Res., Lett., 15,* 871-874, 1988.

Salawitch, R. J., S. C. Wofsy, P. O. Wennberg, R. C. Cohen, J. G. Anderson, D. W. Fahey, R. S. Gao, E. R. Keim, E. L. Woodbridge, R. M. Stimpfle, J. P. Koplow, D. W. Kohn, C. R. Webster, R. D. May, L. Pfister, E. W. Gottlieb, H. A. Michelsen, G. K. Yue, J. C. Wilson, C. A. Brock, H. H.

Jonsson, J. E. Dye, D. Baumgardner, M. H. Proffitt, M. Loewenstein, J. R. Podolske, J. W. Elkins, G. S. Dutton, E. J. Hintsa, A. E. Dessler, E. M. Weinstock, K. K. Kelly, K. A. Boering, B. C. Daube, K. R. Chan, and S. W. Bowen, The distribution of hydrogen, nitrogen, and chlorine radicals in the lower stratosphere: Implications for changes in O_3 due to emission of NO_y from supersonic aircraft, *Geophys. Res. Lett., 21,* 2547-2550, 1994a.

Salawitch, R. J., S. C. Wofsy, P. O. Wennberg, R. C. Cohen, J. G. Anderson, D. W. Fahey, R. S. Gao, E. R. Keim, E. L. Woodbridge, R. M. Stimpfle, J. P. Koplow, D. W. Kohn, C. R. Webster, R. D. May, L. Pfister, E. Gottlieb, H. A. Michelsen, G. K. Yue, M. J. Prather, J. C. Wilson, C. A. Brock, H. H. Jonsson, J. E. Dye, D. Baumgardner, M. H. Proffitt, M. Loewenstein, J. R. Podolske, J. W. Elkins, G. S. Dutton, E. J. Hintsa, A. E. Dessler, E. M. Weinstock, K. K. Kelly, K. A. Boering, B. C. Daube, K. R. Chan, and S. W. Bowen, The diurnal variation of hydrogen, nitrogen, and chlorine radicals: Implications for the heterogeneous hydrolysis of HNO_4, *Geophys. Res. Lett., 21,* 2551-2554, 1994b.

Santee, M. L., W. G. Read, J. W. Waters, L. Froidevaux, G. L. Manney, D. A. Flower, R. F. Jarnot, R. S. Harwood, and G. E. Peckham, Interhemispheric differences in polar stratospheric HNO_3, H_2O, ClO, and O_3, *Science, 267,* 849-852, 1995.

Schoeberl, M. R., and D. F. Strobel, The zonally averaged circulation of the middle atmosphere, *J. Atmos. Sci., 35,* 577-591, 1978.

Schoeberl, M. R., L. R. Lait, P. A. Newman, R. L. Martin, M. H. Proffitt, D. L. Hartmann, M. Loewenstein, J. Podolske, S. E. Strahan, J. G. Anderson, K. R. Chan, and B. Gary, Reconstruction of the constituent distribution and trends in the Antarctic polar vortex from ER-2 flight observations, *J. Geophys. Res., 94,* 16815-16845, 1989.

Schubert, S. D., R. B. Rood, and J. Pfaendtner, An assimilated dataset for Earth science applications, *Bull. Amer. Met. Soc., 74,* 2331-2342, 1993.

Schumann, U., P. Konopka, R. Baumann, R. Busen, T. Gerz, H. Schlager, P. Schulte, and H. Volkert, Estimate of diffusion parameters of aircraft exhaust plumes near the tropopause from nitric oxide and turbulence measurements, *J. Geophys. Res., 100,* 14147-14162, 1995.

Sen, B., G. C. Toon, R. J. Salawitch, J. Jaeglé, R. A. Stachnik, H. M. Pickett, J. J. Margitan, and J.-F. Blavier, Stratospheric Reactive Nitrogen: Comparison of balloon-borne measurements with theory, manuscript in preparation, 1995.

Shah, K. P., D. Rind, and P. Lonergan, 1995: Could high-speed civil transport aircraft impact stratospheric and tropospheric temperatures measured by MSU?, submitted to *J. Geophys. Res.*, 1995.

Shaw, R. J., S. Gilkey, and R. Hines, Engine technology challenges for a 21st century high-speed civil transport, International Symposium on Air Breathing Engines, Tokyo, Japan, September 1993.

Shia, R. L., Y. Young, M. Allen, R. Zureck, and D. Crisp, Sensitivity study of advection and diffusion coefficients in a two-dimensional stratospheric model using excess carbon 14 data, *J. Geophys. Res., 94,* 18467-18484, 1989.

Shia, R.-L., M. K. W. Ko, M. Zou, and V. Kotamarthi, Cross-tropopause transport of excess ^{14}C in a two-dimensional model, *J. Geophys. Res., 98,* 18599-18606, 1993.

Shine, K. P., The middle atmosphere in the absence of dynamical heat fluxes, *Q. J. Roy. Met. Soc., 113,* 603-633, 1987.

Solomon, S., R. R. Garcia, F. S. Roland, and D. J. Wuebbles, On the depletion of Antarctic ozone, *Nature, 321,* 755-758, 1986a.

Solomon, S., J. T. Kiehl, R. R. Garcia, and W. L. Grose, Tracer transport by the adiabatic circulation deduced from satellite observations, *J. Atmos. Sci., 43,* 1603-1617, 1986b.

Solomon, S., R. R. Garcia, and A. R. Ravishankara, On the role of iodine in ozone depletion, *J. Geophys. Res., 99,* 20491-20499, 1994.

Solomon, S., R. W. Portmann, R. R. Garcia, L. W. Thomason, L. R. Poole, and M. P. McCormick, The role of aerosol trends and variability in anthropogenic ozone depletion at northern mid-latitudes, submitted to *J. Geophys Res.,* 1995.

Song, N., Freezing temperatures of $H_2SO_4/HNO_3/H_2O$ mixtures: Implications for polar stratospheric clouds, *Geophys. Res. Lett., 21,* 2709-2712, 1994.

Sparling L. C., M. R. Schoeberl, A. R. Douglass, C. J. Weaver, P. A. Newman, and L. R. Lait, Trajectory modeling of emissions from lower stratospheric aircraft, *J. Geophys. Res., 100,* 1427-1438, 1995.

Spicer, C. W., M. W. Holdren, D. L. Smith, D. P. Hughes, and M. D. Smith, Chemical composition of exhaust from aircraft turbine engines, *J. Eng. Gas Turbines Power, 114,* 111-117, 1992.

Spicer, C. W., M. W. Holdren, R. M. Riggin, and T. F. Lyon, Chemical composition and photochemical reactivity of exhaust from aircraft turbine engines, *Ann. Geophys., 12,* 944-955, 1994.

Steele, H. M., and P. Hamill, Effects of temperature and humidity on the growth and optical properties of sulfuric acid-water droplets in the stratosphere, *J. Aerosol Sci., 12,* 517-528, 1981.

Steele, H. M., M. P. McCormick, and T. J. Swissler, The formation of polar stratospheric clouds, *J. Atmos. Sci., 40,* 2055-2067, 1983.

Stimpfle, R. M., P. O. Wennberg, L. B. Lapson, and J. G. Anderson, Simultaneous *in situ* measurements of OH and HO_2 in the stratosphere, *Geophys. Res. Lett.*, 17, 1905-1908, 1990.

Stimpfle, R. M., J. P. Koplow, R. C. Cohen, D. W. Kohn, P. O. Wennberg, D. M. Judah, D. W. Toohey, L. M. Avallone, J. G. Anderson, R. J. Salawitch, E. L. Woodbridge, C. R. Webster, R. D. May, M. H. Proffitt, K. Aikin, J. J. Margitan, M. Loewenstein, J. R. Podolske, L. Pfister, and K. R. Chan, The response of ClO radical concentrations to variations in NO_2 radical concentrations in the lower stratosphere, *Geophys. Res. Lett., 21,* 2543-2546, 1994.

Stolarski, R. S., and D. B. Considine, Effect of chemical uncertainties on 2-D model predictions of ozone change due to HSCT emissions, manuscript in preparation, 1995.

Stolarski, R. S., and H. L. Wesoky, Editors, *The Atmospheric Effects of Stratospheric Aircraft: A Third Program Report,* NASA Reference Publication 1313, Washington, DC, 1993a.

Stolarski, R. S., and H. L. Wesoky, Editors, *The Atmospheric Effects of Stratospheric Aircraft: A Second Program Report,* NASA Reference Publication 1293, Washington, DC, 1993b.

Stolarski, R. S., and H. L. Wesoky, Editors, *The Atmospheric Effects of Stratospheric Aircraft: A Fourth Program Report,* NASA Reference Publication 1359, Washington, DC, 1995.

Stolarski, R. S., P. Bloomfield, R. D. McPeters, and J. R. Herman, Total ozone trends deduced from Nimbus 7 TOMS data, *Geophys. Res. Lett., 19,* 159-162, 1991.

Strahan, S. E., J. E. Rosenfield, M. Loewenstein, J. R. Podolske, and A. Weaver, Evolution of the 1991-1992 Arctic vortex and comparison with the Geophysical Fluid Dynamics Laboratory SKYHI general circulation model, *J. Geophys. Res.*, *99*, 20713-20723, 1994.

Strobel, D. F., Parameterization of the atmospheric heating rate from 15 to 120 km due to O_2 and O_3 absorption of solar radiation, *J. Geophys. Res.*, *83*, 6225-6230, 1978.

Sweetman, B., U.S. supersonic transport research forges ahead, *INTERAVIA*, 20-22, January 1995.

Tabazadeh A., and R. P. Turco, A model for heterogeneous chemical processes on the surfaces of ice and nitric acid trihydrate particles, *J. Geophys. Res.*, *98*, 12727-12740, 1993.

Tabazadeh, A., R. P. Turco, K. Drdla, and M. Z. Jacobson, A study of Type I polar stratospheric cloud formation, *Geophys. Res. Lett.*, *21*, 1619-1622, 1994.

Taylor, K. E., and J. E. Penner, Response of the climate system to atmospheric aerosols and greenhouse gases, *Nature*, *369*, 734-737, 1994.

Thomason, L. W., and L. R. Poole, A global climatology of stratospheric aerosol surface area density deduced from SAGE II: 1984-1994, manuscript in preparation, 1995.

Thomason, L. W., G. S. Kent, C. R. Trepte, and L. R. Poole, A comparison of the stratospheric aerosol background periods of 1979 and 1989-1991, submitted to *J. Geophys. Res.*, 1995.

Tie, X., Potential impact on stratospheric ozone due to emission of hydrocarbons from high-altitude aircraft, *Tellus*, 46B, 286-293, 1994.

Tie, X., X. Lin, and G. P. Brasseur, Two-dimensional coupled dynamical/chemical/ microphysical simulation of global distribution of El Chichon volcanic aerosols, *J. Geophys. Res.*, *99*, 16779-16792, 1994.

Tolbert, M. A., M. J. Rossi, and D. M. Golden, Heterogeneous interactions of chlorine nitrate, hydrogen chloride, and nitric acid with sulfuric acid surfaces at stratospheric temperatures, *Geophys. Res. Lett.*, *15*, 847-850, 1988.

Toon, O. B., and M. A. Tolbert, Spectroscopic evidence against nitric acid trihydrate in polar stratospheric clouds, *Nature*, *375*, 218-221, 1995.

Toon, O. B., R. P. Turco, and P. Hamill, Denitrification mechanisms in the polar stratospheres, *Geophys. Res. Lett.*, *17*, 445-448, 1990.

Trepte, C. R., and M. H. Hitchman, Tropical stratospheric circulation deduced from satellite aerosol data, *Nature*, *355*, 626-628, 1992.

Trepte, C. R., R. E. Veiga, and M. P. McCormick, The poleward dispersal of Mount Pinatubo volcanic aerosol, *J. Geophys. Res.*, *98*, 18563-18574, 1993.

Tung, K. K., Modeling of tracer transport in the middle atmosphere, in *Dynamics of the Middle Atmosphere*, J. R. Holton, and T. Matsuno, Editors, Terra Scientific Publishing Company, Dordrecht, 417-444, 1984.

Turco, R. P., O. B. Toon, and P. Hamill, Heterogeneous physicochemistry of the polar ozone hole, *J. Geophys. Res.*, *94*, 16493-16510, 1989.

U.S. Standard Atmosphere, M. Dubin, A. Hall, and K. S. W. Champion, Editors, U.S. Government Printing Office, Washington, DC, 1976.

Van Doren, J. M., L. R. Watson, P. Davidovits, D. R. Worsnop, M. S. Zahniser, and C. E. Kolb, Uptake of N_2O_5 and HNO_3 by aqueous sulfuric acid droplets, *J. Phys. Chem., 95,* 1684-1689, 1991.

Vömel, H., S. J. Oltmans, D. J. Hofmann, T. Deshler, and J. M. Rosen, The evolution of the dehydration in the Antarctic stratospheric vortex, *J. Geophys. Res., 100,* 13919-13926, 1995.

Waugh, D. W., R. A. Plumb, J. W. Elkins, D. W. Fahey, K. A. Boering, G. S. Dutton, E. R. Keim, R.-S. Gao, B. C. Daube, S. C. Wofsy, M. Loewenstein, J. R. Podolske, K. R. Chan, M. H. Proffitt, K. K. Kelly, P. A. Newman, and L. R. Lait, Mixing of polar vortex air into middle latitudes as revealed by tracer-tracer scatter plots, submitted to *J. Geophys. Res.*, 1995.

Weaver, C. J., A. R. Douglass, and D. B. Considine, A five year simulation of aircraft emission transport using a three-dimensional model, manuscript in preparation, 1995.

Webster, C. R., R. D. May, M. Allen, L. Jaeglé, and M. P. McCormick, Balloon profiles of stratospheric NO_2 and HNO_3 for testing the heterogeneous hydrolysis of N_2O_5 on sulfate aerosols, *Geophys. Res. Lett., 21,* 53-56, 1994.

Weisenstein, D. K., M. K. W. Ko, J. M. Rodriguez, and N.-D. Sze, Impact of heterogeneous chemistry on model-calculated ozone change due to high-speed civil transport aircraft, *Geophys. Res. Lett., 18,* 1991-1994, 1991.

Weisenstein, D. K., M. K. W. Ko, J. M. Rodriguez, and N.-D. Sze, Effects on stratospheric ozone from high-speed civil transport: Sensitivity to stratospheric aerosol loading, *J. Geophys. Res., 98,* 23133-23140, 1993.

Weisenstein, D. K., M. K. W. Ko, N.-D. Sze, and J. M. Rodriguez, Potential impact of SO_2 emissions from stratospheric aircraft on ozone, submitted to *Geophys. Res. Lett.*, 1995.

Wennberg, P. O., R. M. Stimpfle, E. M. Weinstock, A. E. Dessler, S. A. Lloyd, L. B. Lapson, J. J. Schwab, and J. G. Anderson, Simultaneous *in situ* measurements of OH, HO_2, O_3, and H_2O: A test of modeled stratospheric HO_x chemistry, *Geophys. Res. Lett., 17,* 1909-1912, 1990.

Wennberg, P. O., R. C. Cohen, R. M. Stimpfle, J. P. Koplow, J. G. Anderson, R. J. Salawitch, D. W. Fahey, E. L. Woodbridge, E. R. Keim, R. S. Gao, C. R. Webster, R. D. May, D. W. Toohey, L. M. Avallone, M. H. Proffitt, M. Loewenstein, J. R. Podolske, K. R. Chan, and S. C. Wofsy, The removal of lower stratospheric O_3 by free radical catalysis: *In situ* measurements of OH, HO_2, NO, NO_2, ClO, and BrO, *Science, 266,* 398-404, 1994.

Whitefield, P. D., M. B. Trueblood, and D. E. Hagen, Size and hydration characteristics of laboratory simulated jet engine combustion aerosols, *Particulate Science and Technology, 11,* 25-36, 1993.

Whitefield, P. D., and D. E. Hagen, Particulate characterization of jet engine emission during ground testing, Atmospheric Effects of Aviation Project Annual Meeting, Virginia Beach, VA, 23-28 April 1995.

Williams, L. J., Is there a future for second-generation supersonic travel? After the recession - world commercial aviation at the crossroads, Financial Times Conferences, F. T. Business Enterprises Ltd., London, November 1993.

Williams, L. R., J. A. Manion, D. A. Golden, and M. A. Tolbert, Laboratory measurements of heterogeneous reactions on sulfuric acid surfaces, *Am. Meteor. Soc., 33,* 785-790, 1994.

WMO, *Atmospheric Ozone 1985, Assessment of our Understanding of the Processes Controlling its Present Distribution and Change, Report No. 16,* World Meteorological Organization Global Ozone Research and Monitoring Project, Vol. I-III, 1986.

WMO, *Report of the International Ozone Trends Panel 1988, Report No. 18,* World Meteorological Organization Global Ozone Research and Monitoring Project, Vol. I-II, 1989.

WMO, *Scientific Assessment of Stratospheric Ozone: 1989, Report No. 20,* World Meteorological Organization Global Ozone Research and Monitoring Project, 1990.

WMO, *Scientific Assessment of Ozone Depletion: 1991, Report No. 25,* World Meteorological Organization Global Ozone Research and Monitoring Project, 1992.

WMO, *Scientific Assessment of Ozone Depletion: 1994, Report No. 37,* World Meteorological Organization Global Ozone Research and Monitoring Project, 1995.

Wofsy, S. C., R. J. Salawitch, J. H. Yatteau, M. B. McElroy, B. W. Gandrud, J. E. Dye, and D. Baumgardner, Condensation of HNO_3 on falling ice particles: Mechanisms for denitrification of the polar stratosphere, *Geophys. Res. Lett., 17,* 449-452, 1990.

Wofsy, S. C., K. A. Boering, B. C. Daube, M. B. McElroy, M. Loewenstein, J. R. Podolske, J. W. Elkins, G. S. Dutton, and D. W. Fahey, Vertical transport rates in the stratosphere in 1993 from observations of CO_2, N_2O, and CH_4, *Geophys. Res. Lett., 21,* 2571-2574, 1994.

Woodbridge, E. L., J. W. Elkins, D. W. Fahey, L. E. Heidt, S. Solomon, T. J. Baring, T. M. Gilpin, W. H. Pollock, S. M. Schauffler, E. L. Atlas, M. Loewenstein, J. R. Podolske, C. R. Webster, R. D. May, J. M. Gilligan, S. A. Montzka, K. A. Boering, and R. J. Salawitch, Estimates of total organic and inorganic chlorine in the lower stratosphere from *in situ* and flask measurements during AASE II, *J. Geophys. Res., 100,* 3057-3064, 1995.

Worsnop, D. R., L. Fox, M. S. Zahniser, and S. C. Wofsy, Vapor pressures of solid hydrates of nitric acid: Implications for polar stratospheric clouds, *Science, 259,* 71-74, 1993.

Wuebbles, D. J., D. Maiden, R. K. Seals, Jr., S. L. Baughcum, M. Metwally, and A. K. Mortlock, Emissions scenarios development: Report of the Emissions Scenarios Committee, in *The Atmospheric Effects of Stratospheric Aircraft: A Third Program Report,* NASA Reference Publication 1313, 1993.

Zhang, R., M.-T. Leu, and L. F. Keyser, Heterogeneous chemistry of HONO on liquid sulfuric acid: A new mechanism of chlorine activation on stratospheric sulfate aerosols, submitted to *J. Phys. Chem.*, 1995.

Zhao, J., and R. P. Turco, Particle nucleation in the wake of a jet aircraft in stratospheric flight, *J. Aerosol Sci.*, in press, 1995.

APPENDIX C

AUTHORS, CONTRIBUTORS, AND REVIEWERS

Assessment Chair

Richard S. Stolarski	NASA Goddard Space Flight Center

Lead Authors

Steven L. Baughcum	Boeing Commercial Airplane Group
William H. Brune	Pennsylvania State University
Anne R. Douglass	NASA Goddard Space Flight Center
David W. Fahey	NOAA Aeronomy Laboratory
Randall R. Friedl	Jet Propulsion Laboratory/NASA Headquarters
Shaw C. Liu	NOAA Aeronomy Laboratory
R. Alan Plumb	Massachusetts Institute of Technology
Lamont R. Poole	NASA Langley Research Center
Howard L. Wesoky	NASA Headquarters
Douglas R. Worsnop	Aerodyne Research, Incorporated

Coordinating Editor

Kathy A. Wolfe	Computer Sciences Corporation

Contributors and Reviewers

James G. Anderson	Harvard University
David F. Blake	NASA Ames Research Center
Kristie A. Boering	Harvard University
Mary Anne Carroll	University of Michigan
Ronald C. Cohen	Harvard University
Peter Connell	Lawrence Livermore National Laboratory
David B. Considine	NASA Goddard Space Flight Center
David R. Crosley	SRI International
Paul Crutzen	Max-Planck Institut für Chemie - Mainz
Stephen G. Donnelly	NOAA Aeronomy Laboratory
Manvendra Dubey	SRI International
Ru-Shan Gao	NOAA Aeronomy Laboratory
Marvin A. Geller	State University of New York at Stony Brook
Sam Gilkey	General Electric Aircraft Engines
William L. Grose	NASA Langley Research Center
Neil Harris	University of Cambridge
Paul Heberling	General Electric Aircraft Engines
Matthew H. Hitchman	University of Wisconsin, Madison
Linda A. Hunt	Lockheed Martin
Charles H. Jackman	NASA Goddard Space Flight Center
Kenneth Jucks	Harvard-Smithsonian Center for Astrophysics
Randy Kawa	NASA Goddard Space Flight Center

Jack A. Kaye	NASA Headquarters
Eric R. Keim	NOAA Aeronomy Laboratory
Rose M. Kendall	Computer Sciences Corporation
Douglas E. Kinnison	Lawrence Livermore National Laboratory
Malcolm K. W. Ko	Atmospheric and Environmental Research, Inc.
Mikhail Kogan	Central Aerohydrodynamic Institute (TsAGI)
Charles E. Kolb	Aerodyne Research, Incorporated
John M. Koshoffer	General Electric Aircraft Engines
Michael J. Kurylo	National Institute of Standards and Technology/NASA Headquarters
David H. Lister	Defence Research Agency - Pyestock
Jennifer Logan	Harvard University
Nicole Louisnard	Office National d'Études et Recherches Aerospatiales
Donald L. Maiden	NASA Langley Research Center
James J. Margitan	NASA Jet Propulsion Laboratory
Richard C. Miake-Lye	Aerodyne Research, Incorporated
Hope A. Michelsen	Harvard University
Alan K. Mortlock	McDonnell Douglas Aerospace
Daniel M. Murphy	NOAA Aeronomy Laboratory
Paul A. Newman	NASA Goddard Space Flight Center
Robert C. Oliver	Institute for Defense Analyses
Kenneth Patten	University of Illinois
Joyce E. Penner	Lawrence Livermore National Laboratory
Ian Plumb	Commonwealth Scientific and Industrial Research Organization
Michael J. Prather	University of California, Irvine
Rudolf F. Pueschel	NASA Ames Research Center
Lakshman Randeniya	Commonwealth Scientific and Industrial Research Organization
Jose M. Rodriguez	Atmospheric and Environmental Research, Inc.
Richard B. Rood	NASA Goddard Space Flight Center
Keith R. Ryan	Commonwealth Scientific and Industrial Research Organization
Karen H. Sage	Lockheed Martin
Ross J. Salawitch	NASA Jet Propulsion Laboratory
Arthur L. Schmeltekopf	Retired, NOAA Aeronomy Laboratory
Hans R. Schneider	Harvard University
Mark R. Schoeberl	NASA Goddard Space Flight Center
Ulrich Schumann	DLR Institut für Physik der Atmosphäre
Susan Solomon	NOAA Aeronomy Laboratory
Saadat A. Syed	Pratt & Whitney
Darin W. Toohey	University of California, Irvine
Charles R. Trepte	Science Applications International Corporation
Adrian F. Tuck	NOAA Aeronomy Laboratory
Guido Visconti	Universita' degli Studi l'Aquila
Peter Vohralik	Commonwealth Scientific and Industrial Research Organization
Robert C. Wamsley	NOAA Aeronomy Laboratory
Robert T. Watson	Office of Science and Technology Policy
Clark J. Weaver	Applied Research Corporation
Debra K. Weisenstein	Atmospheric and Environmental Research, Inc.
Paul O. Wennberg	Harvard University
Chowen Chou Wey	NASA Lewis Research Center
Philip D. Whitefield	University of Missouri, Rolla
Leah R. Williams	SRI International
James C. Wilson	University of Denver
Steven C. Wofsy	Harvard University
Donald J. Wuebbles	University of Illinois

APPENDIX D

ACRONYMS AND ABBREVIATIONS

1-D	one-dimensional
2-D	two-dimensional
3-D	three-dimensional
AAOE	Airborne Antarctic Ozone Experiment
ACMAP	Atmospheric Chemistry Modeling and Analysis Program
AEAP	Atmospheric Effects of Aviation Project
AER	Atmospheric and Environmental Research, Inc.
AESA	Atmospheric Effects of Stratospheric Aircraft
ALIAS	Aircraft Laser Infrared Absorption Spectrometer
APL	Applied Physics Laboratory, The Johns Hopkins University
ASHOE/MAESA	Airborne Southern Hemisphere Ozone Experiment/Measurements for Assessing the Effects of Stratospheric Aircraft
ATLAS	Atmospheric Laboratory for Applications and Science
ATMOS	Atmospheric Trace Molecule Spectroscopy
BLISS	Balloon-Borne Laser *In-Situ* Sensor
BMLS	Balloon Microwave Limb Sounder
CAEP	Committee on Aviation Environmental Protection
CAMED	University of Cambridge/University of Edinburgh
CFC	chlorofluorocarbon
CIAP	Climatic Impact Assessment Program
CN	condensation nuclei
CRT	chemical radiative transport
CSIRO	Commonwealth Scientific and Industrial Research Organization
CTM	chemical transport model
DU	Dobson units
EI	emission index
FILOS	Far Infrared Limb Observing Spectrometer
FIRS-2	Far Infrared Spectrometer
GCM	general circulation model
GSFC	Goddard Space Flight Center
GISS	Goddard Institute for Space Studies
HC	hydrocarbon
HSCT	high-speed civil transport
HSRP	High-Speed Research Program

ICAO	International Civil Aviation Organization
IPCC	Intergovernmental Panel on Climate Change
J(HOBr)	photodissociation rate of hypobromous acid
$J(O_2)$	photodissociation rate of molecular oxygen
JPL	Jet Propulsion Laboratory
K_{yy}	horizontal eddy diffusion coefficient
K_{zz}	vertical eddy diffusion coefficient
LLNL	Lawrence Livermore National Laboratory
LTE	local thermodynamic equilibrium
MAP	Middle Atmosphere Program
MLS	Microwave Limb Sounder
MPI	Max-Planck Institute
MPIC	Max-Planck Institute for Chemistry
NASA	National Aeronautics and Space Administration
NAT	nitric acid trihydrate
NCAR	National Center for Atmospheric Research
NMC	National Meteorological Center
NMHC	nonmethane hydrocarbon
NOAA	National Oceanic and Atmospheric Administration
NRC	National Research Council
NSF	National Science Foundation
OCS	carbonyl sulfide
OSLO	University of Oslo
POLARIS	Photochemistry of Ozone Loss in the Arctic Region in Summer
ppbv	parts per billion by volume
ppmv	parts per million by volume
pptv	parts per trillion by volume
PSC	polar stratospheric cloud
PSS	photostationary state
PST	photolytic source term
QBO	quasi-biennial oscillation
SAGE II	Stratospheric Aerosol and Gas Experiment II
SAM II	Stratospheric Aerosol Measurement II
SASS	Subsonic Assessment
SAT	sulfuric acid tetrahydrate
SBUV	Solar Backscatter Ultraviolet Spectrometer
SLS	Stratospheric Limb Sounder
SPADE	Stratospheric Photochemistry, Aerosols and Dynamics Expedition

STEP	Stratosphere-Troposphere Exchange Project
SST	supersonic transport
SUNY	State University of New York
TOMS	Total Ozone Mapping Spectrometer
UAK	University of Alaska
UARP	Upper Atmosphere Research Program
UARS	Upper Atmosphere Research Satellite
UCI	University of California at Irvine
UI	University of Illinois
UNEP	United Nations Environmental Programme
UT	Universal Time
WG3	Emissions Working Group of the International Civil Aviation Organization's Committee on Aviation Environmental Protection
WMO	World Meteorological Organization

APPENDIX E

CHEMICAL FORMULAE AND NOMENCLATURE

Br	bromine atom
Br_y	inorganic bromine
BrCl	bromine chloride
BrO	bromine monoxide
BrO_x	bromine oxides
$BrONO_2$	bromine nitrate
^{14}C	carbon-14
CCl_4	carbon tetrachloride
CFC	chlorofluorocarbon
CFC-11	$CFCl_3$
CFC-12	CF_2Cl_2
CFC-13	$CClF_3$
CFC-113	$CCl_2FCClF2$
CH_3	methyl radical
CH_4	methane
CH_3Br	methyl bromide
CH_3CCl_3	methyl chloroform
CH_3Cl	methyl chloride
CH_2O	formaldehyde
CH_3O	methoxy radical
CH_3O_2	methyl peroxy radical
CH_3OOH	methyl peroxide
Cl	atomic chlorine
Cl_2	molecular chlorine
Cl_y	inorganic chlorine
ClO	chlorine monoxide
ClO_2	chlorine dioxide
ClO_x	chlorine oxides
Cl_2O_2	dichlorine peroxide (ClO dimer)
$ClONO_2$	chlorine nitrate
CO	carbon monoxide
CO_2	carbon dioxide
DMS	dimethyl sulfide
H	atomic hydrogen
H_2	molecular hydrogen
halon-1301	CF_3Br
halon-1211	CF_2ClBr
HBr	hydrogen bromide
HC	hydrocarbon
HCFC-22	$CHClF_2$
HCFC-141b	$CFCl_2CH_3$
HCl	hydrogen chloride
HCO	formyl radical
HF	hydrofluoric acid
HNO_3	nitric acid
HNO_4	peroxynitric acid
HO_2	hydroperoxy radical
HO_x	hydrogen oxides
H_2O	water
H_2O_2	hydrogen peroxide
HOBr	hypobromous acid
HOCl	hypochlorous acid
HONO	nitrous acid
H_2SO_4	sulfuric acid
IO	iodine monoxide
N	atomic nitrogen
N_2	molecular nitrogen
NAD	nitric acid dihydrate
NAT	nitric acid trihydrate
NO	nitric oxide
NO_2	nitrogen dioxide
NO_3	nitrogen trioxide, nitrate radical
NO_x	nitrogen oxides
NO_y	odd nitrogen (= $NO + NO_2 + HNO_3 + 2N_2O_5 + ClONO_2 + HO_2NO_2$ + PAN + ...,)
N_2O	nitrous oxide
N_2O_5	dinitrogen pentoxide
NMHC	nonmethane hydrocarbon
O	atomic oxygen
$O(^1D)$	atomic oxygen (first excited state)
O_2	molecular oxygen
O_3	ozone
O_x	odd oxygen
OClO	chlorine dioxide
OCS	carbonyl sulfide
OH	hydroxyl radical
SAT	sulfuric acid tetrahydrate
SO_2	sulfur dioxide
SO_x	sulfur oxides
soot	A particulate product of incomplete combustion with the empirical formula C_nH_n

NASA
National Aeronautics and Space Administration

Report Documentation Page

1. Report No.	2. Government Accession No.	3. Recipient's Catalog No.
NASA RP-1381		

4. Title and Subtitle
1995 Scientific Assessment of the Atmospheric Effects of Stratospheric Aircraft

5. Report Date
November 1995

6. Performing Organization Code

7. Author(s)
R. S. Stolarski, S. L. Baughcum, W. H. Brune, A. R. Douglass, D. W. Fahey, R. R. Friedl, S. C. Liu, R. A. Plumb, L. R. Poole, H. L. Wesoky, D. R. Worsnop

8. Performing Organization Report No.

10. Work Unit No.

9. Performing Organization Name and Address
NASA Office of Aeronautics

11. Contract or Grant No.

13. Type of Report and Period Covered
Reference Publication

12. Sponsoring Agency Name and Address
National Aeronautics and Space Administration
Washington, DC 20546

14. Sponsoring Agency Code

15. Supplementary Notes

16. Abstract

This report provides a scientific assessment of our knowledge concerning the impact of proposed high-speed civil transport (HSCT) aircraft on the atmosphere. It comes at the end of Phase I of the Atmospheric Effects of Stratospheric Aircraft element of the NASA High-Speed Research Program. The fundamental problem with stratospheric flight is that pollutant residence times are long because the stratosphere is a region of permanent temperature inversion with stable stratification. Using improved two-dimensional assessment models and detailed fleet emissions scenarios, the assessment examines the possible impact of the range of effluents from aircraft. Emphasis is placed on the effects of NO_x and H_2O on the atmospheric ozone content. Measurements in the plume of an in-flight Concorde supersonic transport indicated a large number of small particles. These measurements, coupled with model sensitivity studies, point out the importance of obtaining a more detailed understanding of the fate of sulfur in the HSCT exhaust. Uncertainties in the current understanding of the processes important for determining the overall effects of HSCTs on the atmosphere are discussed and partially quantified. Research directions are identified to improve the quantification of uncertainties and to reduce their magnitude.

17. Key Words (Suggested by Author(s))	18. Distribution Statement
stratosphere, high speed civil transport, supersonic transport, aircraft, ozone, climate, nitrogen oxides, assessment, pollution	Unclassified - Unlimited Subject Category 45

19. Security Classif. (of this report)	20. Security Classif. (of this page)	21. No. of pages	22. Price
Unclassifed	Unclassified	110	